Aus der
Medizinischen Klinik und Poliklinik I
Klinikum der Universität München
Direktor: Professor Dr. med. Steffen Massberg

Dissertation

zum Erwerb des Doctor of Philosophy (Ph.D.)

an der Medizinischen Fakultät der

Ludwig-Maximilians-Universität zu München

## *Mechanisms of embryonic thrombopoiesis*

vorgelegt von:

Huan Liu

aus:

Shandong, China

Jahr:

2021

Mit Genehmigung der Medizinischen Fakultät der

Ludwig-Maximilians-Universität zu München

**First evaluator (1. TAC member):** *Prof. Dr. Steffen Massberg*
**Second evaluator (2. TAC member):** *Prof. Dr. Christian Schulz*
**Third evaluator:** *apl. Prof. Dr. Michael Spannagl*
**Fourth evaluator:** *Priv. Doz. Dr. Dr. Fabian Hauck*

**Dean:** **Prof. Dr. med. Thomas Gudermann**

Datum der Verteidigung:

09.12.2021

# Table of content

# List of figures

# List of abbreviations

| | |
|---|---|
| 3D | 3-dimensional |
| AGM | Aorta-gonad-mesonephros |
| BM | Bone marrow |
| BSA | Bovine serum albumin |
| CFU | Colony-forming units |
| dpc | Days post coitum |
| EDTA | Ethylenediaminetetraacetic acid |
| EMP | Erythromyeloid progenitor |
| FITC | Fluorescein isothiocyanate |
| FL | Fetal liver |
| GFP | Green fluorescent protein |
| HE | Hemogenic endothelium |
| HPCs | Hematopoietic progenitor cells |
| HSC | Hematopoietic stem cells |
| IL | Interleukin |
| IP injection | Intraperitoneal injection |
| LT-HSCs | Long-term HSCs |
| MEP | Megakaryocytic-erythrocytic progenitor |
| min | Minute |
| MK | Megakaryocyte |
| mL | Milliliter |
| mm | Millimeter |
| mM | Millimolar |
| MP-IVM | Multiphoton Intravital microscopy |
| Mpl | Myeloproliferative leukemia oncogene |
| MPV | Mean platelet volume |
| mRNA | Messenger RNA |
| NF-E2 | Nuclear factor-erythroid 2 |
| nm | Nanometer |
| OPO | Optical parametric oscillator |
| PBS | Phosphate buffer saline |
| PFA | Paraformaldehyde |

| | |
|---|---|
| PI | Propidium Iodide |
| PMTs | Photomultipliers |
| RFP | Red Fluorescent Protein |
| rh | Recombinant human |
| rm | Recombinant mouse |
| Rock | Rho kinase |
| ROS | Reactive oxygen species |
| RT | Room temperature |
| RUNX | Runt-related transcription factor |
| SEM | Standard error of the mean |
| TO | Thiazole orange |
| TPO | Thrombopoietin |
| vWF | von Willebrand factor |
| WT | Wild type |
| YS | Yolc sac |
| µg | Microgram |
| µL | Microliter |
| µm | Micrometer |

# Abstract

Platelets are generated by specialized cells called megakaryocytes (MKs) throughout embryonic development and adulthood. In adult bone marrow, MKs form and release proplatelets into circulation which mature into functional peripheral platelets. However, platelet generation in embryos is not fully understood. This is due to limitations of existing mouse models, challenges in handling fragile embryonic structures and lack of suitable imaging methods. Our goal was to assess the physiological generation of platelets in embryos.

We used flow cytometry to globally assess the different components of embryonic megakaryopoiesis and thrombopoiesis. We quantified platelets in embryonic blood and MKs in the fetal liver from wild type mice and mouse models of absent definitive hematopoiesis with c-Myb deficient embryos, and deficient megakaryocyte differentiation and thrombocytopenia with NFE2 deficient embryos. We found a dramatic increase of platelet count from E13.5 to E14.5, which could be the result of an observed strong increase in absolute MK number and further maturation with increasing fetal liver MK ploidy. Embryos with absence of c-Myb showed normal peripheral platelet count and MK numbers in fetal liver, although MKs had an immature phenotype. This finding suggests that megakaryopoiesis and thrombopoiesis in the fetal liver could be of dual original from yolk sac progenitors and later definitive hematopoietic precursors. Moreover, the master regulator of MK differentiation, NFE2, appeared to have also a role in embryonic thrombopoiesis. NFE2 deficient embryos presented with thrombocytopenia and increased numbers of apparently less mature MKs.

Second, we developed a highly advanced protocol for direct visualization of embryonic thrombopoiesis *in vivo* over time by adapting multiphoton intravital microscopy (MP-IVM) in the fluorescent thrombopoietic reporter mouse model Rosa26 mTmG x Pf4 Cre. We imaged directly platelet generation from MKs in the yolk sac and fetal liver identifying various types of proplatelets at different stages of embryonic development. We found that fetal liver MKs had higher thrombopoietic activity than yolk sac MKs. Embryonic platelets were released from MKs either by proplatelet or by membrane bud formation. Membrane

bud formation seemed to be the predominant form of platelet generation.

Our modified embryonic flow cytometry protocol and our novel three-dimensional MP-IVM protocol can be applied for studies of thrombopoiesis, hematopoiesis and other dynamic developmental processes. Comprehending the underlying mechanism by which embryonic platelets are generated could be critical to develop novel therapeutic strategies for congenital defects of hematopoiesis and thrombopoiesis such as neonatal thrombocytopenia. Our work could help to foster embryonic disease modeling beyond the hematopoietic system.

# 1.  Introduction

## 1.1  Embryonic platelet function

Platelets are a crucial component of hemostasis in mammals. In adults, they are key players for hemostasis and wound healing [1]. Platelets interact with leukocytes and components of the coagulation system in close proximity to the vessel wall under inflammatory conditions, mediating a complex process termed thromboinflammation [2]. Furthermore, they can contribute to immunity, infection control, but also cancer development [2-5].

Presumably, platelets have a different structure, size and function in embryos. Embryonic platelet functions are probably diverse, but less understood. Known examples are hemostasis upon injury and bleeding [6], development of lymphatic and venous vessels [7] and closure of ductus arteriosus [8].

There is lack of data how megakaryocytes (MKs) are generating embryonic platelets. Our goal is to define the physiological process of platelet generation in the embryo and compare its properties to canonical platelet generation in the adult bone marrow (BM).

## 1.2  Thrombopoiesis in bone marrow

In adult mice, platelets are produced by MKs in the bone marrow (BM). Besides, platelet production could also be allocated to the lungs under thrombocytopenic conditions or inflammation [9]. Megakaryopoiesis means the process through which megakaryocytes are derived from hematopoietic stem cells (HSCs), mainly in the BM [10].

In steady state of hematopoiesis, megakaryocytes are derived through a series of multipotent progenitor (MPP), common myeloid progenitor (CMP), and megakaryocyte-erythroid progenitor (MEP) cells [11, 12]. MEP give rise to erythroid progenitors and unipotent megakaryocytic precursors [13, 14]. These diploid MK progenitors will perform sequential rounds of DNA replication in the absence of cell division, resulting in DNA

ploidy ranging from 2N to 128N [15]. This process is paralleled by growth of cell dimension and protein levels. Finally, long extensions of the cytoplasm develop and are shed as platelets into the circulation, which is the major form of platelet generation in the adult BM [16].

In detail, mature MKs move near to the BM vascular sinusoids [17] and proplatelet-like structures have been observed extending from MKs through junctions in the lining of blood sinuses and therefore circulation [18]. Proplatelets have periodic platelet-sized swellings, which will become mature platelets into circulation [19]. Moreover, Nishimura et al.[20] showed that platelet release from megakaryocytes can be induced by interleukin-1α (IL-1α) via a new rupture mechanism, which yields higher platelet numbers under stress conditions.

## 1.3 Embryonic hematopoiesis and thrombopoiesis

### 1.3.1 Primitive and definitive hematopoiesis

Embryonic blood cell formation first occurs within the yolk sac (YS), where primordial red blood cells and several classes of colony-forming units (CFUs)/hematopoietic progenitor cells (HPCs) are found [21]. HSCs of the early stage originate within the major arteries of the developing embryo, including the dorsal aorta, the vitelline and umbilical arteries [22]. HSCs are also found in the YS and placenta by E11.5 [23, 24]; nonetheless, it is still unknow if this occurs through *de novo* generation within these structures or through inward migration. Derived from mesoderm, hemogenic endothelium (HE) contributes to primitive and definitive hematopoietic lineages [25].

HSC-independent hematopoiesis consists of two waves of hematopoietic progenitors that emerge in the YS [26]. As shown in **Figure 1.1**, the first, 'primitive' wave contains of primitive erythroid, megakaryocyte, and macrophage lineages. The second, 'erythromyeloid progenitor' (EMP) wave consists of definitive erythroid, megakaryocyte, macrophage, neutrophil, as well as mast cell lineages [27].
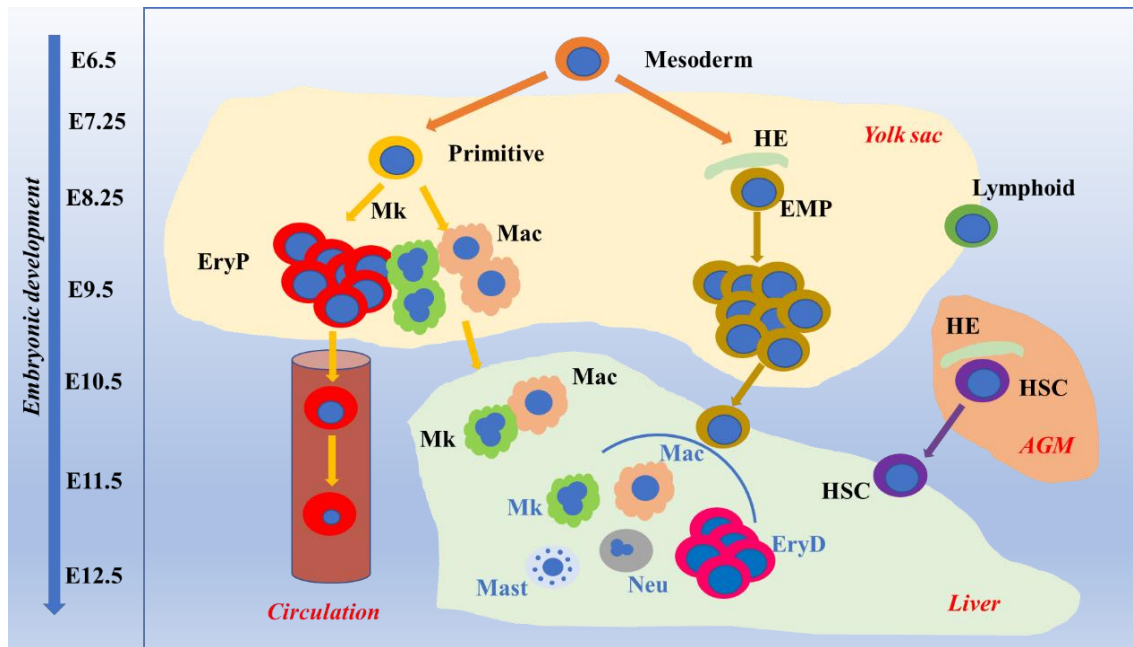
**Figure 1.1    Hematopoietic ontogeny scheme of the embryo**
**Adapted from Palis J，2016 [27]**

HSCs rise from the aorta in the aorta-gonad-mesonephros (AGM) region as well as from other large arterial vessels of the embryo. Some HSCs associated with the main embryonic vasculature are derived from YS precursors [28]. Commonly, both EMP and HSC arise from the HE [27]. HSCs migrate to the fetal liver (FL) [29], where they undergo massive expansion and form the definitive hematopoietic lineages; by E16.5, they begin to colonize the BM. In the BM, they will reside, self-renew and produce a continuous supply of all blood lineages throughout adult life   [25]. Apparently, the FL is a site of hematopoietic cells from both primitive and definitive origin, which is presumably also the case for megakaryopoiesis and thrombopoiesis. The relative contribution of both origins to total blood cell populations is still unknown.

### 1.3.2  Embryonic megakaryopoiesis and thrombopoiesis

The first circulating platelets in the embryo are provided by primitive megakaryocytes [30], which have a common progenitor with primitive erythrocytes in the YS [31]. At the beginning, megakaryocyte-erythrocyte progenitors (MEPs) differentiate into MK progenitor cells [13]. The first MK wave is detected in the YS, and characterized by the

occurrence of diploid MKs [13]. MKs with higher ploidy are uncommon at this developmental age. The second wave of hematopoiesis in the YS, and subsequently FL, gives rise to MKs that are able to polyploidize, but are still smaller than adult MKs [16].

Previously, platelet biogenesis was believed to be a uniform, canonical process in the adult BM and in the FL, meaning that MKs shed long proplatelets into the vasculature [16]. In fact, compared with adult thrombopoiesis, embryonic thrombopoiesis is less understood. Some studies indicated the proportion of reticulated platelets of total platelets is higher in contrast to the adult organism [32, 33], which could indicate a different form of thrombopoiesis in the embryo. As such, dynamic development of MKs and their mode of embryonic platelet production has not been studied in detail but could help understand the potential differences between embryonic and adult thrombopoiesis. When and how exactly thrombopoiesis emerges and proceeds in the embryo are unanswered questions. Understanding the mechanism by which platelets are generated is critical and could lead to novel strategies for the treatment of fetal or congenital diseases such as fetal thrombocytopenia [34, 35].

Importantly, the methodologies used in previous studies have significant limitations with regard to the observation and tracking of embryonic MKs and platelets. To better understand how platelet production proceeds in the embryo, we studied imaging methods for visualization and quantification of embryonic MKs and platelets *in vivo*.

## 1.4   Fetal liver development

As early as E8, the murine hepatic lineage is occurring in a portion of the ventral foregut endoderm adjacent to the developing cardiac structures. While the embryo develops, the endoderm forms a gut tube and the primordial liver structure moves to the midgut. The liver diverticulum forms by E9 and expands into a liver bud by E10 [36]. During this period, it is colonized by hematopoietic cells to become the major fetal hematopoietic organ. The liver expands as embryo develops. By E15, hepatoblasts are differentiating into both hepatocyte and biliary cells [36, 37].
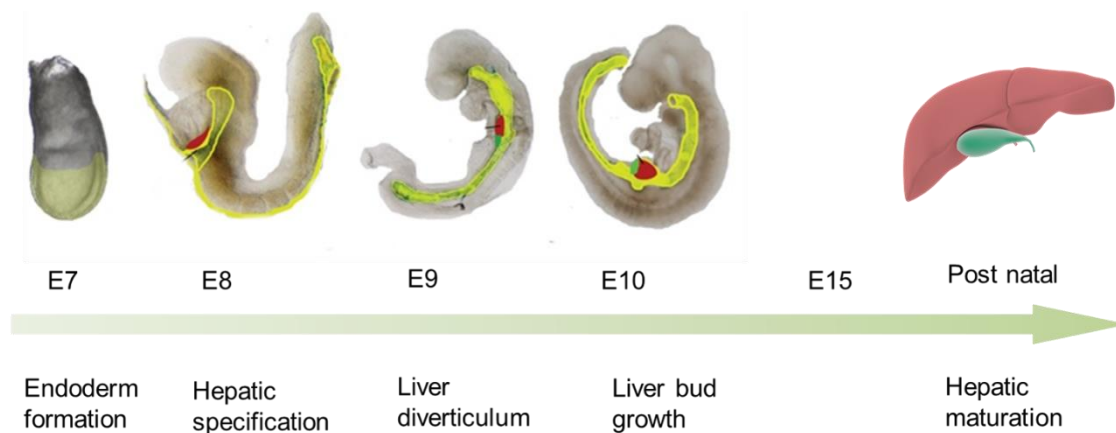
**Figure 1.2 Schematic presentation of mouse liver development**
**(Adapted from Zorn, 2008 [36] ) Yellow, endoderm tissue; red, liver; green, gall**
**bladder.**

At the end of prenatal stage, HSCs migrate from FL to BM and they reside there throughout adulthood [38, 39]. The first functional long-term HSCs (LT-HSCs) in the FL can be found by 17.5 dpc (days post coitum) in mice [23, 38].

## 1.5    Influence of c-Myb on embryonic hematopoiesis

The c-Myb gene is essential for the development of definitive hematopoiesis in the embryo. c-Myb was originally identified as an oncogene in two avian retroviruses that induce leukemia [40, 41]. There are many studies investigating *in vitro* the function of c-Myb, indicating that c-Myb is essential for the survival, proliferation as well as differentiation of hematopoietic cells [41, 42]. It's *in vivo* role for embryonic hematopoiesis has been also studied. At E13, c-Myb deficient embryos appeared normal, which suggested that c-myb is not essential for early hematopoietic development. By E15, however, the mutant mice were severely anemic. These c-Myb deficient embryos died thus due to lack of successful development of erythroid and myeloid lineages [43]. Importantly, overexpression of c-Myb constrains the differentiation of erythroid and myeloid cell lines [41, 44].

The role of c-Myb for thrombopoiesis, especially in the embryonic setting, is little understood. c-Myb hypomorphic adult mice show higher MK progenitor numbers, while early HPCs tend to differentiate into MKs [45, 46]. Accordingly, hypomorphic mutations of c-myb can induce MK expansion in the fetus and more thrombocytosis in adults [45, 47, 48]. However, the MKs that develop in c-Myb deficient mice display a reduction in ploidy [31, 46]. Moreover, the mechanisms of such effect it is not clear yet. This could due to defects in maturation/differentiation as well as the cell cycle being altered [41].

## 1.6  Influence of NFE2 on embryonic hematopoiesis

The nuclear factor-erythroid 2 (NFE2) transcription factor was identified over 30 years ago as a critical regulator for globin gene expression [49]. In mice, NFE2 is expressed in hematopoietic tissues, for example FL, adult BM, and spleen [50]. On a cellular level, NFE2 is mainly expressed in hematopoietic cells, including erythroid cells, megakaryocytes, and mast cells [51-53].

NFE2 is very critical in regulating MK biogenesis and function [49]. In MKs, NFE2 is important for maturation, transcriptional regulation, and platelet biogenesis [49, 54]. Transcription factor RUNX1 targets NFE2 and co-regulates MK [55]. In addition to transcriptional regulation of genes involved in platelet biogenesis, NFE2 can increase the accumulation of intracellular reactive oxygen species (ROS) [49, 56]. ROS can distinctly regulate MK proliferation, differentiation, and maturation through influencing microenvironment of the BM vascular niche and osteoblastic niche [57].

NFE2 knockout mouse were essential to elucidate the function *in vivo*. NFE2 knockout mice lack circulating platelets, i.e., suffer from absolute thrombocytopenia. This leads to the death of more than 90 % of NFE2-deficient pups because of peri/postnatal bleeding; their MKs show no cytoplasmic platelet formation [58].

Interestingly NFE2 knockout mice that survive into adulthood do not die of hemorrhage or show syndromes of bleeding, even though they lack almost completely peripheral

platelets [58]. Accordingly, those mice have a severe deficiency in proplatelet production [59]. Since they suffer from absolute thrombocytopenia but are otherwise viable if surviving the perinatal period, other important factors of the coagulation system are likely to compensate for this failure.

Although anemia was observed intermittently in surviving adult NFE2 knockout mice, these mice appeared otherwise normal in other organ functions. Both sexes were fertile [58]. However, the role of NFE2 for embryonic thrombopoiesis is less understood, especially for early and mid-gestational thrombopoiesis in the FL.

## 1.7  Influence of thrombopoietin on thrombopoiesis

Kelemen and Tanos defined thrombopoietin (TPO) as a humoral substance responsible for platelet production [60]. TPO is widely expressed in multiple organs, including liver, kidney, and smooth muscle [61-63]. It is the main regulator of adult megakaryopoiesis and thrombopoiesis [64-67].

TPO promotes differentiation of HSCs into the megakaryocytic lineage, in this way stimulates platelet production [65, 66]. Mice treated with TPO have increased MK numbers, size and polypoidization in the BM and elevated peripheral platelet level [66]. TPO has similar effect for *in vitro* BM cell culture. TPO-treated mice show higher generation of granules, demarcation membranes and cytoplasmic fragmentations, in this way generated more platelets [62, 68].

There are TPO receptor on MKs and platelets [69], which is known as the myeloproliferative leukemia oncogene (Mpl) receptor. Mpl receptor binds and internalizes TPO in situations of thrombocytosis [64, 65]. In thrombocytopenia, low levels of Mpl receptor expression and therefore decreased TPO clearance facilitate an increase of thrombopoiesis, as TPO is more abundant. Besides, the Mpl receptor plays a major role in platelet homeostasis [64, 70].

Even though TPO is predominantly produced at a constant rate in the liver, its level can be regulated by platelet level. Folman et al. reported that the plasma TPO level is inversely proportionate to circulating platelet counts [64]. Interestingly, in NFE2 knockout mice with absolute thrombocytopenia, TPO level are not elevated. [58].

As a therapeutic agent in humans, TPO has been approved for use in certain patients with thrombocytopenia [71]. Recombinant human TPO (rhTPO) can effectively stimulate MK and platelet production after intravenous administration [72].

Whether TPO plays a comparably important role in embryonic thrombopoiesis is unknown. In addition, it is not reported whether maternal TPO can cross the placenta barrier thereby influencing fetal platelet biogenesis.

## 1.8 Intravital real-time imaging with multiphoton microscopy

Although embryonic megakaryopoiesis and thrombopoiesis is studied extensively, it is limited by restrictions of intravital imaging. The majority of reports use *ex vivo* methods such as histological staining or *in vitro* cell culture to study embryonic megakaryopoiesis and thrombopoiesis. Obviously, these approaches are insufficient to study real-time and intravital changes of the embryonic environment.

Multiphoton fluorescence light microscopy was invented by Denk, Webb and coworkers [73]. This microscopy improved three-dimensional (3D) *in vivo* imaging of tissues and organs dramatically. Two-photon excitation is a description of a fluorescence process. In this process, a single fluorophore molecule got excited and generate two-photons [74]. Compared to single photon excitation, high power infrared lasers are applied to excite fluorophores with 2 photons with twice the wavelength and half the energy [73, 75, 76]. This method presents several advantages over confocal microscopy. It enables a deeper penetration depth through the tissue with less photo-bleaching and photo-toxicity. Besides, it excites the fluorophore uniquely and accurately at the desired focal plane [75]. This helps limiting tissue damage and dramatically increases the viability of biological

specimens [76].

These properties make multiphoton microscopy an optimal method for *in vivo* imaging of living tissues over longer time periods. The combination of multiphoton intravital microscopy (MP-IVM) and transgenic mice that express cell-specific fluorescence reporter proteins has facilitated novel studies of pathologic alterations in the mammalian organism [77]. MP-IVM can be widely used for imaging diverse and complex organ structures and processes, such as megakaryopoiesis and thrombopoiesis in BM [18, 20] or platelet generation in the adult lung [9, 17].

To date, *in vivo* studies investigating thrombopoiesis in the developing mouse fetus are very incomplete due to the difficult handling and fragility of fetal organs for microscopic studies. Besides, the mouse embryos are fairly small and strictly depend on maintaining feto-maternal circulation. All these demands challenge experimental conditions of embryo live imaging.

We applied MP-IVM to the embryo setting with transgenic fluorescent reporter mouse strains to establish new imaging methods in murine YS and FL in a 3D, *in vivo* and real-time setting.

## 1.9   Aim of the study

The aim of this doctoral thesis was to study characteristics of embryonic platelet generation by megakaryocytes in different fetal organs. Therefore, we performed extensive quantitative analysis of embryonic platelets and MKs in blood, YS and FL over different stages of murine development to give a global view on embryonic thrombopoiesis and its components. Furthermore, we used transgenic knock-out mice of c-Myb and NFE2, key transcriptional factors for hematopoiesis and thrombopoiesis, to evaluate their impact on embryonic thrombopoiesis. We applied advanced intravital real-time imaging with MP-IVM to give evidence that embryonic thrombopoiesis is a dynamic process with key differences compared to the adult organism. For this purpose, we had to establish a

novel murine imaging model to study the dynamic processes of embryonic platelet formation *in vivo.* This model and its complex technology enabled us to explore in detail different modes of platelets generation.

# 2. Materials and methods

## 2.1 Study approval

Animal studies were approved by the local regulatory agency (Regierung von Oberbayern, Munich, Germany) with project number 55.2-1-54-2532-207-2016.

## 2.2 Mice

C57BL/6, Pf4-Cre (Stock No: 008535) [78], Rosa26 mTmG (Stock No: 007676)[79], c-Myb (Stock No: 004757) [43] mice were obtained from The Jackson Laboratory (Boston, MA, USA). All mice were on C57BL/6 background (after being backcrossed at least 5 generations). NFE2 mice (Stock No: 002767) were generated on a 129/Sv-C57BL/6 strain background as previously described [4]. The mice were maintained and bred under specific-pathogen free and fed standard mouse diet. All pregnant animals undergoing procedures were over 10 weeks old. All mice were sacrificed after each surgery.

## 2.3 Timed mating and breeding strategy

Embryonic development was estimated as embryonic day 0.5 (E0.5) if a vaginal plug was present the following morning after mating. Pregnant females were used for subsequent experiments on indicated time points.

For flow cytometry experiments, we time mated C57BL/6 male and female mice to yield embryos which served as the control wild type (WT) samples for the embryonic thrombopoiesis analysis. We mated c-Myb +/- male and c-Myb +/- female mice to generate homozygous c-Myb -/- embryos. Similarly, we mated NFE2 +/- male and NFE2 +/- female mice to generate homozygous NFE2 -/- embryos. We used homozygous c-Myb -/- and homozygous NFE2 -/- embryos to investigate the influence of c-Myb and NFE2 on embryonic thrombopoiesis.

For multiphoton *in vivo* microscopy, we crossbred Rosa26-mTmG and Pf4-Cre mice to create Rosa26-mTmG × Pf4-Cre embryos for the use as a fluorescent reporter. Cre

activity is essential for defining the spatial and temporal extent of Cre-mediated recombination. Here with mTmG, this double-fluorescent Cre reporter mouse expresses membrane-targeted tandem dimer Tomato (mT) prior to Cre-mediated excision and membrane-targeted green fluorescent protein (mG) after excision. Besides, mG labeling is Cre-dependent [78, 79]. In these mice, mT is expressed in cells without activation of the Pf4 promoter as red fluorescent protein. mG is expressed in cells with Pf4 promoter activation as green fluorescent protein. We time-mated male Rosa26-mTmG × Pf4-Cre and female C57BL/6 mice to generate heterozygous Rosa26-mTmG × Pf4-Cre embryos expressing the fluorescent marker mTmG under the control of the Pf4 promoter with concomitant Cre expression.

## 2.4  Flow cytometry
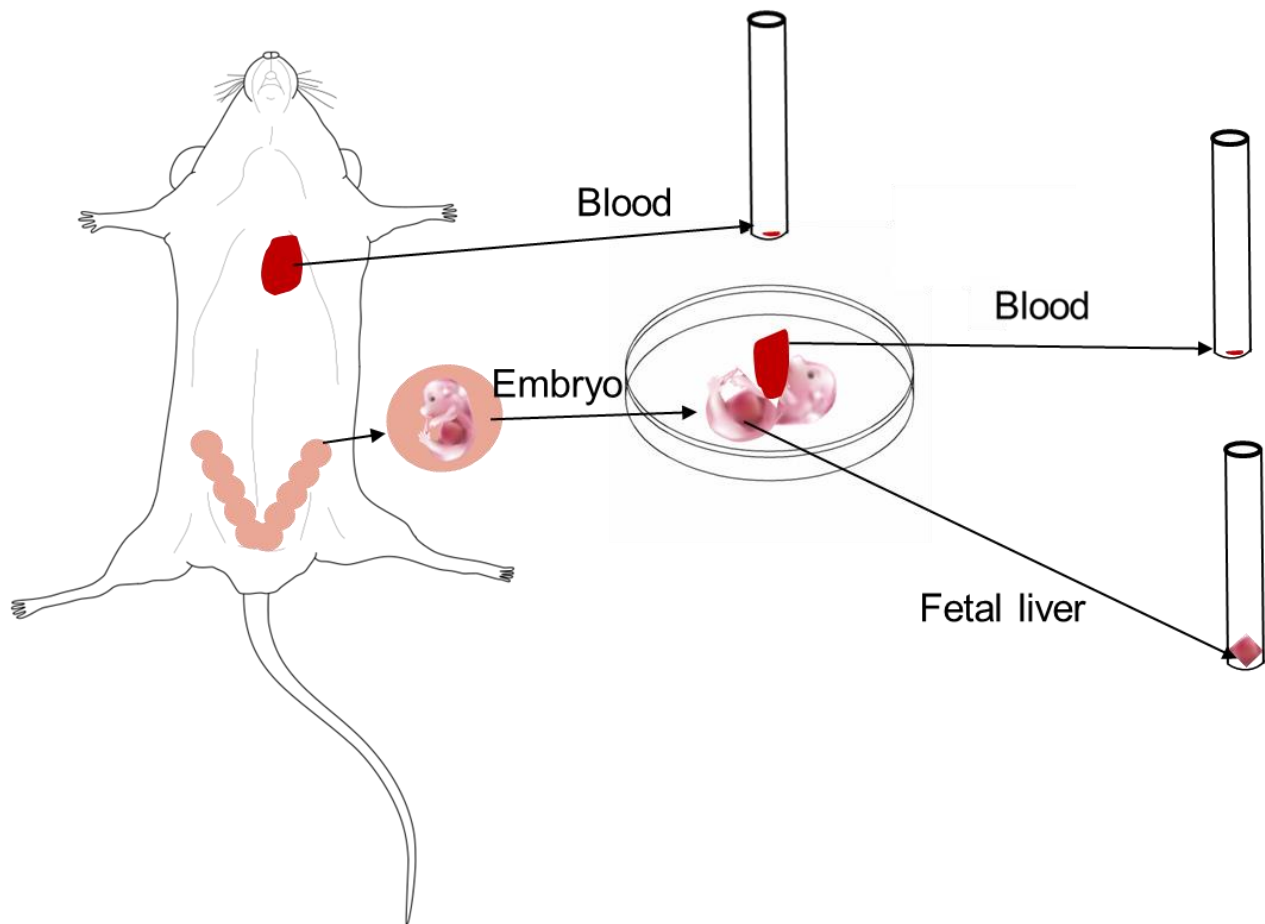


**Figure 2.1  Schematic presentation of mother animal and embryo processing**

### 2.4.1 Blood collection, processing, and fluorescence staining

We performed flow cytometry analysis with peripheral blood. As shown in **Figure 2.1**, full blood from the mother mice was taken by cardiac puncture with a syringe containing Acid-Citrate-Dextrose (ACD, containing 39 mM citric acid, 75 mM sodium citrate, 135 mM dextrose; 1:7 volume). The blood was kept on room temperature for further procedures. Embryos at specific ages were isolated from pregnant mice. Collection of 2 µL of fetal blood was performed through lateral neck dissection and added to 98 µL PBS for platelet and reticulated platelet staining. Platelets within a total volume of 100 µL were stained with the fluorescent-labelled antibody anti-CD42d-APC (1: 100, Biolegend, San Diego, USA) for 25 min at room temperature. The sample was then diluted again with PBS to 400 µL. For reticulated platelet staining, 2 µL of blood was diluted with 98 µL 4% formaldehyde. Then the sample was stained with anti-CD42d-APC and thiazole orange (100 ng/ml, SigmaAldrich, Poole, Dorset) for a further 25 min at room temperature. The sample was diluted again with PBS to 400 µL.

### 2.4.2 Fetal liver isolation, processing, and fluorescence staining

The fetal liver was isolated from surrounding tissue by blunt dissection and set aside in a solution of saline (NaCl 0.9%) on ice **(Figure 2.1)**. With a 5 mL syringe paired with a 20-gauge needle, the fetal liver was aspirated and expelled several times to dissociate the tissue mechanically. The dissociated liver was filtered through a 70 µm cell strainer (Miltenyl Bioec GmbH, Bergisch Gladbach, Germany). The filtered sample was centrifuged at 300g for 10 min at 4℃. After centrifugation, the supernatant was discarded and the cells were resuspended in 500 µL PBS for further procedure. 100 µL of cell suspension were prepared for fetal liver cell number counting with a Neubauer counting chamber (Paul Marienfeld, Lauda-Königshofen, Germany).

Cell staining and flow cytometry analysis were done as previously described [80]. For MK fraction assessment, we used 99 µL of the aforementioned cell suspension and stained the cells with fluorescent-labelled antibodies anti-CD41-FITC (1:100, Thermo Fisher

Scientific Company, San Diego, USA) and anti-CD42d-APC (1:100) for 30 minutes at 4℃ in dark. Then we washed the cells with 3mL PBS and centrifuged the cells with 300g for 10 min at 4℃. After centrifugation, the supernatant was discarded and the cell pellet was resuspended with 400 µL PBS. After that the cells were transferred for flow cytometry.

For MK ploidy assessment, we used propidium iodide (PI) (Sigma-Aldrich, Taufkirchen, Germany) to check the polyploidy extent. In experiment, we first stained 99 µL of cell suspension with anti-CD41-FITC (1:100) and anti-CD42d-APC (1:100) and washed as above. Afterwards, we resuspended the cells in 500 µL PBS and fixed the cell suspension with 500 µL 1% paraformaldehyde (PFA, Pierce, Bonn, Germany) for 10 minutes on ice. After fixation, cells were washed and resuspended with 500ul DNA staining buffer (1× PBS + 2mM MgCl2 + 0.05% Saponin + 0.01mg/mL PI + 10U/mL RNase A) overnight at 4 ℃. Then, after washing and resuspending with 400 µL PBS, the cells were transferred to flow cytometric measurement.

### 2.4.3 Flow cytometry acquisition and analysis of peripheral blood and fetal liver

For platelet counting, 4 x $10^4$ beads (Thermo Fisher, MA, USA) were added and blood samples were transferred to a flow cytometer (Beckman Coulter, Gallios Flow Cytometer 773231AD). A total of 500 beads were counted. Acquired data sets were analyzed with a dedicated flow cytometry analysis software (FlowJo LLC, Oregon, USA). Within this software, platelets were gated and distinguished by forward scatter /sideward scatter parameters and CD42d expression, as shown in results. Platelet counts were calculated based on collected volume and counted number of cells. Reticulated platelets were identified as a subpopulation of platelets exhibiting bright fluorescence with thiazole orange staining, as shown in results. The fraction of reticulated platelets of the total platelet population was then multiplied by the total platelet count to give the total reticulated platelet count.[81] MKs were gated and distinguished by forward scatter /sideward scatter appearance, CD41 and CD42d expression, as shown in results. Ploidy analysis was performed as shown in results.

## 2.5 Multiphoton intravital microscopy

### 2.5.1 Experimental setup
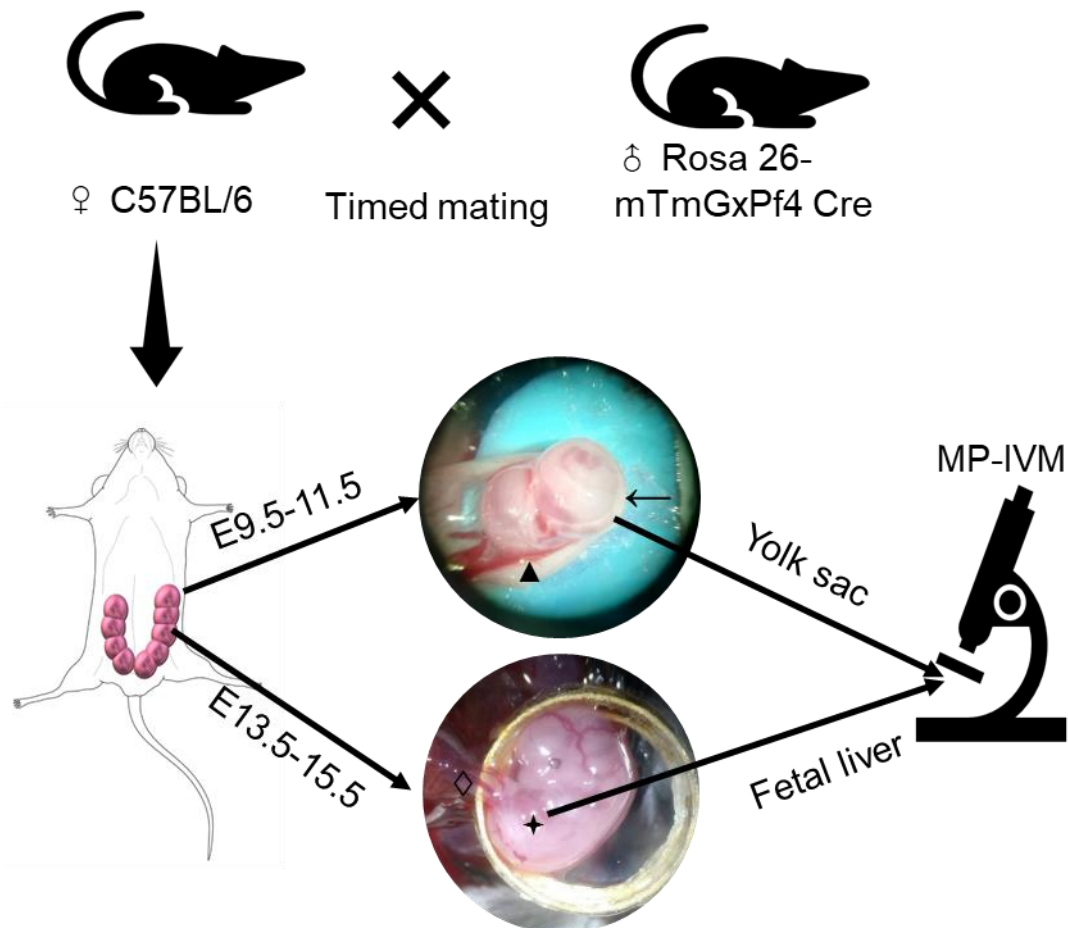


**Figure 2.2   Scheme of mice mating and experimental setup for yolk sac and fetal liver live imaging**

Timed mating was done with male Rosa 26-mTmG x Pf4 Cre mice and female wild type mice. Pregnant mice were used for yolk sac (YS) and fetal liver (FL) multiphoton intravital microscopy (MP-IVM). Embryos at E9.5-11.5 were suitable for YS imaging [82] and embryos at E13.5-16.5 for FL imaging. Abdominal ultrasound was checked regularly to monitor pregnancy.

▲: placenta; ←: complete yolk sac with embryo inside; ◊: umbilical cord; ✦: fetal liver.

### 2.5.2 Surgical preparation of dams and embryos for yolk sac and fetal liver imaging

Surgery of pregnant mouse was performed under deep anesthesia by intraperitoneal injection of midazolam (5 mg/kg body weight; Ratiopharm), medetomidine (0.5 mg/kg body weight; Pfizer), and fentanyl (0.05 mg/kg body weight; CuraMed Pharma GmbH) (MMF)

After anesthesia was initiated, the mouse was temporally kept in a sleeping box. For the experiment, the anesthetized dam was fixed on the surgery plate by tapes fixing her arms and legs. The surgery plate was placed on a heating stage. MMF was re-injected intraperitoneally every half an hour to maintain the anesthesia. Eyes were covered with cream (Bepanthen) to prevent drying. During the subsequent operation, anesthetic depth was assessed regularly via toe pinch. When deep anesthesia was achieved, the surgical procedure would start.

The abdominal skin was disinfected with Octenisept spray (Schülke & Mayr, Norderstedt, Germany). A 1.5 cm skin incision was made on the lateral side of the abdomen, and subsequently, the underside portion of the peritoneal membrane was cut. For imaging of embryos, a single uterine horn containing several embryos was carefully exposed and fixed on a plastic holder with a tissue adhesive (Histoacryl®). Warm saline and ultrasound gel (SONOSID®) were added continuously to keep the hydration of the exposed uterus and embryo. The uterine wall was cut, revealing the individual amniotic sacs, each containing one fetus and the respective placenta. During the whole preparation and imaging process, the embryo is connected with the mother through the umbilical cord to maintain its circulation.

For YS imaging, the membranes surrounding the YS were carefully removed and cleaned. Warm ultrasound gel was added to surround the embryo and YS to assure tissue hydration. A holder with a coverslip was placed on the top of the exposed YS. For FL imaging, YS and amniotic sac were cut to expose the fetus. The lateral abdominal skin of the embryo was removed if it was too thick to reduce the light scattering and improve light

penetration. Then, the preparation was moved to the microscope. During surgery, the blood and liquid was absorbed by the tissue and cotton bud in time to avoid blurred version.

The coverslip holders were customized by 3D printing technology thereby adjusting coverslip size for the appropriate embryonic age and size. We designed the new holders using computer-aided design (CAD) software (Autodesk® Fusion 360™), a biocompatible plastic resin (MiiCraft BV-007A) and a 3D printer (MiiCraft).

Each surgical procedure was documented with the respective project number from the regulatory agency.

### 2.5.3 Multiphoton intravital microscopy of yolk sac and fetal liver thrombopoiesis

The stage with the mother and embryo were located under the microscope objective. First, expression of green fluorescent protein (GFP) was checked by epifluorescence mode with fluorescence illumination (X-Cite 120Q) to select the appropriate embryos with Pf4-Cre recombination. If the embryo expressed Cre recombinase, the MK and platelet would successfully express GFP. This would enable subsequent MP-IVM for the identification of MKs and platelets. However, in the absence of Cre recombination and thus no GFP expression, embryos were not used for image acquisition.

A multiphoton microscope (LaVision Biotech) with an upright Olympus stand, all enclosed in a custom-built incubator maintaining 37°C, was used for imaging. The microscope was equipped with a Chameleon Ti:Sapphire laser (Coherent, Inc., Santa Clara, CA, USA) with an output 900-1100nm range pulsed laser for excitation and four photomultipliers (PMTs) with simultaneous four channel acquisitions. Images were acquired using a CFI75 LWD 16X objective (Nikon) with saline (for YS) or ultrasound gel (for FL) as immersion medium. Emitted fluorescent signals were collected by photomultipliers (PMTs). Images were acquired using ImSpector software. Fluorescence excitation was provided by laser tuned to 1100 nm with an optical parametric oscillator (OPO) for simultaneous excitation of tdTomato. 800 nm excitation wavelength was used for imaging GFP. The power of the laser and OPO were adjusted according to the thickness of scanning volume. The

magnifications were recorded in each specific image. Image stacks (z-axis) were recorded with 1.5 µm or 2 µm step size with a total axial depth of 20-90 µm tissue volume. Sequential images were acquired as time lapse to allow observation of fetal blood flow and real-time cell movements. During MP-IVM of anesthetized mice, periodic tissue motion caused by heart beati and respiration induced significant shifts of the imaged region. To adjust for the relevant tissue movement and displacement during MP-IVM, we applied VivoFollow software (University of Bern) for real-time *in vivo* imaging stabilization [17, 18]. Acquired images were analyzed using Imaris software (Bitplane). For videos with excessive tissue motions, optional post-acquisition drift correction was performed with Imaris Software.

## 2.6 Thrombopoietin injection

### 2.6.1 Thrombopoietin injection and animal processing
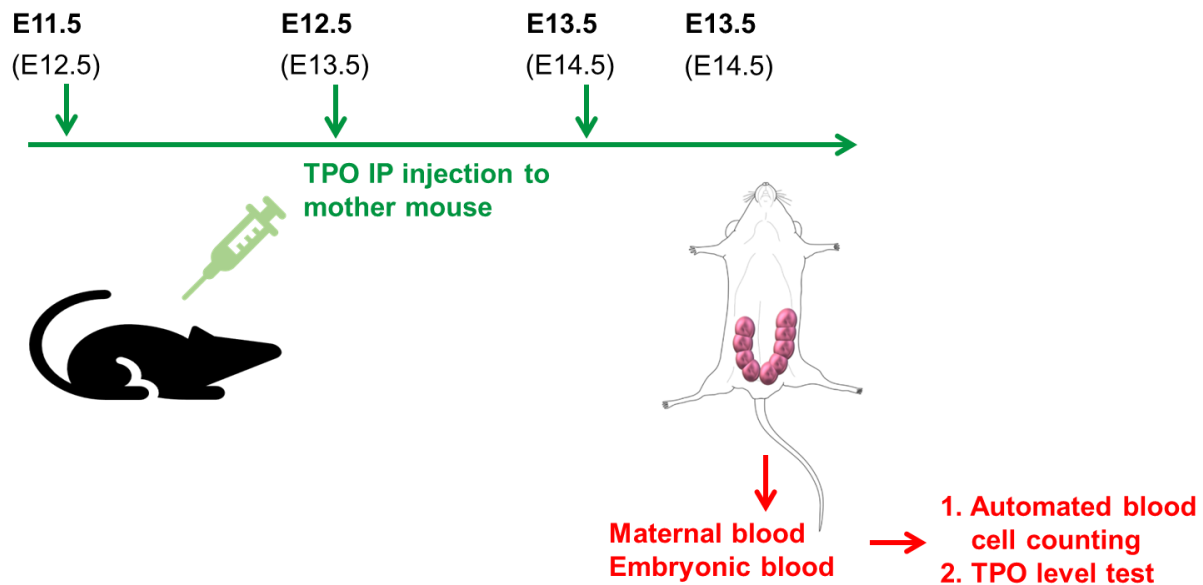


**Figure 2.3  Scheme of mice injection of thrombopoietin**

TPO, thrombopoietin. IP injection, intraperitoneal injection

To check the effect of exogenous thrombopoietin (TPO), we timed mated BL6 male and female mice. Pregnancy was confirmed by presence of vaginal plug the next morning after

mating. We performed once daily intraperitoneal (IP) injections of recombinant murine thrombopoietin (rmTPO, ImmunoTools) with a dose of 8ng per gram of mouse body weight per day over three consecutive days. Accordingly, to measure blood cell count and TPO level in mother animals of gestational age G13.5 and embryos of E13.5, the injection would be performed on G11.5, G12.5 and G13.5 (**Figure 2.3)**. The maternal blood was then taken between 3-4 h after the last injection at day G13.5. The embryos were isolated from dams at E13.5. Analysis was also performed on G14.5/E14.5 after three consecutive injections.

### 2.6.2 Blood collection and automated blood cell count

Peripheral blood from the mother mice was taken by cardiac puncture with a syringe containing ACD as described above. The blood was kept at room temperature for further procedure.

Fetal blood was collected through lateral neck dissection and drawn up to a tube coated with ethylenediaminetetraacetic acid (EDTA) (Sarstedt, Germany). The blood of all embryos from one dam was collected one by one and gathered together. We gathered blood of the whole litter to get enough volume for automated blood cell count as well as serum isolation for TPO measurements.

Platelet count and mean platelet volume (MPV) were measured from 50 µL blood sample by hematology analyzer ABX Micros ES 60 (HORIBA, Kyoto, Japan).

### 2.6.3 Serum thrombopoietin immunoassay

The remaining blood was centrifuged with 2000g for 20min. The supernatant (serum) was collected for TPO level measurements. We performed immunoassay with Quantikine Mouse Thrombopoietin ELISA Kit (R&D Systems, Minneapolis, USA) to measure serum TPO levels. The experiment was performed according to datasheet of the manufacture. This immunoassay detects both endogenous TPO and exogenous rmTPO.

## 2.7   Statistical analysis

Statistical analyses were performed with GraphPad Prism software (San Diego, USA). In figures, all data are presented as mean ± SEM. Error bars in figures indicate standard error of the mean (SEM). An unpaired student 's t-test was used for comparison between two groups. For comparison of multiple groups with one variable, one-way ANOVA testing was performed. A p value less than 0.05 was considered statistically significant.

P values are presented in figures as follows:

**Table 2.1   P value presentation in figures. (Adapted from Prism User Guide)**

| P value | Meaning | Figure label |
|---|---|---|
| < 0.0001 | Extremely significant | **** |
| 0.0001 to 0.001 | Extremely significant | *** |
| 0.001 to 0.01 | Very significant | ** |
| 0.01 to 0.05 | Significant | * |
| ≥ 0.05 | Not significant | ns |

# 3. Results

## 3.1 Platelet and megakaryocyte counts in C57BL/6 (BL6) mother animals and embryos

We measured platelet count in embryo peripheral blood from E11.5 to E18.5 to report patterns of thrombopoiesis. As is known, the major source of MKs in embryo is fetal liver [10, 16]. Here, we also report the MK patterns in fetal liver, including MK number and ploidy in different developing stage. We also assessed the parameter in c-Myb and NFE2 mice. There, we use BL6 embryos and dams as wildtype (WT) control.

### 3.1.1 Gating strategy for platelet quantification
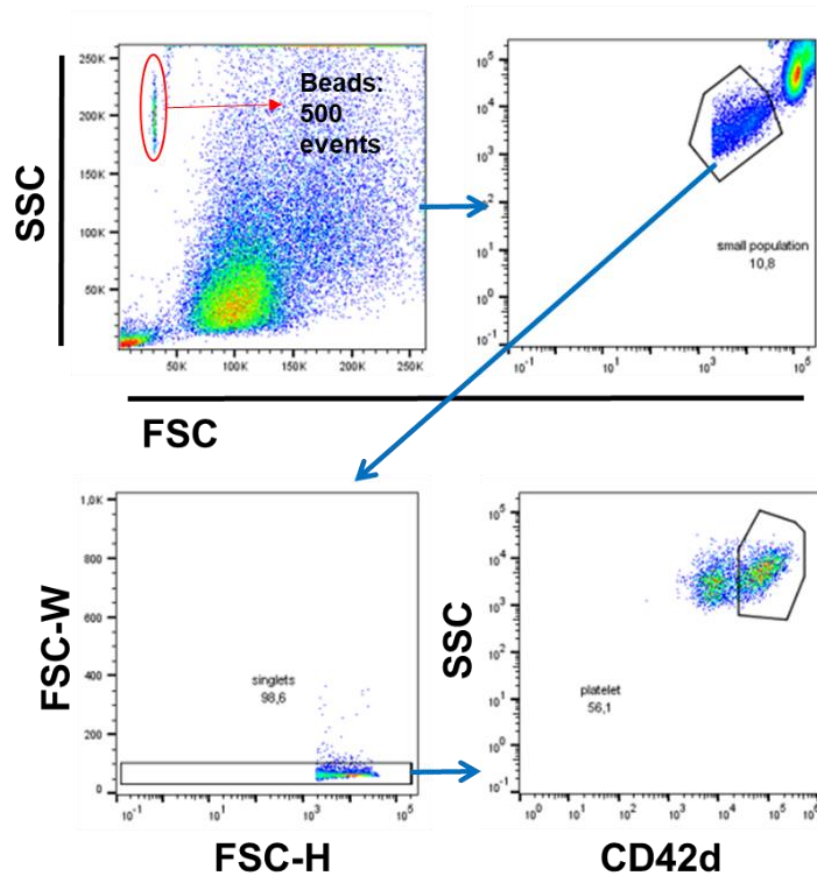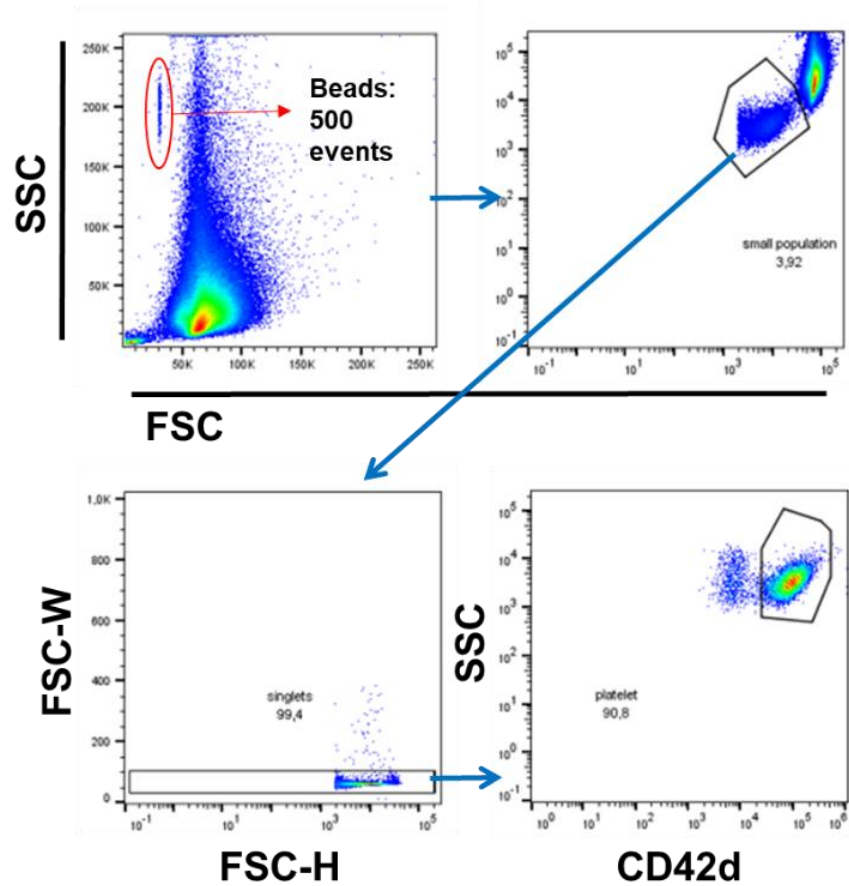
**Figure 3.1   Gating strategy of platelet quantification in maternal and embryonic blood**

Platelet counts are measured from 2 µL blood volume by flow cytometry. Peripheral platelets from maternal **(A)** and embryonic blood **(B)** were gated with the same gating strategy. Platelets were defined as 1) low signal in forward scatter/sideward scatter (FSC/SSC), 2) singlets by FSC width and 3) CD42d positive [9].

## 3.1.2 Embryonic peripheral blood platelet count



| | | | | | | | |
|---|---|---|---|---|---|---|---|
| n (dams) | 2 | 4 | 6 | 6 | 3 | 4 | 1 |
| n (embryos) | 18 | 38 | 47 | 40 | 24 | 35 | 9 |
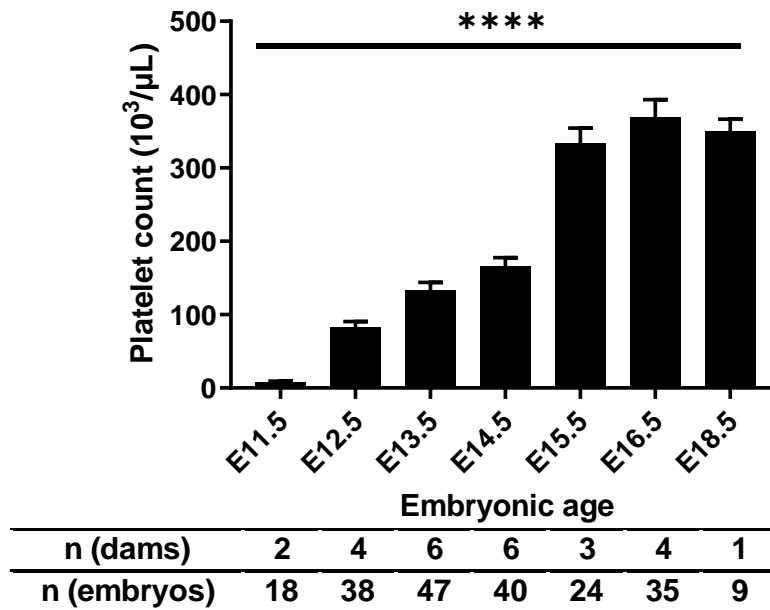
**Figure 3.2   Platelet count in embryonic blood**

We quantified the peripheral blood platelet count in embryos at different stages of embryonic development. At E11.5, blood platelet count was lowest with $8.14 \pm 1.0*10^3/\mu L$, with continuing increase up to E14.5 ($165.3 \pm 12.3*10^3/\mu L$). A strong increase was observed from E14.5 to E15.5 ($333.1 \pm 21.4*10^3/\mu L$), with stable platelet counts until E18.5 ($349.4 \pm 17.0*10^3/\mu L$). ****$p<0.0001$, one-way ANOVA test. The number of mother animals (dams) and embryos are noted below the graph.

### 3.1.3 Maternal peripheral blood platelet count



| n (dams) | 2 | 4 | 6 | 6 | 3 | 4 | 1 |
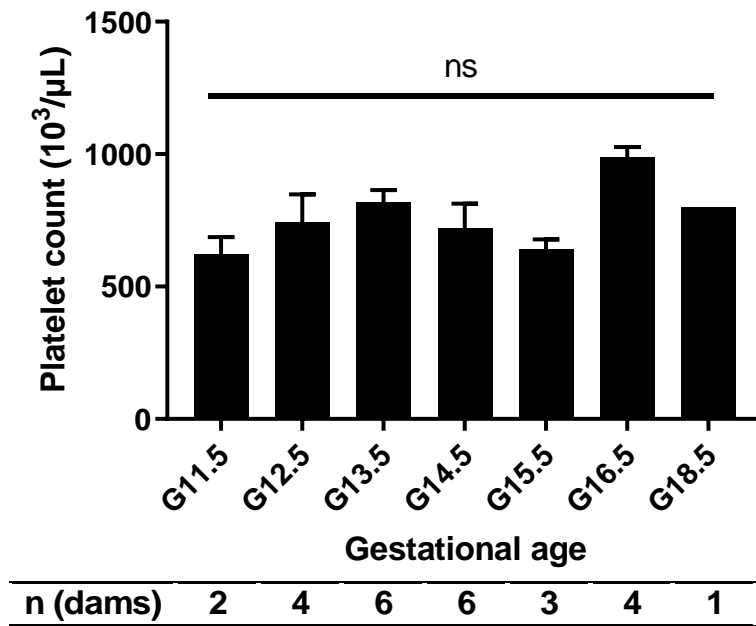
**Figure 3.3   Platelet count in maternal blood**

We quantified the peripheral blood platelet count in mother animals at different stages of gestation (G). At G11.5, maternal blood platelet count was lowest ($620.8 \pm 65.7 \times 10^3/\mu L$). At G16.5, maternal blood platelet count was highest ($986.3 \pm 40.5 \times 10^3/\mu L$), although statistical testing with the ANOVA test found no significant difference across gestational age. The numbers of dams are noted below the graph.

### 3.1.4 Forward scatter width of platelets from wild type maternal and embryonic blood
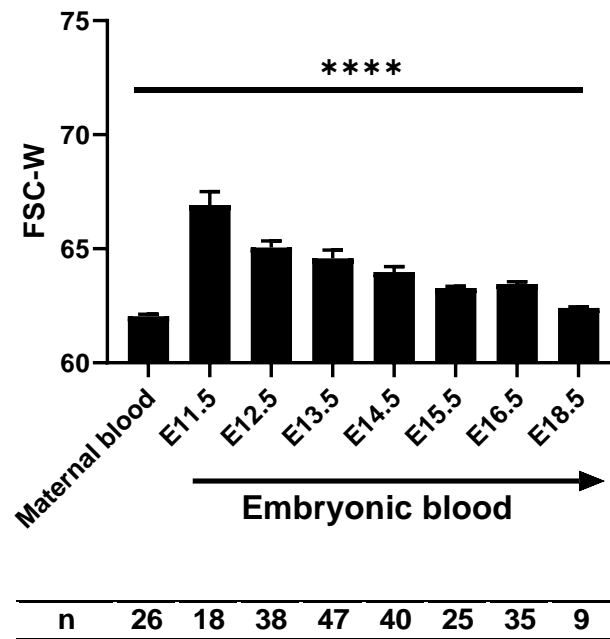


**Figure 3.4   Forward scatter width of platelets from maternal and embryonic blood**

Flow cytometry was used to measure forward scatter width (FSC-W) as a parameter for particle size to estimate platelet size in embryonic and maternal blood [83]. The gating strategy according to **Figure 3.1** was used. In maternal blood, the mean FSC-W was 62.0 ± 0.1, which was significantly lower than the FSC-W of early embryonic platelets from E11.5 (66.9 ± 0.6). With further embryonic development, FSC-W decreased to 62.4 ± 0.1 (E18.5), which is more similar to maternal platelet FSC-W. Differences at development were statistically significant with one-way ANOVA test ($p < 0.000$). The number of dams and embryos are noted below the graph.

### 3.1.5 Gating strategy for reticulated platelet quantification

## A  E14.5 embryonic blood
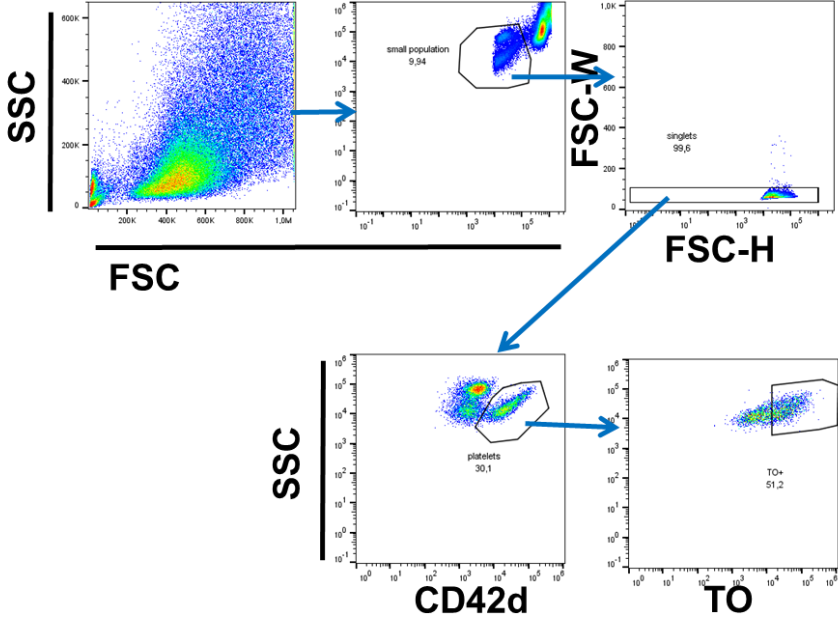


## B  G14.5 maternal blood
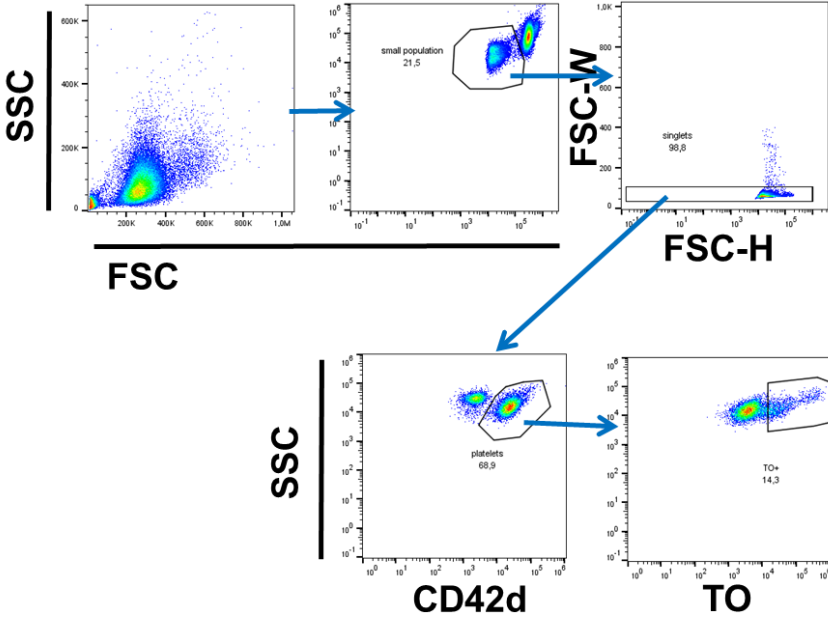
**Figure 3.5   Gating strategy for quantification of reticulated platelets in maternal and embryonic blood**

Newly formed platelets, so-called reticulated platelets, are anucleated but contain rough endoplasmic reticulum and messenger RNA (mRNA). Reticulated platelet exist in adult mouse blood [84]. Reticulated platelet count is measured from 2 µL blood volume by flow cytometry. Blood was stained with a fluorescent antibody against CD42d and with thiazole orange (TO). Thiazole orange stains nucleic acids in platelet [85]. Maternal **(A)** and embryonic blood **(B)** were gated with the same gating strategy. We used a comparable gating strategy as **Figure 3.1** with additional gating for thiazole orange (TO) positive particles representing reticulated platelets.

### 3.1.6  Reticulated platelet fraction in embryonic peripheral blood



| Embryonic age | E11.5 | E12.5 | E13.5 | E14.5 | E15.5 | E16.5 | E18.5 |
|---|---|---|---|---|---|---|---|
| n (dams) | 2 | 4 | 6 | 6 | 3 | 4 | 1 |
| n (embryos) | 9 | 19 | 32 | 26 | 12 | 15 | 3 |
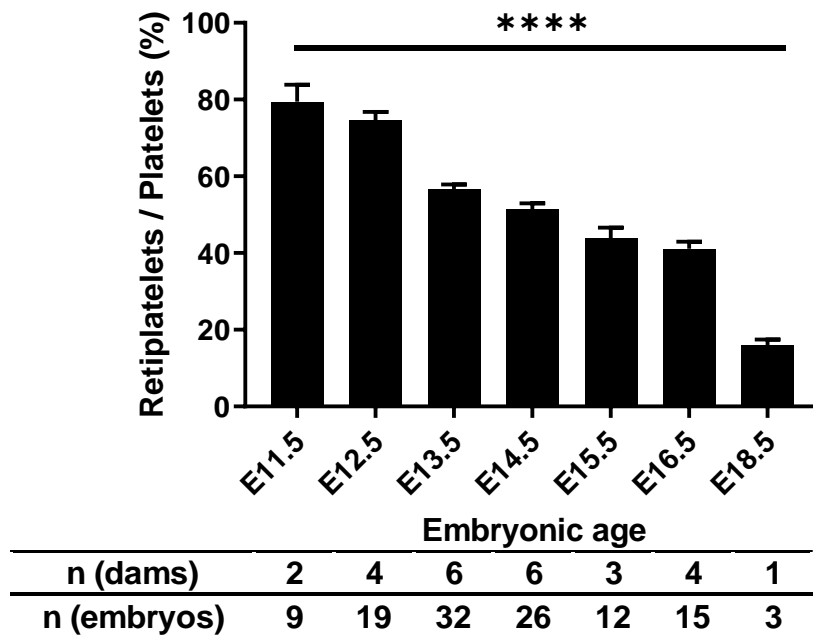
**Figure 3.6   Reticulated platelet fraction in embryonic peripheral blood**

As seen in this figure, the majority of embryonic platelets is reticulated from E11.5 until 14.5. At E11.5, the fraction amounted to 79.4 ± 4.5 % of all blood platelets. With embryonic

development, the proportion decreased continuously to 16.0 ± 1.4% at E18.5 (p<0.0001, one-way ANOVA test). The latter value is comparable to the fraction of adult reticulated platelets. Number of mother animals (dams) and embryos are noted below the graph.

### 3.1.7  Reticulated platelet fraction in maternal peripheral blood



| n (dams) | 2 | 4 | 6 | 6 | 3 | 4 | 1 |
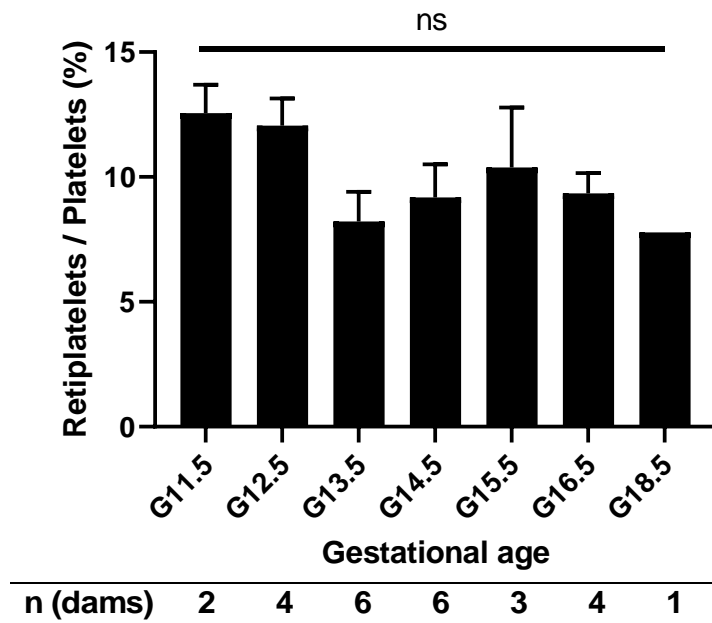
**Figure 3.7    Reticulated platelet level in maternal peripheral blood.**

We analysed reticulated platelet proportion in dams. Reticulated platelet fraction ranged from minimum 8.2 ± 1.2 % at G13.5 to maximum 12.5 ± 1.2 % at G11.5, although these differences over gestational age did not reach statistical significance (p=0.34, one-way ANOVA test). The numbers of dams are noted below the graph.

## 3.1.8 Reticulated platelet count in embryonic peripheral blood



| | | | | | | | |
|---|---|---|---|---|---|---|---|
| **n (dams)** | 2 | 4 | 6 | 6 | 3 | 4 | 1 |
| **n (embryos)** | 9 | 19 | 32 | 26 | 12 | 15 | 3 |
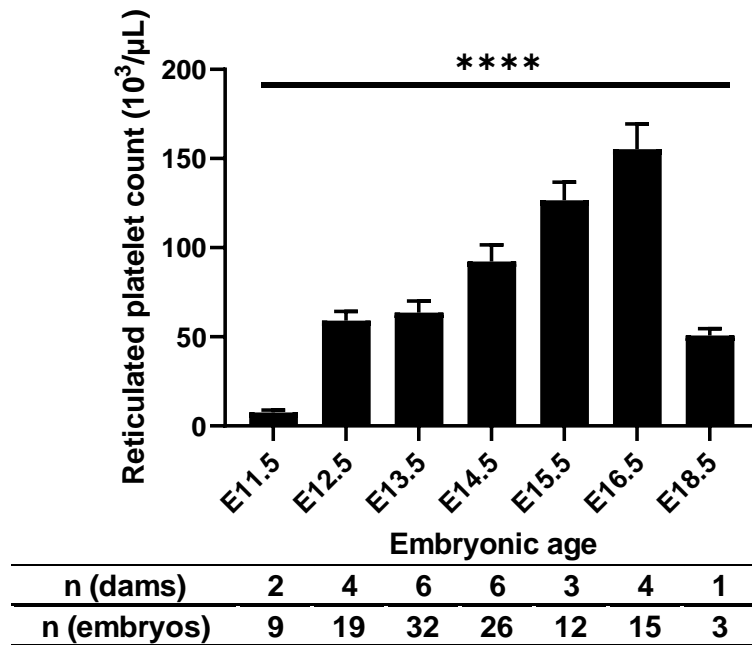
**Figure 3.8   Reticulated platelet count in embryonic peripheral blood**

Reticulated platelet blood concentration was calculated from the overall peripheral blood platelet count multiplied with the fraction of reticulated platelets in the embryo. In parallel to the overall peripheral platelet count, reticulated platelet numbers were low at E11.4 (7.6 $\pm$ 1.3 x $10^3$/µL), with increasing numbers over time until E16.5 (155.3 $\pm$ 14.0 x $10^3$/µL). After that, reticulated platelet counts decreased to 50.8 $\pm$ 3.9 x $10^3$/µL at E18.5. $p < 0.0001$, one-way ANOVA test. The number of mother animals (dams) and embryos are noted below the graph.

### 3.1.9   Reticulated platelet count in maternal peripheral blood
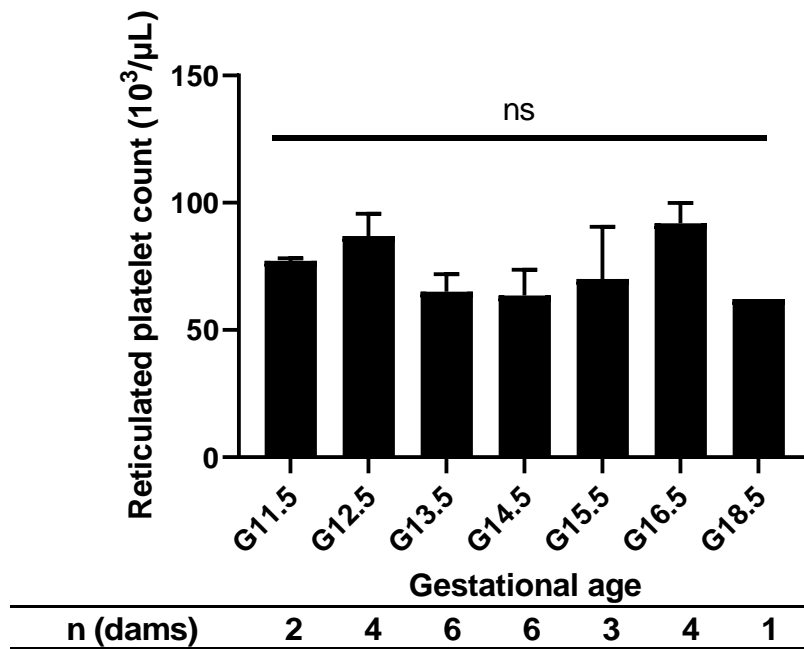


**Figure 3.9   Reticulated platelet count in maternal peripheral blood**

Reticulated platelet count of maternal blood ranged from minimum $62.2 \pm 0 \times 10^3$/µL at G18.5 to maximum $91.9 \pm 8.0 \times 10^3$/µL at G11.5, although these differences over gestational age were not statistically significant (p=0.27, one-way ANOVA test). The numbers of dams are noted below the graph.

### 3.1.10 Fetal liver growth
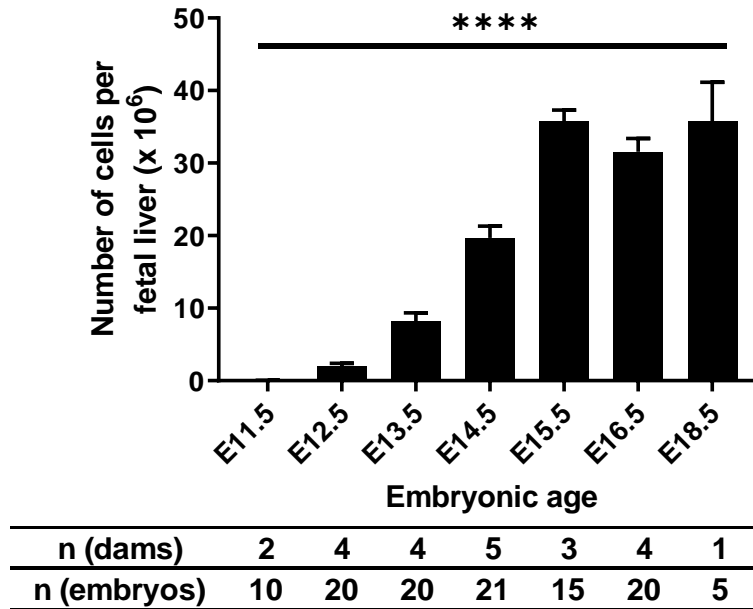


**Figure 3.10   Fetal liver cell numbers during embryonic development**

Between E11.5 and E15.5, the fetal liver (FL) undergoes a period of accelerated growth with rising FL cell numbers[36]. From as little as $0.05 \pm 0.02$ x $10^6/\mu L$ of FL volume at E11.5, the FL cell number expands by >700 fold to $35.7 \pm 1.6$ x $10^6/\mu L$ at E15.5. After this exponential growth phase, FL cell numbers are stable until E18.5 ($35.8 \pm 5.4$ x $10^3/\mu L$). p<0.0001, one-way ANOVA test. The number of mother animals (dams) and embryos are noted below the graph.

### 3.1.11    Gating strategy for megakaryocyte quantification
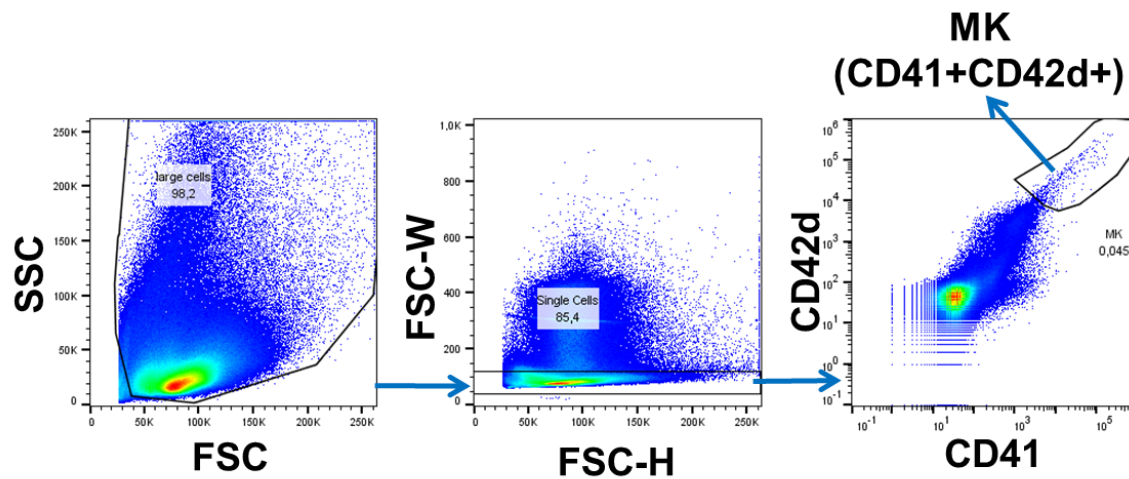


**Example from E15.5 fetal  liver**

**Figure 3.11    Gating strategy for quantification of fetal liver megakaryocytes**

Using flow cytometry, we quantified megakaryocytes **(**MK) in FL. MKs from FL were defined as 1) large FSC/SSC cells, singlets in FSH-H/FSC-W and double positive for the thrombopoietic surface markers CD41 and CD42d [86].

### 3.1.12 Megakaryocyte proportion in fetal liver
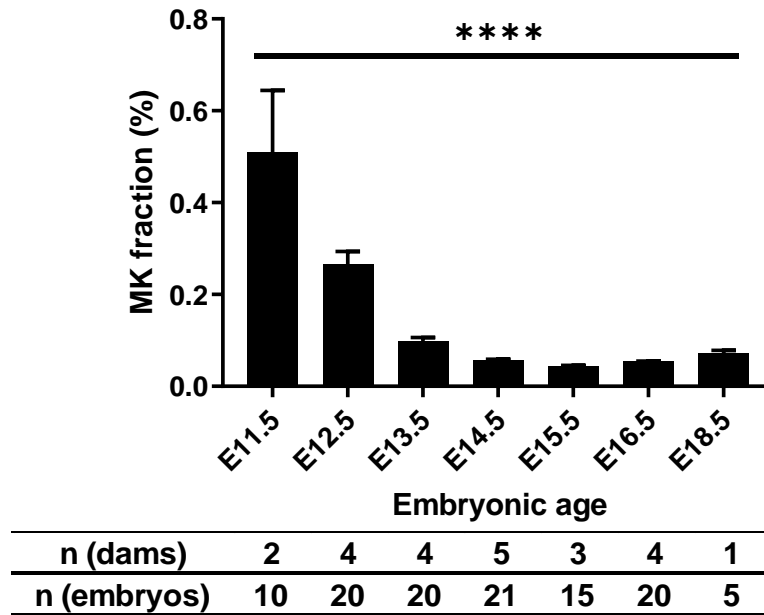


**Figure 3.12   Fraction of megakaryocytes to total cell number in fetal liver**

Fraction of megakaryocytes to the total cell number in the developing FL was assessed by flow cytometry. The fraction of MKs of total fetal liver cells is low and decreases from maximum 0.51 ± 0.14 % at E11.5 to minimum 0.04 ± 0.0 % at E15.5, remaining on low levels further on. p<0.0001, one-way ANOVA test. The number of mother animals (dams) and embryos are noted below the graph.

## 3.1.13 Megakaryocyte cell number in fetal liver



| n (dams) | 2 | 4 | 4 | 5 | 3 | 4 | 1 |
|---|---|---|---|---|---|---|---|
| n (embryos) | 10 | 20 | 20 | 21 | 15 | 20 | 5 |
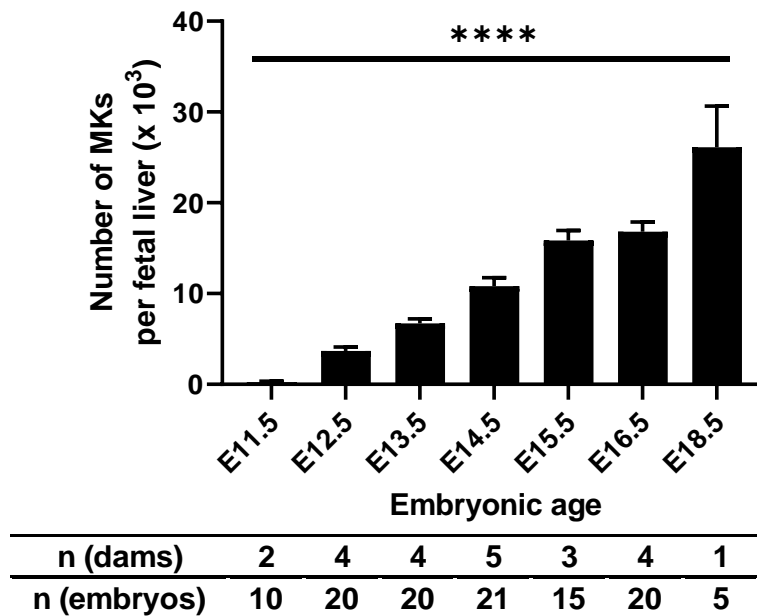
**Figure 3.13    Absolute megakaryocyte cell count in fetal liver**

Absolute megakaryocyte (MK) numbers per FL were calculated from the FL cell count multiplied with the fraction of MK in FL. During FL development, total cell numbers strongly increased as shown in **Figure 3.10**. In parallel, also fetal MK numbers rise significantly. Absolute MK counts grew from $0.3 \pm 0.1 \times 10^3$ at day E11.5 to $26.1 \pm 4.5 \times 10^3$ at day E18.5, a 87-fold increase of MK number. $p < 0.0001$, one-way ANOVA test. The number of mother animals (dams) and embryos are noted below the graph.

### 3.1.14  Megakaryocyte cell size in fetal liver



| n (dams) | 2 | 4 | 4 | 5 | 3 | 4 | 1 |
|---|---|---|---|---|---|---|---|
| n (embryos) | 10 | 20 | 20 | 21 | 15 | 20 | 5 |
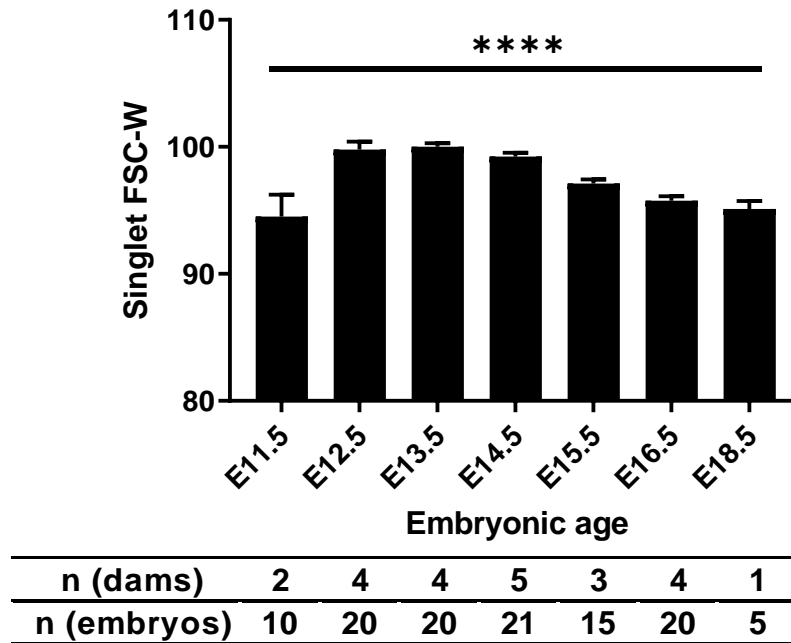
**Figure 3.14   Megakaryocyte forward scatter width in fetal liver**

Fetal liver MK FSC-W was lowest at E11.5 (94.5 ± 5.4) and increased the following days up to 100.0 ± 1.3 at E13.5. From then on, a progressive decrease was observed until E18.5 (95.1 ± 1.4). These dynamic changes in FSC-W parameter were statistically significant ($p < 0.0001$, one-way ANOVA test.) Average number of embryos in this experiment per dam was 4.8 embryos. The number of mother animals (dams) and embryos are noted below the graph.

### 3.1.15　Megakaryocyte maturation in fetal liver assessed by ploidy
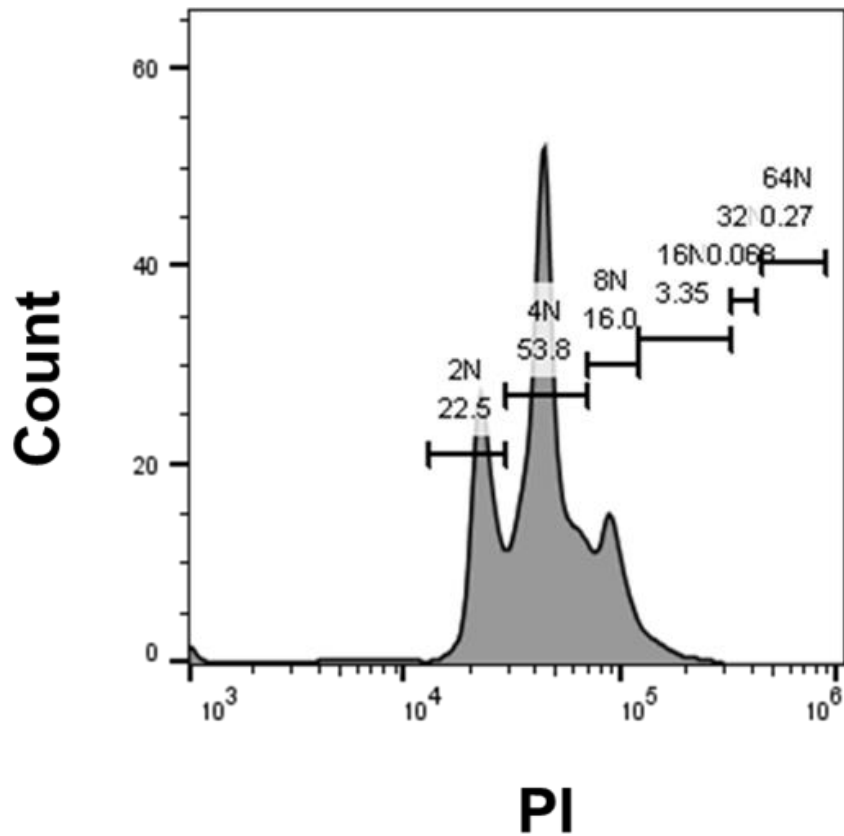


**Figure 3.15　Ploidy analysis of fetal liver megakaryocytes by flow cytometry**

Maturation of fetal liver MKs was assessed with ploidy analysis using propidium iodide (PI) staining. The aforementioned MK gating strategy in flow cytometry was used to identify MKs. Histograms were divided as approximated the different ploidy classes in terms of DNA content. We set boundaries of DNA with markers between peaks with geometric mean analysis[87]. The frequency of cells with each ploidy level was calculated by dividing the number of specific ploidy cells by the total cell number in this histogram. Representative analysis from ED16 shows the presence of MKs with different ploidy ranging from 2N to 64N.
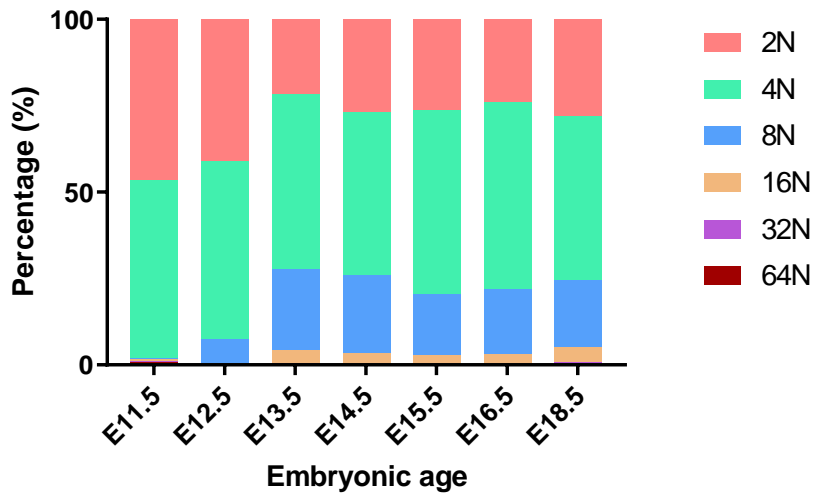
Upper chart — Percentage (%) vs Embryonic age (stacked bar chart)

| | E11.5 | E12.5 | E13.5 | E14.5 | E15.5 | E16.5 | E18.5 |
|---|---|---|---|---|---|---|---|
| n (dams) | 2 | 4 | 4 | 5 | 3 | 4 | 1 |
| n (embryos) | 10 | 20 | 20 | 21 | 15 | 20 | 5 |

Legend: 2N, 4N, 8N, 16N, 32N, 64N



Lower chart — Percentage (%) vs Embryonic age (line chart)

| | E11.5 | E12.5 | E13.5 | E14.5 | E15.5 | E16.5 | E18.5 |
|---|---|---|---|---|---|---|---|
| n (dams) | 2 | 4 | 4 | 5 | 3 | 4 | 1 |
| n (embryos) | 10 | 20 | 20 | 21 | 15 | 20 | 5 |

Legend: 2N, 4N, 8N, 16N, 32N, 64N
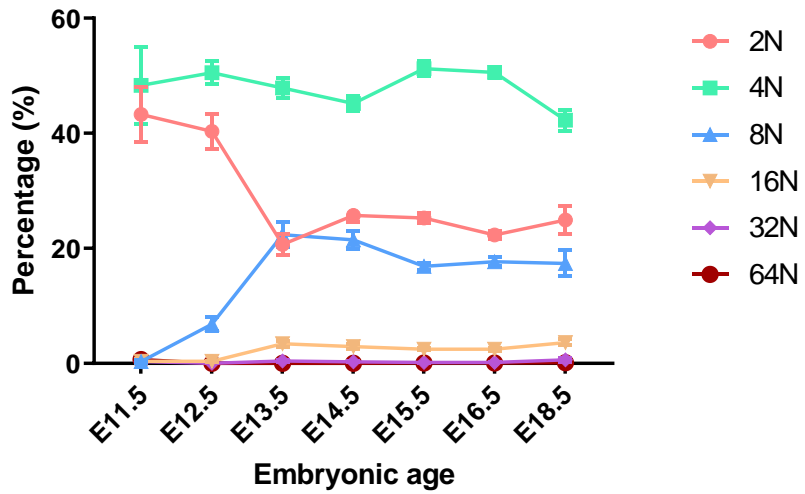
**Figure 3.16   Assessment of megakaryocytes ploidy during fetal liver development**

FL MK ploidy was measured across embryonic development. Development of different ploidy fractions is shown as bar graph (upper panel) and connected dots (lower panel) The 2N MK fraction was highest at E11.5 with 43.3 ± 4.9 % and decreased until E13.5 (20.7 ± 1.8 %) with stable fraction afterwards.

The 4N MK fraction was the dominant fraction at different embryonic age. At E11.5, the 4N MK fraction was 48.3 ± 6.6 %. The percentage stage stayed at similar level until E18.5. The 8N MK fraction was minor at E11.5 (0.3 ± 0.3 %) and increased to 6.8 ± 1.2 % at E12.5 and 22.4 ± 2.2 % at E13.5. The level kept stable afterwards.

The 16N MK took small proportion at E11.5 (0.4 ± 0.4 %) and E12.5 (0.4 ± 0.1 %). The fraction increased to 3.4 ± 0.5 % at E13.5 and was constant afterwards.

The 32N and 64N MK proportion was very small (less than 1%) throughout the whole embryo development.

The increase of 8N MK fraction paralleled with a decreased 2N fraction could hint to MK maturation over time in the FL.

The number of mother animals (dams) and embryos are noted below the graph.

## 3.2 Impact of c-Myb on embryonic thrombopoiesis

MKs in embryos originates from primitive hematopoiesis and definitive hematopoiesis. c-Myb homozygous deficient embryos are lack of primitive hematopoiesis. It is known that homozygous c-Myb -/- embryos are lethal at E15.5 due to severe anemia and hypoxia [43]. We applied c-Myb transgenic mouse model and checked platelet and MK levels at E14.5 to test the effect of primitive MKs absence.

### 3.2.1 Phenotype of c-Myb transgenic embryos
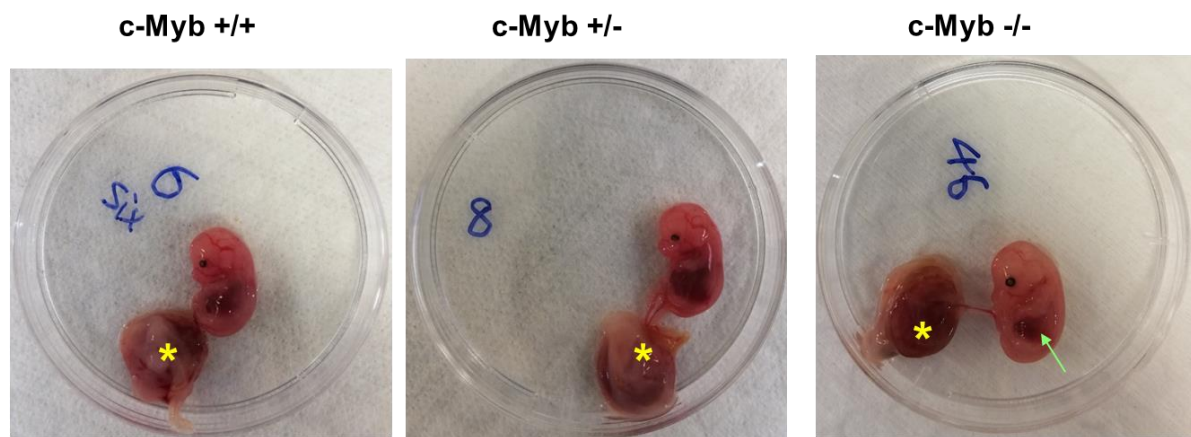


**Figure 3.17   Phenotype of c-Myb transgenic embryos**

Images of E14.5 embryos with different c-Myb transgene genotypes. Heterozygous c-Myb +/- male mice were time mated with heterozygous c-Myb +/- female mice to yield different genotypes in embryos. c-Myb +/+ (left) and heterozygous c-Myb +/- (center) embryos appear normal without signs of anemia. c-Myb -/- (right) are lacking definitive hematopoiesis with thus smaller fetal livers and therefore appear pale due to severe anemia.

(* yellow star) placenta

(→ green arrow) smaller fetal liver in c-Myb -/- embryos

### 3.2.2 Peripheral blood platelet count in dams and embryos with different c-Myb genotypes

**A**  **E14.5 embryonic blood platelet count**



| Genotype | BL6 | c-Myb +/+ | c-Myb +/- | c-Myb -/- |
|---|---|---|---|---|
| n (embryos) | 40 | 4 | 15 | 3 |

**B**  **G14.5 maternal blood platelet count**



| Genotype | BL6 | c-Myb +/- |
|---|---|---|
| n (dams) | 6 | 4 |
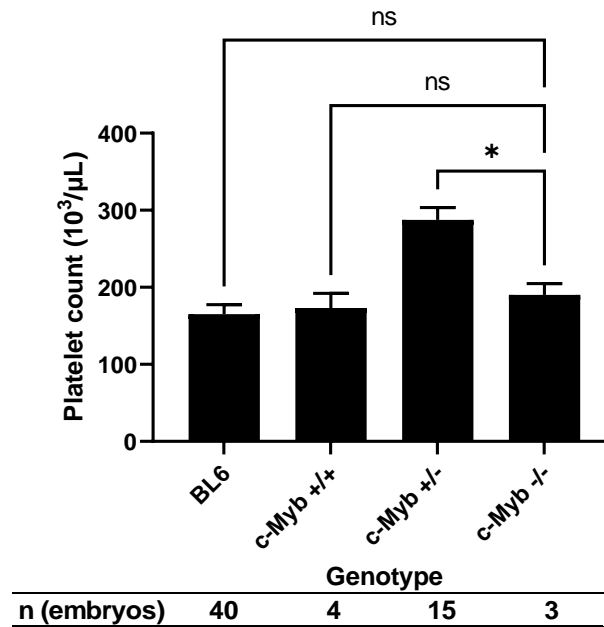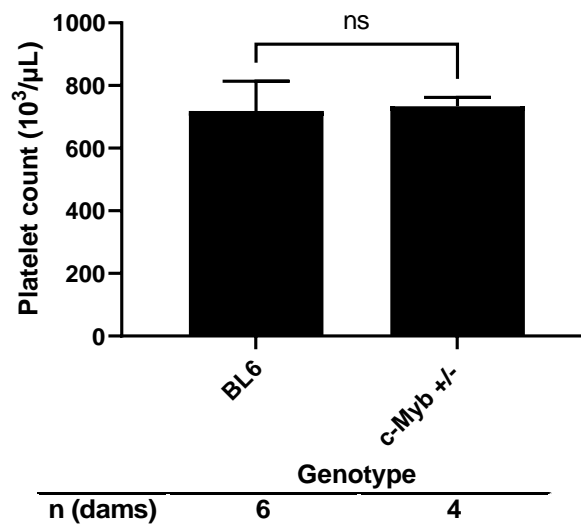
**Figure 3.18    Platelet count in c-Myb dams and embryos at E14.5**

We applied flow cytometry to check for differences in platelets and MKs numbers in mother animals with different c-myb genotypes and their respective embryos at E14.5: Homozygous c-Myb -/- embryos were compared to heterozygous c-Myb +/-, and c-Myb +/+ embryos. We define BL6 embryos dams as wildtype (WT) control. Our WT dams were compared to heterozygous c-Myb +/- dams. The analysis and gating strategy for platelets was used as previously described (see **Figure 3.1**).

Embryonic platelet count in c-Myb -/- embryos ($190.0 \pm 14.8 \times 10^3/\mu L$) was similar as c-Myb +/+ ($173.3 \pm 19.0 \times 10^3/\mu L$) and WT embryos ($165.3 \pm 12.3 \times 10^3/\mu L$), but significantly lower than heterozygous c-Myb +/- embryos ($287.3 \pm 16.1 \times 10^3/\mu L$, p=0.02) **(A)**. In contrast, maternal WT and c-Myb +/- peripheral platelet counts were comparable ($719.0 \pm 94.4 \times 10^3/\mu L$ vs $733 \pm 28.4 \times 10^3/\mu L$, p=0.91) **(B)**. The number of mother animals (dams) and embryos are noted below the graph.

### 3.2.3  Platelet size in dams and embryos with different c-Myb genotypes

**A**          **E14.5 platelet FSC-W in embryonic blood**



| n (embryos) | 40 | 4 | 15 | 3 |
|---|---|---|---|---|

**B**    **G14.5 platelet FSC-W in maternal blood**
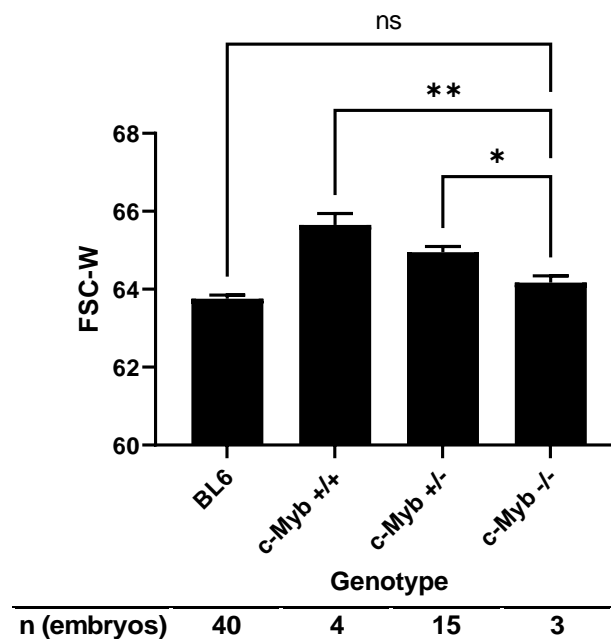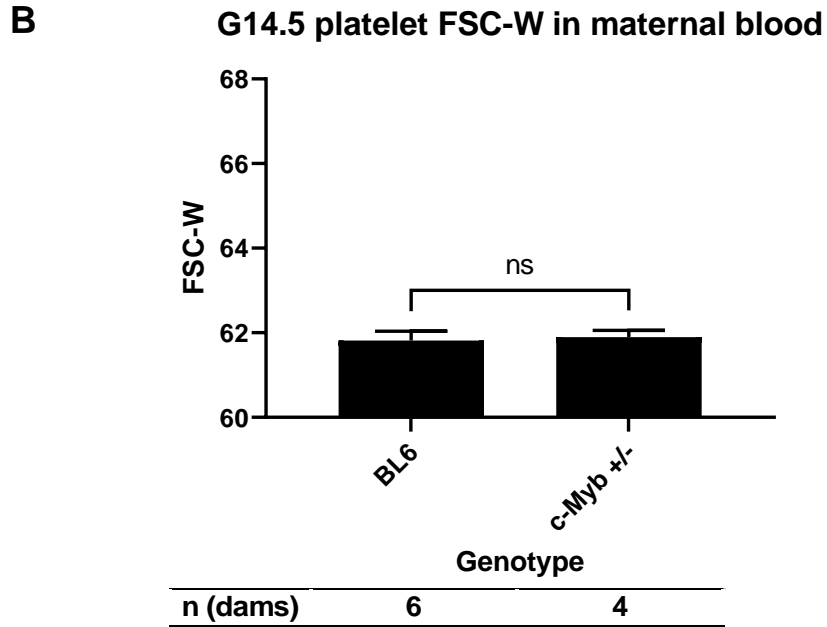


**Figure 3.19    Platelet forward scatter width in c-Myb dams and embryos at E14.5**

To compare platelet size in embryos with different c-Myb genetic background, we used the forward scatter width (FSC-W) parameter from flow cytometry analysis [83]. The platelet gating strategy was previously shown in **Figure 1.1**.

In c-Myb -/- embryos platelets showed a lower FSC-W (64.2 ± 0.3) as c-Myb +/- platelets (65.0 ± 0.6, p=0.04) and c-Myb +/+ platelets (65.7 ± 0.6, p=0.01). But it was similar with BL6 (WT) platelets (64.0 ± 1.5), indication no relevant impact on platelet size by c-myb **(A)**.

In c-Myb +/- maternal blood, the platelet presented almost identical FSC-W (61.8 ± 0.5) with BL6 mothers (61.8 ± 0.3), indicating similar platelet size **(B)**.

The number of mother animals (dams) and embryos are noted below the graph.

### 3.2.4 Reticulated platelet fraction in dams and embryos with different c-Myb genotypes

**A**     **E14.5 embryonic blood reticulated platelet fraction**



| n (embryos) | 26 | 4 | 15 | 3 |

**B**     **G14.5 maternal blood reticulated platelet fraction**



| n (dams) | 6 | 4 |
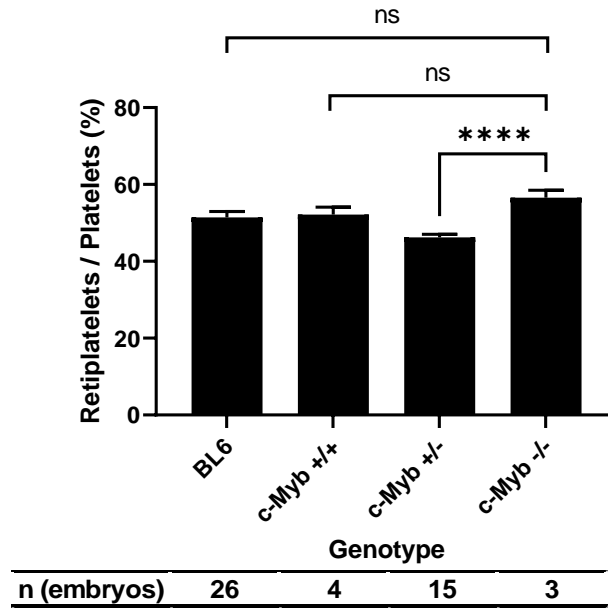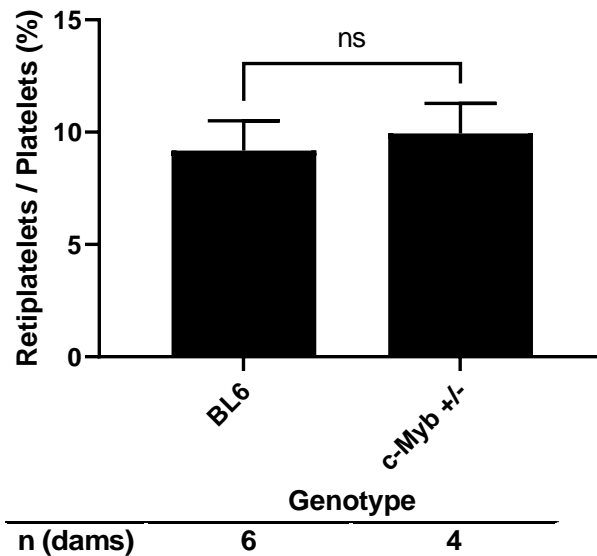
**Figure 3.20   Reticulated platelet fraction in c-Myb dams and embryos at E14.5**

Subsequently, we evaluated the fraction of reticulated platelets in embryos and dams with different c-Myb background. The analysis and gating strategy as previously described was used (see **Figure 3.5**).

The c-Myb -/- embryonic blood presented higher reticulated platelet fraction (56.5 ± 1.9 %) than c-Myb +/- embryonic blood (46.3 ± 0.8 %, p<0.0001), although it was similar with c-Myb +/+ (52.2 ± 1.9 %) and BL6 (51 ± 1.5 %) embryonic blood **(A)**.

The reticulated platelet fraction in c-Myb +/- maternal blood (9.9 ± 1.3 %) was also similar to the BL6 maternal blood (9.2 ± 1.3 %) **(B)**.

These results show that c-Myb does not seem to have a profound effect on reticulated platelet generation.

The number of mother animals (dams) and embryos are noted below the graph.

### 3.2.5 Reticulated platelet count in dams and embryos with different c-Myb genotypes

**A**      **E14.5 embryonic blood reticulated platelet count**



| n (embryos) | 26 | 4 | 15 | 3 |

**B**     **G14.5 maternal blood reticulated platelet count**



| | | |
|---|---|---|
| **n (dams)** | **6** | **4** |
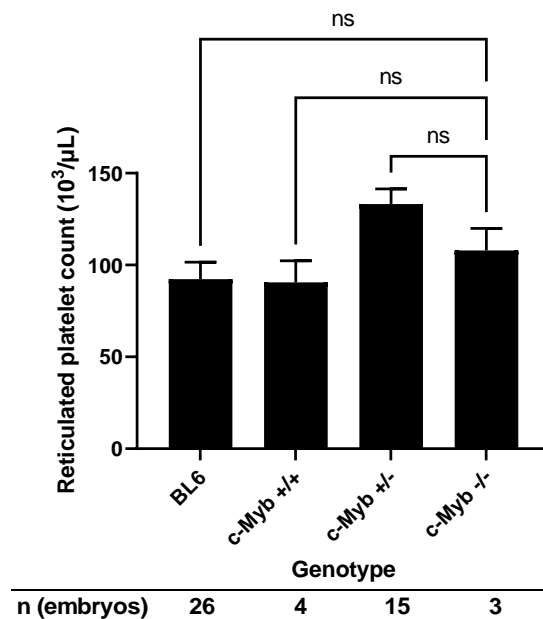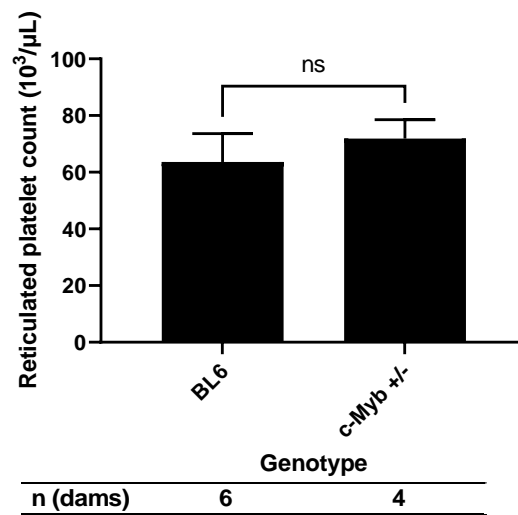
**Figure 3.21   Reticulated platelet count in c-Myb dams and embryos at E14.5**

The reticulated platelet count is calculated by multiplying the platelet count with the fraction of reticulated platelets.

In embryos **(A)**, there was no significant difference between c-Myb +/- (107.9 ± 12.1 x $10^3$/µL), c-Myb +/- (133.2 ± 8.2 x $10^3$/µL), c-Myb +/+ (90.6 ± 11.6 x $10^3$/µL) and BL6 (92.3 ± 9.4 x $10^3$/µL).

The c-Myb +/- dams' reticulated platelet count (63.3 ± 10.1 x $10^3$/µL) was similar with BL6 dams (71.9 ± 6.6 x $10^3$/µL) **(B)**.

The number of mother animals (dams) and embryos are noted below the graph.

## 3.2.6 Fetal liver cell numbers in embryos with different c-Myb genotypes



| n (embryos) | 26 | 4 | 15 | 3 |
|---|---|---|---|---|
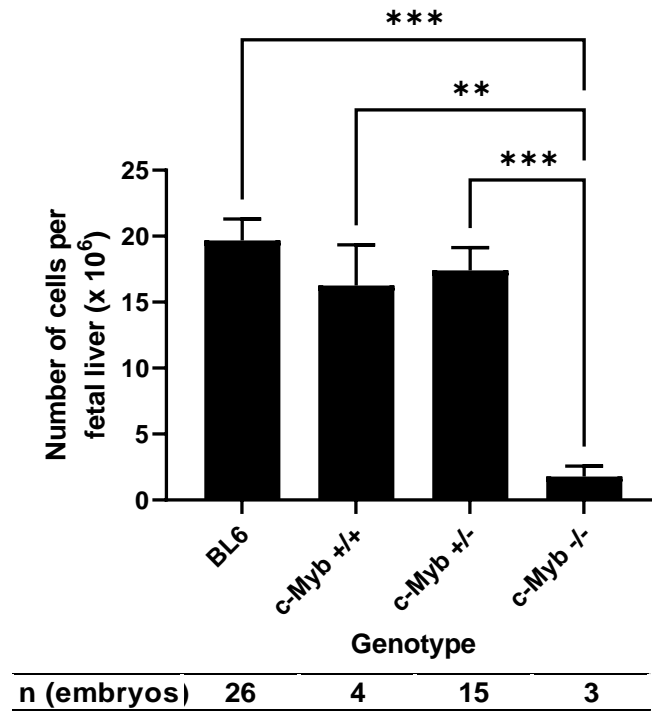
**Figure 3.22    Fetal liver cell numbers in c-Myb and BL6 embryos at E14.5**

As previously described, the fetal liver size of c-Myb -/- embryos is smaller due to the lack of definitive hematopoiesis, which contributes the majority of fetal liver cells during embryonic development. Thus, fetal liver cell counts were significantly lower in c-Myb -/- ($1.8 \pm 0.8 \times 10^6$ per fetal liver) than BL6 ($19.7 \pm 1.6 \times 10^6$ per fetal liver, p=0.0001), c-Myb +/+ ($16.3 \pm 3.1 \times 10^6$ per fetal liver, p=0.001) and c-Myb +/- ($17.4 \pm 1.7 \times 10^6$ per fetal liver, p=0.0001) embryos.

The number of embryos is noted below the graph. n (BL6 dams) =6, n (c-Myb +/- dams) = 4.

### 3.2.7 Megakaryocyte cell count in fetal liver of embryos with different c-Myb genotypes

**A**        **E14.5 megakaryocyte fraction in fetal liver**



| n (embryos) | 26 | 4 | 15 | 3 |
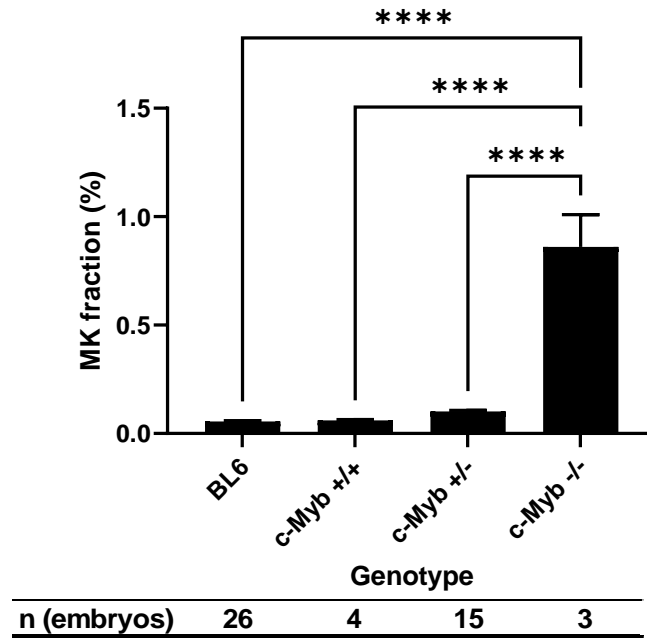
**B**        **E14.5 megakaryocyte number per fetal liver**



| n (embryos) | 26 | 4 | 15 | 3 |
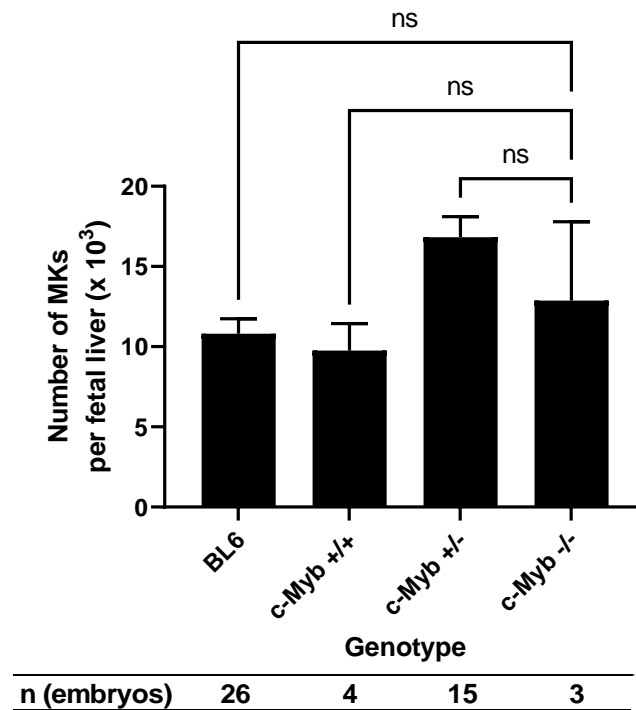
**Figure 3.23   Fetal liver megakaryocyte fraction and cell number in c-Myb and BL6 embryos at E14.5**

We used flow cytometry to quantify cell numbers and MKs in FL by staining with specific thrombopoietic surface markers CD41 and CD42d to detect MKs. A previously described analysis and gating strategy for MKs was used (see **Figure 3.11**).

c-Myb -/- embryos had a significantly higher FL MK fraction (0.86 ± 0.15 %) than BL6 (0.06 ± 0.00 %, p<0.0001), c-Myb +/+ (0.06 ± 0.00 %, p<0.0001) and c-Myb +/- (0.10 ± 0.01 %, p<0.0001) embryos **(A)**.

Total FL MK number was calculated by multiplying MK fraction with total FL cell count. c-Myb -/- embryos had comparable absolute MK numbers (12.8 ± 4.9 $\times 10^3$/FL) in their fetal liver as BL6 (10.8 ± 0.9 $\times 10^3$/FL), c-Myb +/+ (9.8 ± 1.7 $\times 10^3$/FL) and c-Myb +/- (16.8 ± 1.3 $\times 10^3$/FL) embryos **(B)**. These results suggest that MKs in c-Myb -/- FL are not less than other genotypes at E14.5.

The number of embryos are noted below the graph. n (BL6 dams) =6, n (c-Myb +/- dams) = 4.

## 3.2.8 Megakaryocyte size in fetal liver of embryos with different c-Myb genotypes



| n (embryos) | 26 | 4 | 15 | 3 |
| --- | --- | --- | --- | --- |
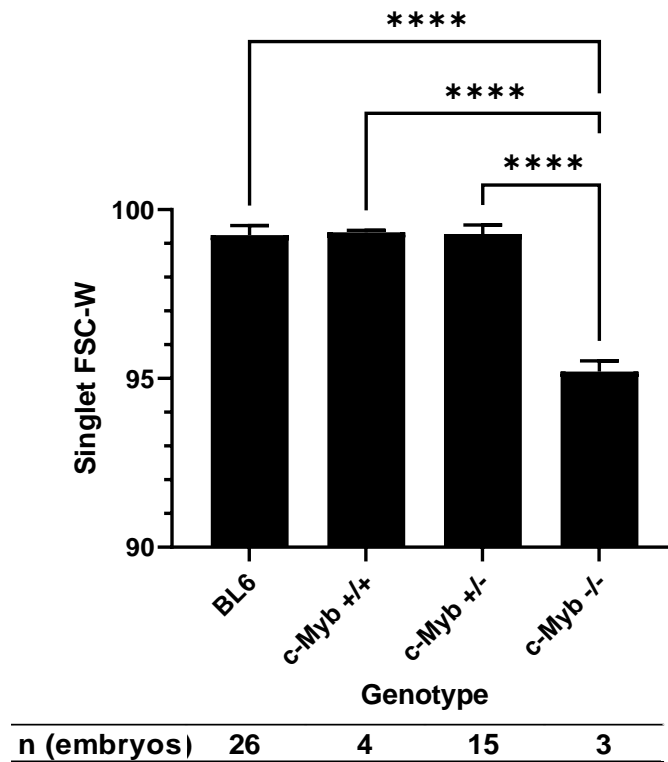
**Figure 3.24   Fetal liver megakaryocyte forward scatter width in c-Myb and BL6 embryos at E14.5**

The FSC-W of FL MK in c-Myb -/- (95.20 ± 0.56) was significantly smaller than c-Myb +/- (99.28 ± 1.03, p<0.0001), c-Myb +/+ (99.33 ± 0.12, p<0.0001) and BL6 FSC-W (99.24 ± 1.31, p<0.0001). This implies that MKs in the FL of in c-Myb -/- embryos could be smaller, representing potentially primitive, less mature MKs from a non-FL origin or primitive hematopoiesis.

The number of embryos are noted below the graph. n (BL6 dams) =6, n (c-Myb +/- dams) = 4.

### 3.2.9 Megakaryocyte ploidy in fetal liver of embryos with different c-Myb genotypes

**A**

**E14.5 MK ploidy fraction**



| n (embryos) | 26 | 4 | 15 | 3 |
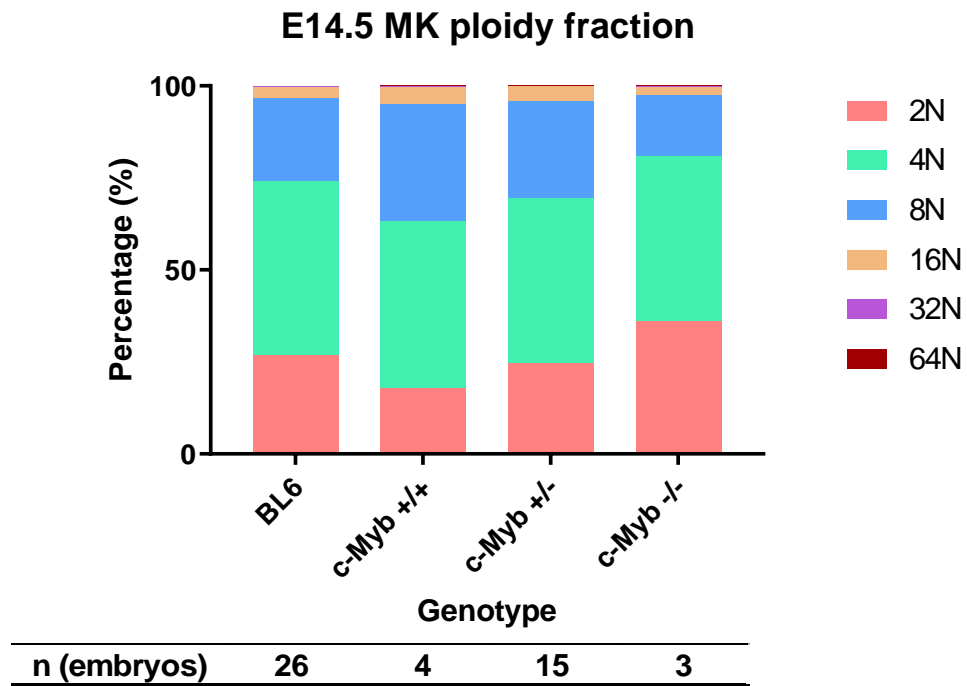
**B**

| | 2N+4N vs 8N+16N |
|---|---|
| c-Myb +/- | 69% vs 30% |
| c-Myb -/- | 80% vs 18% |
| p-value (Chi-square test) | 0.05 |

**Figure 3.25   Assessment of fetal liver megakaryocyte ploidy in c-Myb embryos at E14.5**

Ploidy was assessed with flow cytometry using propidium iodide staining of MKs. A previously described analysis and gating strategy was used (see **Figure 3.15**).

In all embryos **(A)**, the majority of MKs were we found to have 2N and 4N. The 2N fraction

was lowest in c-Myb +/+ MKs (17.7 ± 0.8 %) and highest in c-Myb -/- MKs (35.9 ± 17.9 %). The 4N fraction was similar across all groups (between 44.8 ± 7.0% and 45.5 ± 0.7 %). In contrast to 2N, the 8N fraction was lowest in c-Myb -/- MKs (16.8 ± 9.6 %) and highest in c-Myb +/+ (31.8 ± 0.5 %). The 16N fraction was low in all groups, ranging from 2.1 ± 1.2 % to 4.5 ± 0.3 %. The 32N and 64N fraction was very small (less than 1%) in all groups.

Therefore, we observed a strong trend that c-Myb -/- embryos contained MKs with lower ploidy than c-Myb +/- and c-Myb +/+ embryos **(B)**. This could represent a population of primitive MKs from a non-fetal liver origin or primitive hematopoiesis.

Parts of the litter were used. Average number of WT and c-Myb embryos in this experiment per dam was 3.5 and 5.5 embryos. The number of embryos are noted below the graph. n (BL6 dams) =6, n (c-Myb +/- dams) = 4.

To conclude, even though c-Myb -/- embryos had smaller FL size and lower FL cell numbers, they presented similar level of platelets and their reticulated forms in peripheral blood. This could be explained by their similar absolute FL MK numbers compared with the BL6 or c-Myb +/- embryos. These results confirmed that c-Myb has a strong impact on definitive hematopoiesis, but showed that the role of c-Myb role for thrombopoiesis is less important as potentially primitive thrombopoiesis is capable of producing sufficient platelet numbers, therefore compensating any decrease or failure of definitive thrombopoiesis. Furthermore, the FL contained smaller MKs with less ploidy, which could represent primitive thrombopoiesis taking place also in the fetal liver at E14.5.

## 3.3 Impact of NFE2 on embryonic thrombopoiesis

Transgenic NFE2-deficient mice are an established model for studying thrombopoiesis and has been used in embryonic settings[49]. The transcription factor NFE2 is mainly involved in thrombopoiesis and megakaryocyte differentiation. Homozygous NFE2 -/- mice lack peripheral blood platelets and can die of hemorrhage. Less than 10% of the live born homozygotes NFE2 -/- survive to adulthood, and surviving neonates are smaller than littermates. Thus, the majority of NFE2 -/- mice die already in the perinatal or neonatal period as a consequence of hemorrhage [58]. Adult homozygous NFE2-/- knock-out mice show severely impaired platelet production [49, 88].    The major role of NFE2 is regulating MK maturation and biogenesis of platelets. Here, we investigated the platelets and MKs in embryo at E14.5 to clarify the effect of NFE2 on embryonic thrombopoiesis.

### 3.3.1 Phenotype of NFE2 transgenic embryos
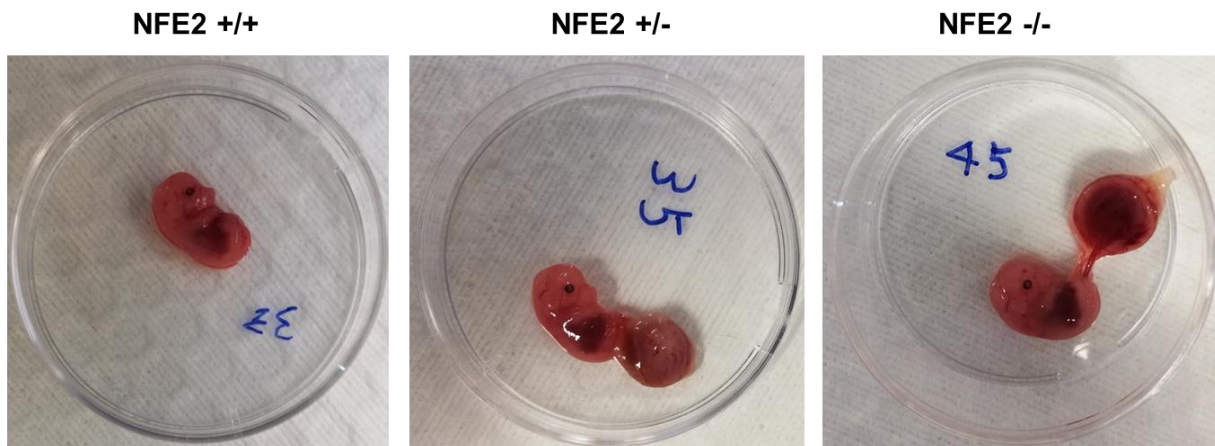


**Figure 3.26    Phenotype of NFE2 transgenic embryos**

Heterozygous NFE2 +/- male mice were time mated with NFE2 +/- female mice. Images of E14.5 embryos of NFE2 +/+ (left), NFE2 +/- (center) and NFE2 -/- (right) genetic background are shown. Outward appearance of these different genotypes seems to be comparable, particularly erythropoiesis in NFE2 -/- embryo is probably not severely affected [58].

## 3.3.2 Peripheral blood platelet count in dams and embryos with different NFE2 genotypes

**A**

**E14.5 embryonic blood platelet count**



| | | | | |
|---|---|---|---|---|
| n (embryos) | 40 | 6 | 17 | 7 |

**B**

**G14.5 maternal blood platelet count**



| | | |
|---|---|---|
| n (dams) | 6 | 6 |
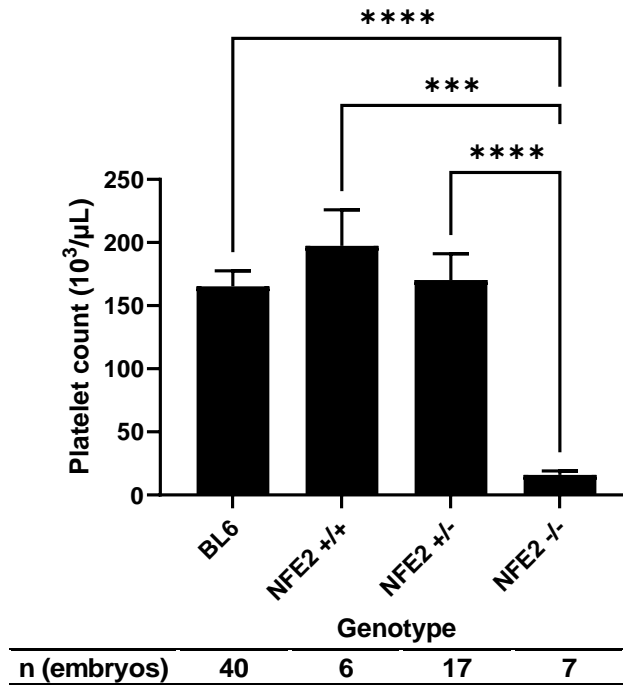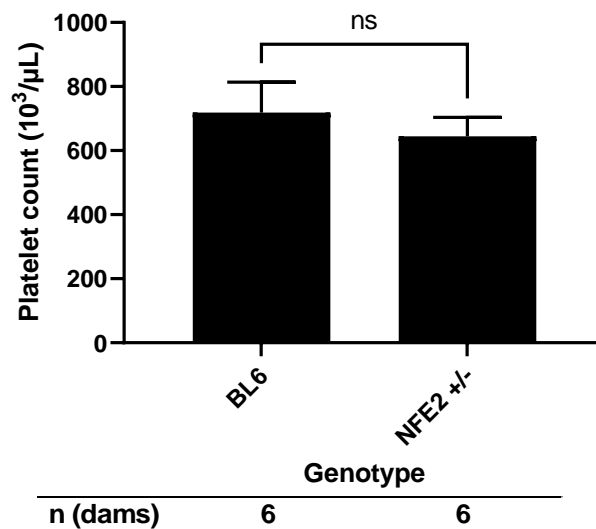
**Figure 3.27   Platelet count in NFE2 embryos and dams at E14.5**

We applied flow cytometry for the evaluation of embryonic platelet numbers in E14.5 embryos with different genetic backgrounds of NFE2. The gating strategy from previous flow cytometry experiments for platelet identification and quantification was used (see **Figure 3.1**).

In E14.5 embryos **(A)**, NFE2 -/- resulted in severe thrombocytopenia with very low platelet counts (15.9 ± 3.2 $\times10^3$/µL). In contrast, NFE2 +/+ (197.4± 28.6 $\times10^3$/µL) and heterozygous NFE2 +/- littermates (170.3 ± 20.9 $\times10^3$/µL) had normal platelet counts compared to BL6 controls.

As for the dams **(B)**, heterozygous NFE2 +/- mother animals showed comparable platelet counts to BL6 mother mice (719.0 ± 94.4 $\times 10^3$/µL vs. 644.6 ± 58.8 $\times10^3$/µL, p=0.54).

The number of mother animals (dams) and embryos are noted below the graph.

### 3.3.3   Platelet size in dams and embryos with different NFE2 genotypes

**A**          **E14.5 platelet FSC-W in embryonic blood**



| | BL6 | NFE2 +/+ | NFE2 +/- | NFE2 -/- |
|---|---|---|---|---|
| **n (embryos)** | 40 | 6 | 17 | 7 |

**B**

### G14.5 platelet FSC-W in maternal blood



| | | |
|---|---|---|
| **n (dams)** | **6** | **6** |
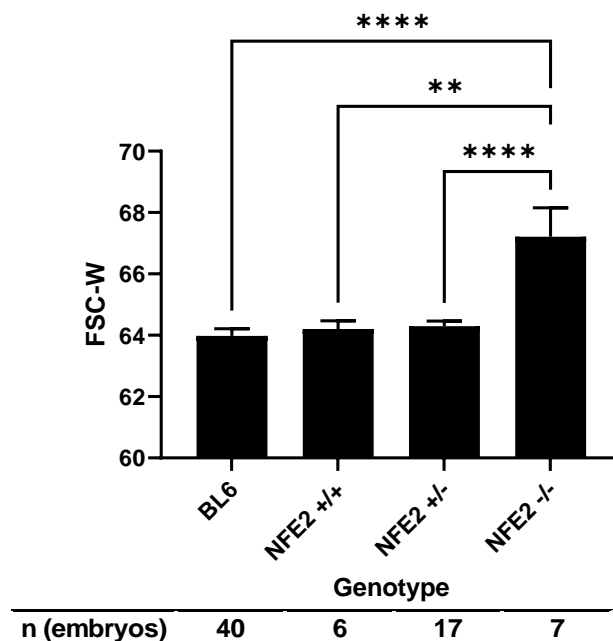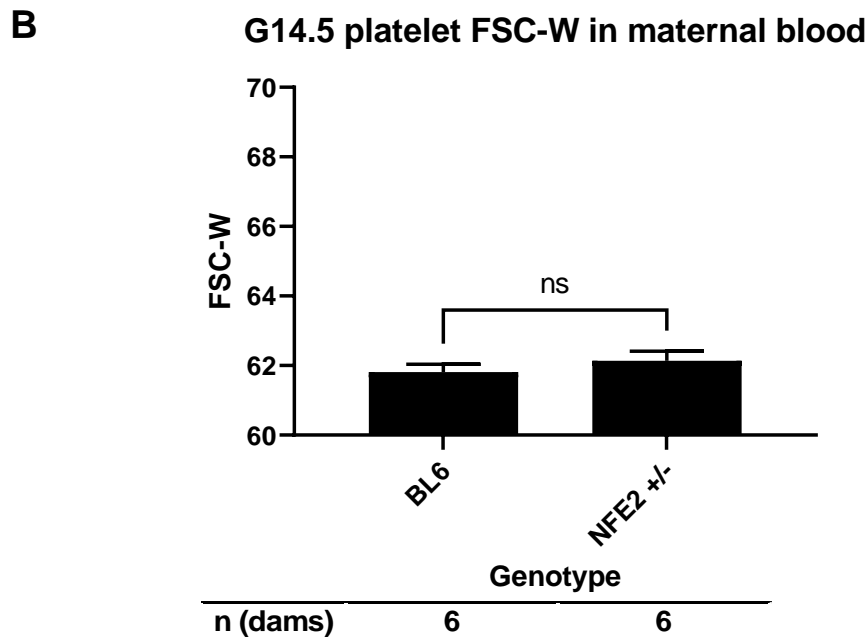
**Figure 3.28   Platelet forward scatter width in NFE2 embryos and dams at E14.5**

To compare platelet size in embryos with different NFE2 genetic background, we used the forward scatter width (FSC-W) parameter from flow cytometry analysis [83, 89]. NFE2 -/- platelets showed a significantly higher FSC-W (67.2 ± 0.9) than heterozygous NFE2 +/- platelets (64.3 ± 0.2), NFE2 +/+ platelets (64.2 ± 0.3), or BL6 embryonic platelets (64.0 ± 0.2) **(A)**. This indicates that NFE2 -/- platelets are larger than their counterparts in WT or heterozygous embryos.

In NFE2 +/- maternal blood, platelets presented similar FSC-W (62.1 ± 0.3) compared with BL6 (61.8 ± 0.2) **(B)**.

The number of mother animals (dams) and embryos are noted below the graph.

### 3.3.4 Reticulated platelet fraction in dams and embryos with different NFE2 genotypes

**A**     **E14.5 embryonic blood reticulated platelet fraction**



| n (embryos) | 26 | 4 | 18 | 7 |

**B**     **G14.5 maternal blood reticulated platelet fraction**



| n (dams) | 6 | 6 |
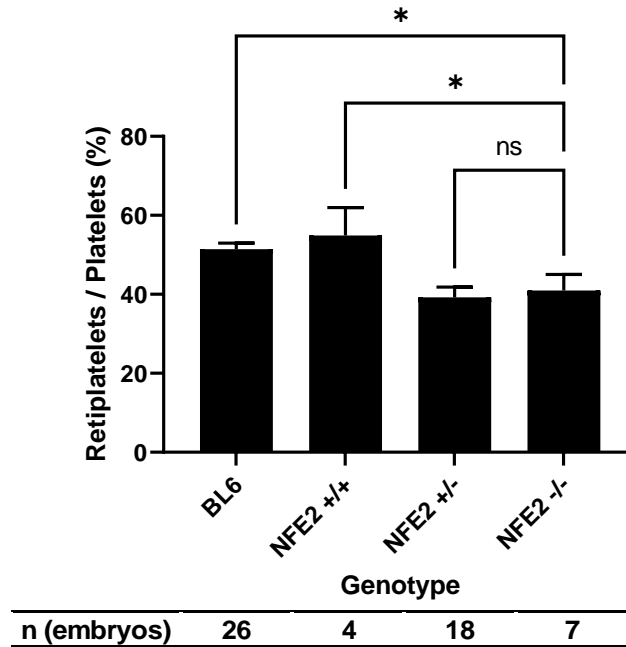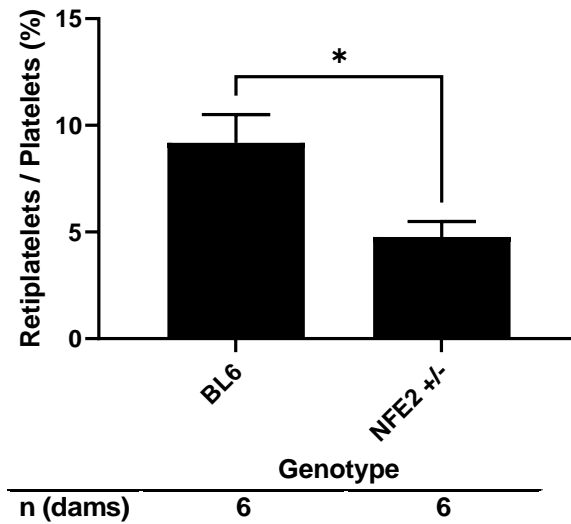
**Figure 3.29    Reticulated platelet fraction in NFE2 embryos and dams at E14.5**

We measured reticulated platelet fraction by flow cytometry as previously described (see **Figure 3.5**). Heterozygous NFE2 +/- embryos displayed similar reticulated platelet fraction (39.2 ± 11.0 %) compared with homozygous NFE2 -/- embryos (41.0 ±10.8 %). In contrast, BL6 (51.4 ± 7.7 %, p=0.01) or NFE2 +/+ embryos (54.9 ± 14.2 %, p=0.02) showed a higher reticulated platelet fraction at E14.5 **(A)**.

Also, heterozygous NFE2 +/- mother animals showed a reduced reticulated platelet fraction compared to BL6 mother animals (9.2 ± 3.2 % vs. 4.8 ±1.6 %, p=0.02) **(B)**.

The number of mother animals (dams) and embryos are noted below the graph.

### 3.3.5 Reticulated platelet count in dams and embryos with different NFE2 genotypes



**A**  **E14.5 embryonic blood reticulated platelet count**

| n (embryos) | 26 | 4 | 18 | 7 |
|---|---|---|---|---|

**B**       **G14.5 maternal blood reticulated platelet count**



| n (dams) | 6 | 6 |
|---|---|---|
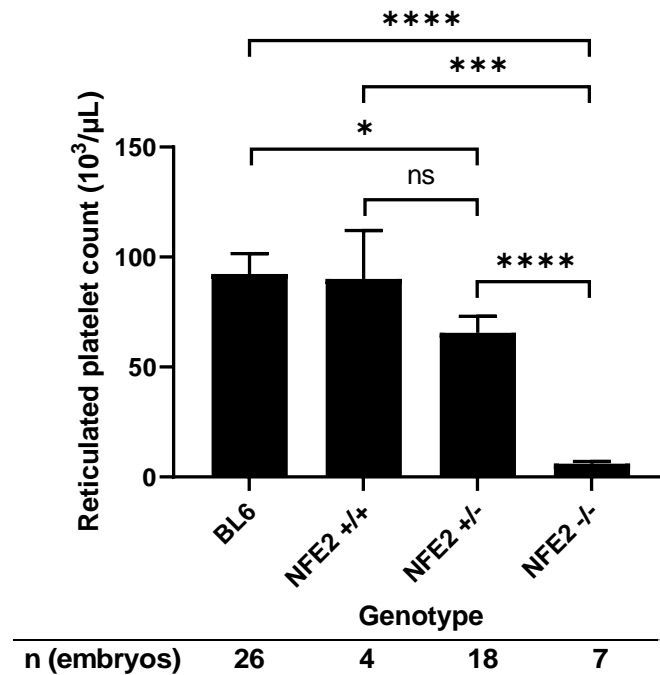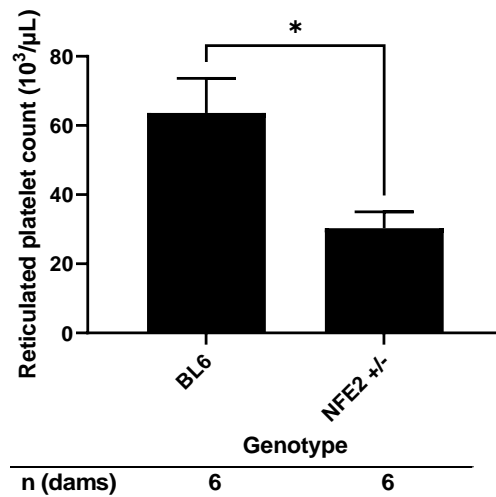
**Figure 3.30    Reticulated platelet count in NFE2 dams and embryos at E14.5**

The reticulated platelet count was calculated by multiplying the overall platelet count with the fraction of reticulated platelets. As NFE2 -/- embryos were severely thrombopenic, reticulated platelet count was very low ($6.0 \pm 1.1$ x$10^3$/µL) compared to NFE2 +/- ($65.6 \pm 7.5$ x$10^3$/µL, $p<0.0001$), NFE2 +/+ ($90.1 \pm 22.0$ x$10^3$/µL, $p=0.0002$), and BL6 embryos ($92.3 \pm 9.4$ x$10^3$/µL, $p<0.0001$). NFE2 +/- embryos showed no significant difference with NFE2 +/+ embryos in reticulated platelet count ($p=0.24$), but it was significantly lower than that in BL6 embryos ($p=0.04$) **(A)**.

For maternal blood and in accordance with the results from the previous fraction analysis, the NFE2 +/- reticulated platelet count ($30.3 \pm 4.7$ x$10^3$/µL) was significantly lower than in WT mice ($63.6 \pm 10.1$ x$10^3$/µL, $p=0.02$) **(B)**.

The number of mother animals (dams) and embryos are noted below the graph.

The analysis of reticulated platelets in NFE2 embryos shows that NFE2 could also have a gene dose dependent impact on the generation of reticulated platelets. Already in heterozygous embryos or dams, the fraction and count of reticulated platelets is lower than in WT animals.

## 3.3.6 Fetal liver cell number in embryos with different NFE2 genotypes
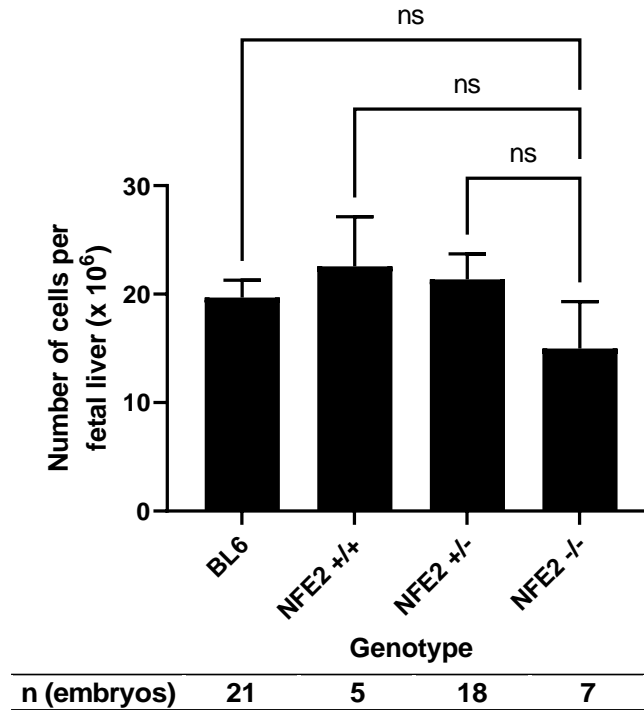


**Figure 3.31    Fetal liver cell number in NFE2 and BL6 embryos at E14.5**

As we have already shown in a previous figure **(Figure 3.31)**, the fetal liver of NFE2 -/- embryos was similar in size compared with NFE2 +/- and NFE2 +/+ embryos. Accordingly, the NFE2 -/- fetal liver cell counts (15.0 ± 4.3 x10$^6$ per fetal liver) were also comparable with NFE2 +/- (21.4 ± 2.4 x10$^6$ per fetal liver), NFE2 +/+ (22.6 ± 4.6 x10$^6$ per fetal liver) and BL6 (19.7 ± 1.6 x10$^6$ per fetal liver). This could suggest that hematopoietic lineages beyond thrombopoiesis are not severely affected by NFE2 depletion.

The number of embryos are noted below the graph. n (BL6 dams) =6, n (NFE2 +/- dams) = 6.

### 3.3.7 Megakaryocyte cell count in fetal liver of embryos with different NFE2 genotypes

**A**  **E14.5 megakaryocyte fraction in fetal liver**



| n (embryos) | 21 | 5 | 18 | 7 |
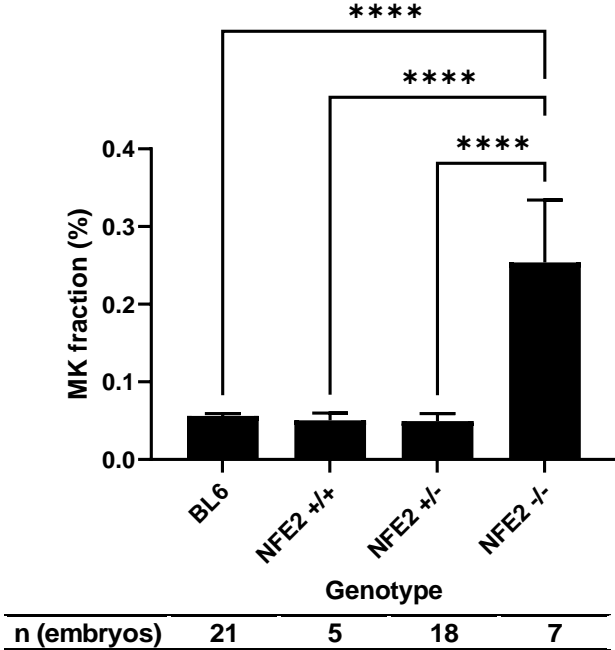
**B**  **E14.5 megakaryocyte numbers per fetal liver**



| n (embryos) | 21 | 5 | 18 | 7 |
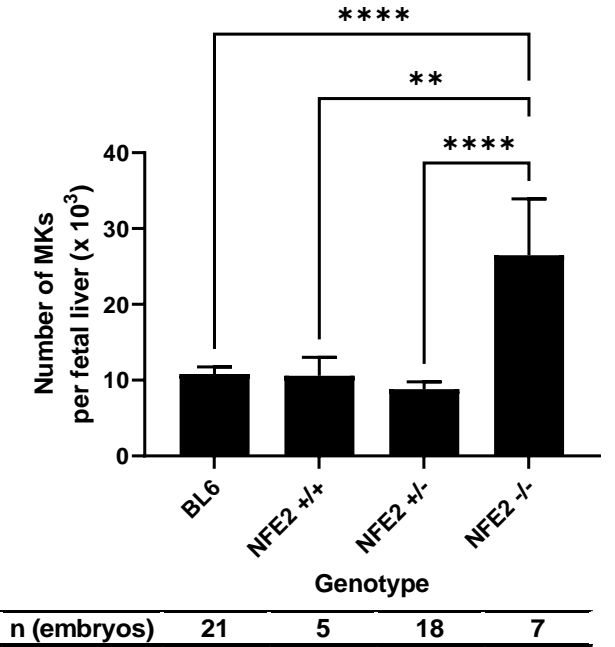
**Figure 3.32   Fetal liver megakaryocyte fraction and cell number in NFE2 and BL6 embryos at E14.5**

We used flow cytometry to quantify cell numbers and MKs in FL by staining with specific thrombopoietic surface markers CD41 and CD42d. A previously described analysis and gating strategy for MKs was used (see **Figure 3.11**). NFE2 -/- embryos showed a significantly higher FL MK fraction (0.25 ± 0.1 %) than NFE +/- (0.05 ± 0.01 %), NFE2 +/+ (0.05 ± 0.01 %) and BL6 (0.06 ± 0.0 %) groups **(A)**. In line with the previous observation of MK fraction, the absolute MK number was higher in NFE2 -/- embryos (26.5 ± 7.4 x $10^3$) than heterozygous NFE2 +/- (8.8 ± 1.0 x $10^3$), NFE2 +/+ (10.6 ± 2.4 x $10^3$) and BL6 (10.8 ± 0.9 x $10^3$) embryos **(B)**.

Parts of the litters were used. Average number of BL6 and NFE2 embryos in this experiment per dam was 4.3 and 5.2 embryos, respectively. The number of embryos are noted below the graph. n (BL6 dams) =6, n (NFE2 +/- dams) = 6.

## 3.3.8 Megakaryocyte size in fetal liver of embryos with different NFE2 genotypes



| n (embryos) | 21 | 5 | 18 | 7 |
|---|---|---|---|---|
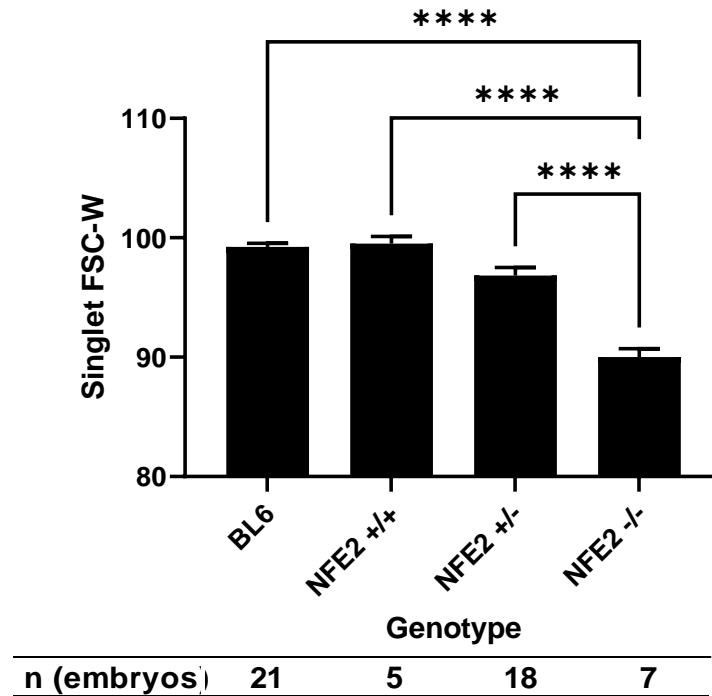
**Figure 3.33 Fetal liver megakaryocyte forward scatter width in NFE2 and BL6 embryos at E14.5**

The fetal liver MK FSC-W in NFE2 -/- (90.0 ± 0.7) was significantly smaller than NFE2 +/- (96.9 ± 0.6), NFE2 +/+ (99.5 ± 0.6) and WT (99.2 ± 0.3). Parts of the litters were used. Average number of BL6 and NFE2 embryos in this experiment per dam was 4.3 and 5.2 embryos, respectively. The number of embryos are noted below the graph. n (BL6 dams) =6, n (NFE2 +/- dams) = 6.

### 3.3.9 Megakaryocyte ploidy in fetal liver of embryos with different NFE2 genotypes

**A**

**E14.5 MK ploidy distribution**



| n (embryos) | 21 | 5 | 18 | 7 |
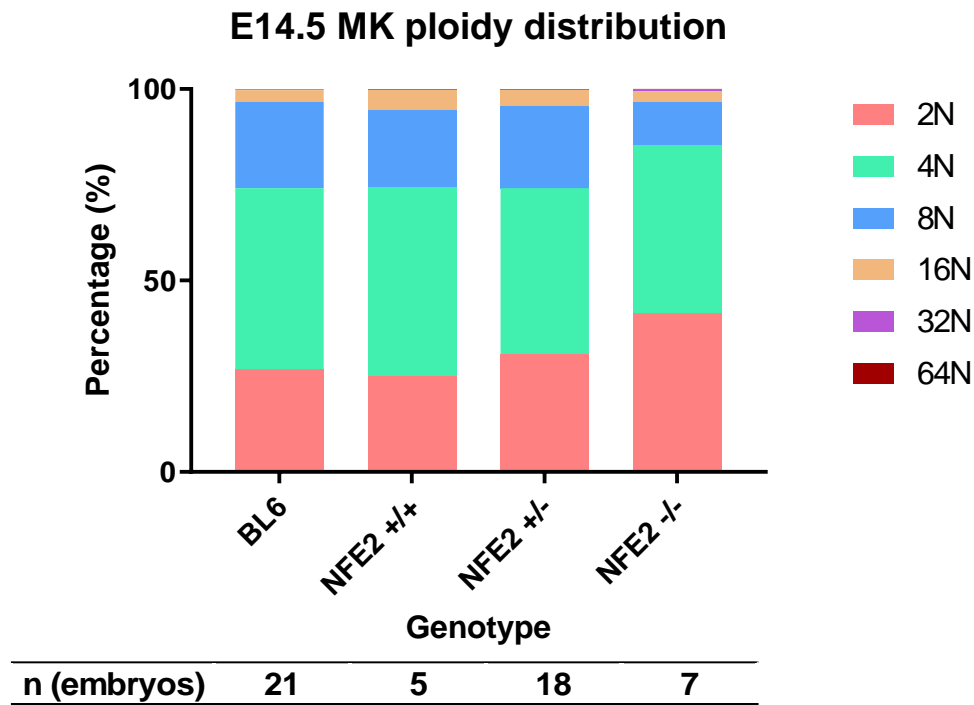
**B**

| | 2N+4N vs 8N+16N |
|---|---|
| NFE2 +/- | 74% vs 25% |
| NFE2 -/- | 85% vs 14% |
| p-value (Chi-square test) | 0.04 |

**Figure 3.34    Assessment of fetal liver megakaryocyte ploidy in NFE2 embryos at E14.5**

MK ploidy was assessed with flow cytometry using propidium iodide staining of MKs. A previously described analysis and gating strategy was used (see **Figure 3.15**). Across all genotypes, the majority of FL MKs had 4N ploidy **(A)**. There was a significantly higher

fraction of 2N MKs in NFE2 -/- (41.34 ± 16.23 %) compared with NFE2 +/- (30.69 ± 6.11 %), NFE2 +/+ (24.85 ± 2.41 %) and WT (25.70 ± 5.31 %) (p=xxx). The fraction of 4N MKs in NFE2 -/- (43.91± 13.97 %) was similar to NFE2 +/- (43.46 ± 6.08 %), NFE2 +/+ (49.43 ± 4.81 %) and WT (45.18 ± 5.85 %). In contrast, the fraction of 8N MKs in NFE2 -/- (11.32 ± 4.05 %) was significantly lower than NFE2 +/- (21.39 ± 6.75 %), NFE2 +/+ (20.29 ± 4.57 %) and WT (21.48 ± 7.03 %) (p=xx). The 16 n MK fraction in NFE2 -/- (2.92 ± 1.37 %) was again comparable with NFE2 +/- (3.99 ± 2.13 %), NFE2 +/+ (5.11 ± 2.88 %) and WT (2.97 ± 1.88 %). In NFE2 -/-, the combined fraction of 2N+4N was 85% and 8N+16N was 14%, which represented a significantly different proportion than NFE2 +/-.

The number of embryos is noted below the graph. n (BL6 dams) =6, n (NFE2 +/- dams) = 6.

To conclude, even though NFE2 -/- embryos were severely thrombocytopenic, they had higher fetal liver MK counts with smaller MK size and less ploidy than their BL6 or NFE2 +/- counterparts. In NFE2 -/- embryos, there seems to be a larger fraction of immature MKs compared to NFE2 +/-. These results confirm that NFE2 has a strong impact on platelet production, probably by impairing MK maturation.

## 3.4 Multiphoton intravital microscopy imaging revealed different patterns of embryonic thrombopoiesis in yolk sac and fetal liver

There is yet no visual method in live embryos to show how platelet is generated and how MKs are shedding. Here, we developed a protocol for intravital visualization of embryonic thrombopoiesis over time by multiphoton intravital microscopy (MP-IVM) in Rosa 26 mTmG x Pf4 Cre embryos. We imaged platelet generation from MKs in the yolk sac (YS) and fetal liver (FL) identifying various types of proplatelets at different stages of embryonic development. Exceeding image acquisition technology enabled direct visualization of platelet production from MKs into blood circulation in the three-dimensional environment of the fetal liver over time (four-dimensional measurement). After analyse our video data, we summarized the MK characters as well as shedding pattern in embryos.

### 3.4.1 MP-IVM for imaging of yolk sac and fetal liver structures and thrombopoiesis



Green cells: MK progenitors, MKs and platelets
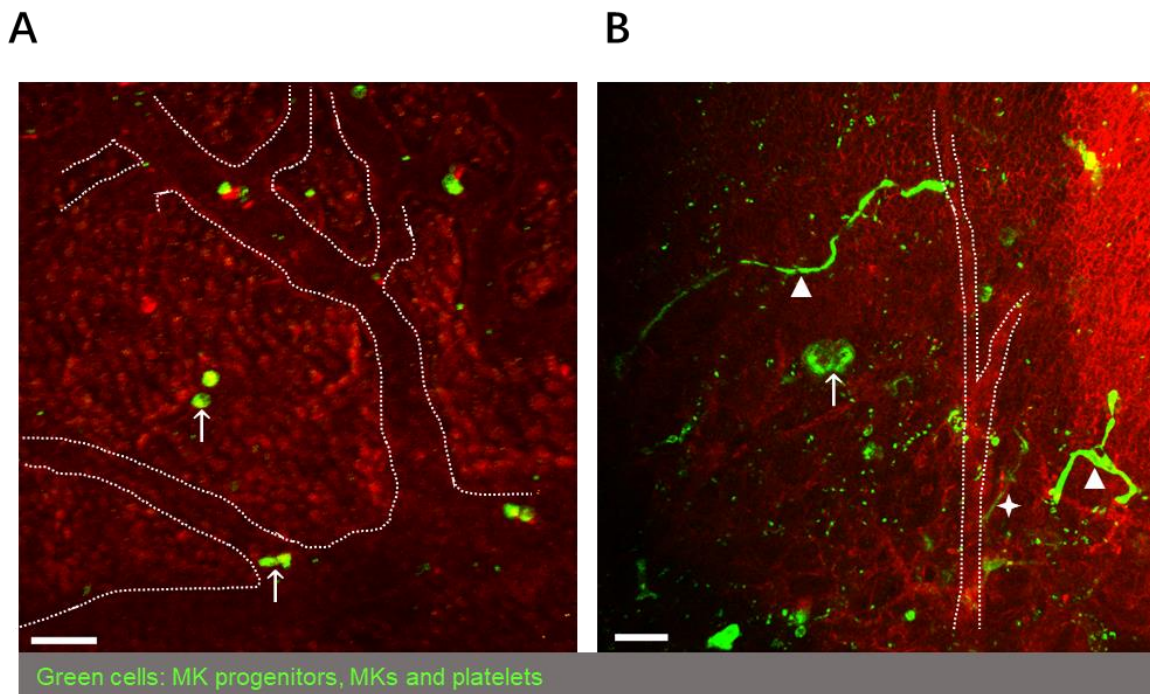
**Figure 3.35   Representative examples of different megakaryocyte morphologies in yolk sac and fetal liver**

Multiphoton intravital microscopy (MP-IVM) was applied for real-time imaging of YS and FL. Optical section from a 3D z-projection of YS (**A**, E10.5, scan depth: 25.5 μm) and FL (**B**, E14.5, scan depth: 57 μm).

Symbols: white ↑, MK; white ▲, MKs with large protrusion; white ✦, proplatelet. Dashed line represents main vessel wall. Bar, 50 μm.

MP-IVM showed parenchymal and vascular structures as well as cells of YS and FL. MKs presented with different sizes and morphologies, and were distributed intravascular and extravascular. Some MKs extended long protrusions or multiple mid-size protrusions, whereas some MKs were circular without protrusion.

For YS imaging, we applied MP-IVM on embryos at E10.5 and E11.5. For FL imaging, we applied MP-IVM on embryos from E13.5 to E15.5. Subsequently, we quantified the size and morphology of YS and FL MKs.

## 3.4.2 Analysis of megakaryocyte size by multiphoton intravital microscopy



| | | Yolk sac | | Fetal liver | |
| --- | --- | --- | --- | --- | --- |
| n (dams) | 8 | 6 | 6 | 7 | 6 |
| n (embryos) | 22 | 9 | 13 | 14 | 12 |
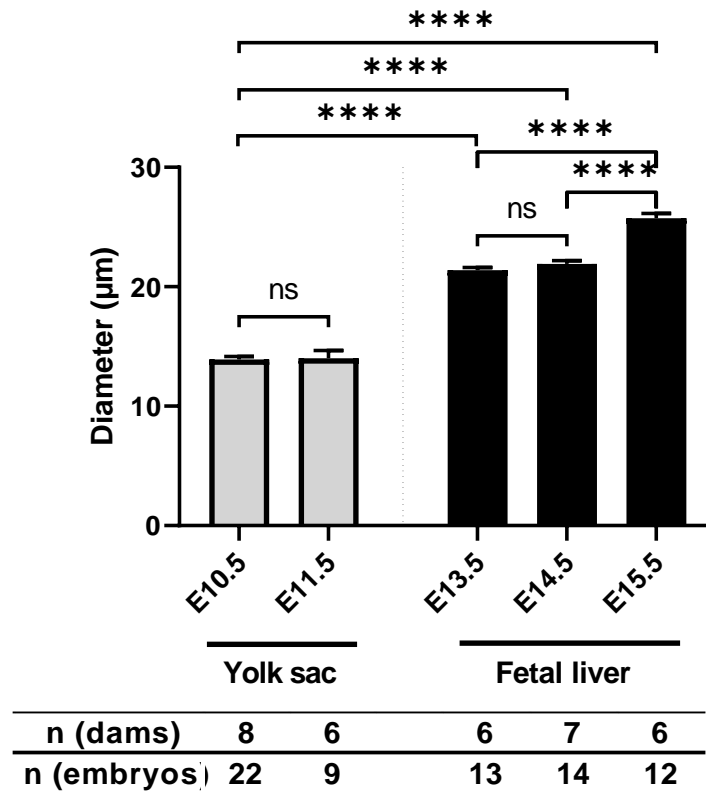
**Figure 3.36   Megakaryocyte size in yolk sac and fetal liver**

From MP-IVM datasets of live imaging, we measured the size of GFP+ cells with the largest diameter > 7 μm. GFP+ cells represent the megakaryocytic lineage due expression of GFP+ under the specific control of the thrombopoietic-lineage reporter system PF4-Cre. In YS, the diameter of MKs was 13.9 ± 0.2 μm at E10.5, which was similar with that at E11.5 (14.0 ± 0.7 μm). In FL at E13.5, MK diameter was 21.4 ± 0.2 μm. This was comparable to E14.5 (21.9 ± 0.3 μm). At E15.5, FL MK were significantly larger (25.7 ± 0.4 μm). Overall, MKs were smaller in YS than in FL by MP-IVM.

The number of dams and embryos are noted below the graph.

### 3.4.3 Quantification of yolk sac and fetal liver megakaryocyte concentration by multiphoton intravital microscopy
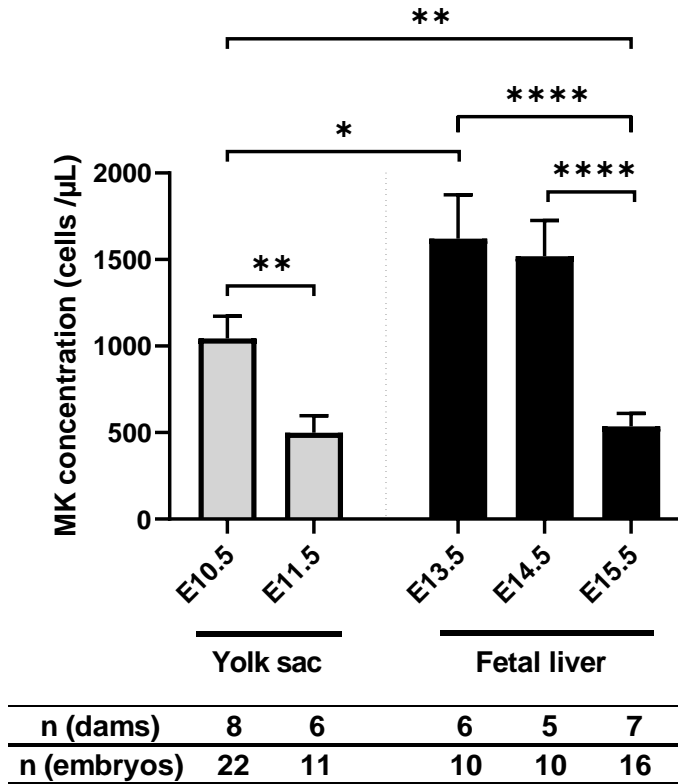


**Figure 3.37    Megakaryocyte concentration in yolk sac and fetal liver**

We measured the number of MKs per µL of imaged 3D dataset from MP-IVM. In YS, there were more MKs at E10.5 (1045 ± 128 cells per µL) than E11.5 (499 ± 93 cells per µL, p=0.009).

In FL, MK density decreasing from E13.5 (1621 ± 252 cells per µL) to E14.5 (1519 ± 207 cells per µL) and E15.5 (535 ± 76 cells per µL, p <0.0001). This decrease of MK concentration was consistent with our findings in flow cytometry for both YS and FL.

The number of dams and embryos are noted below the graph.

**3.4.4 Different forms of platelet shedding from embryonic megakaryocytes: Proplatelet formation and membrane budding**

**A**



**B**
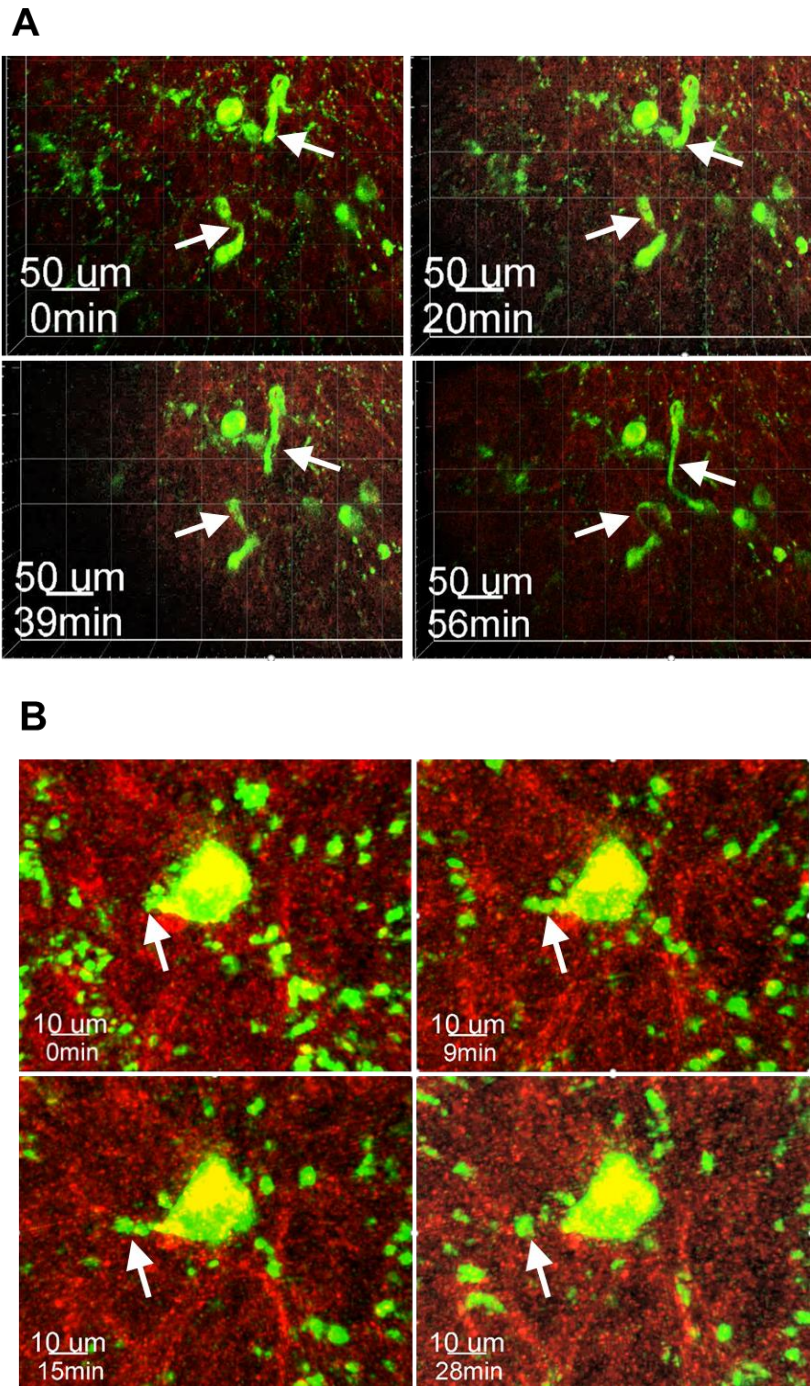


**Figure 3.38    Representative images of proplatelet formation and membrane budding from embryonic megakaryocyte**

We observed two distinct forms of platelet shedding from MKs by MP-IVM: As expected, MKs showed conventional proplatelet formation by extending long membrane particles into the vasculature **(A)**. Detailed observation of resting MKs revealed a different from of platelet generation by expelling smaller particles without long proplatelet formation, which we termed membrane budding **(B)**. These representative images are obtained from FL at E15.5 by MP-IVM.

### 3.4.5 Prevalence of membrane bud formation and proplatelet formation of yolk sac and fetal liver megakaryocytes
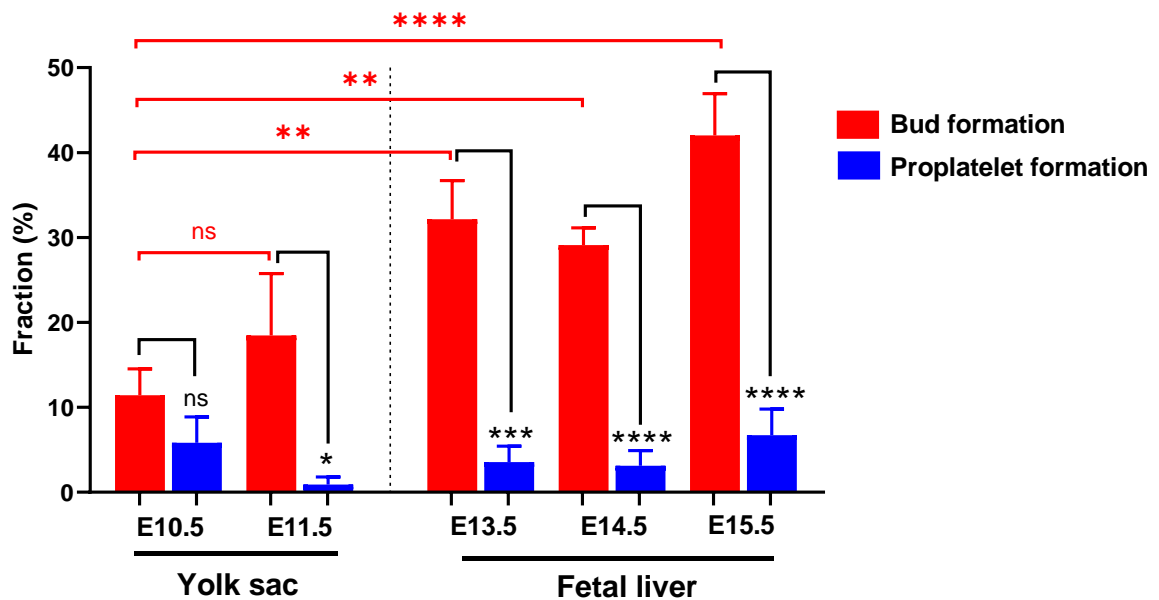


| n (dams) | 7 | 5 | 5 | 4 | 5 |
|---|---|---|---|---|---|
| n (embryos) | 17 | 8 | 9 | 7 | 9 |
| n (MKs) | 171 | 54 | 151 | 137 | 101 |

**Figure 3.39   Prevalence of membrane bud formation and proplatelet formation of yolk sac and fetal liver megakaryocytes**

Using MP-IVM, we assessed the presence of both membrane bud and proplatelet formation from MKs, including MKs with and without a release event. We classified the forms of platelet generation as membrane budding if the extension or membrane protrusion was less than 10 µm in length. Proplatelet formation was referred to as a

membrane protrusion longer than 10 μm. The fraction of each type of platelet generation was calculated of all observed MKs.

Statistical comparison between membrane bud and proplatelet formation fraction at the same age of embryos is shown with black lines. The fraction of membrane bud formation was also compared between YS E10.5 and all other embryonic ages of YS and FL, as shown with red lines in the figure. The number of dams, embryos and observed MKs are noted below the graph.

In YS at E10.5, fraction of bud forming MKs was numerically higher than proplatelet forming MKs (11.4 ± 3.1% vs. 5.8 ± 3.1%, p=0.25). However, at E11.5, the fraction of bud forming MKs (18.4 ± 7.3 %) was 20x higher than the fraction of proplatelet forming MKs (0.89 ± 0.89 %, p=0.03). In FL, the fraction of bud forming MKs was significantly higher than the fraction of proplatelet forming MKs at E13.5 (32.2 ± 4.6 % vs. 3.5 ± 1.9 %, p= 0.0002), at E14.5 (29.1 ± 2.0 % vs. 3.1 ± 1.8 %, p <0.0001) and at E15.5 (42.0 ± 4.9 % vs. 6.7 ± 3.1 %, p <0.0001).

Overall, the fraction of bud forming MKs was higher in the FL than YS. The fraction of bud forming MKs itself remained stable in the YS (p=0.60) and the FL (p=0.08). For proplatelet formation, there were no difference at different embryonic age in YS (p=0.88) and FL (p=0.43).

These results indicate that membrane bud formation and their release from MKs could be a major contributor of platelet generation in both YS and FL. Proplatelet formation seems to be a rather rare event in embryonic thrombopoiesis. As follows, we aimed at quantifying the platelet release frequency by both forms of platelet generation.

### 3.4.6 Prevalence of membrane bud release and proplatelet release from yolk sac and fetal liver megakaryocytes



| | E10.5 | E11.5 | E13.5 | E14.5 | E15.5 |
|---|---|---|---|---|---|
| n (dams) | 7 | 5 | 5 | 4 | 5 |
| n (embryos) | 17 | 8 | 9 | 7 | 9 |
| n (MKs) | 171 | 54 | 151 | 137 | 101 |
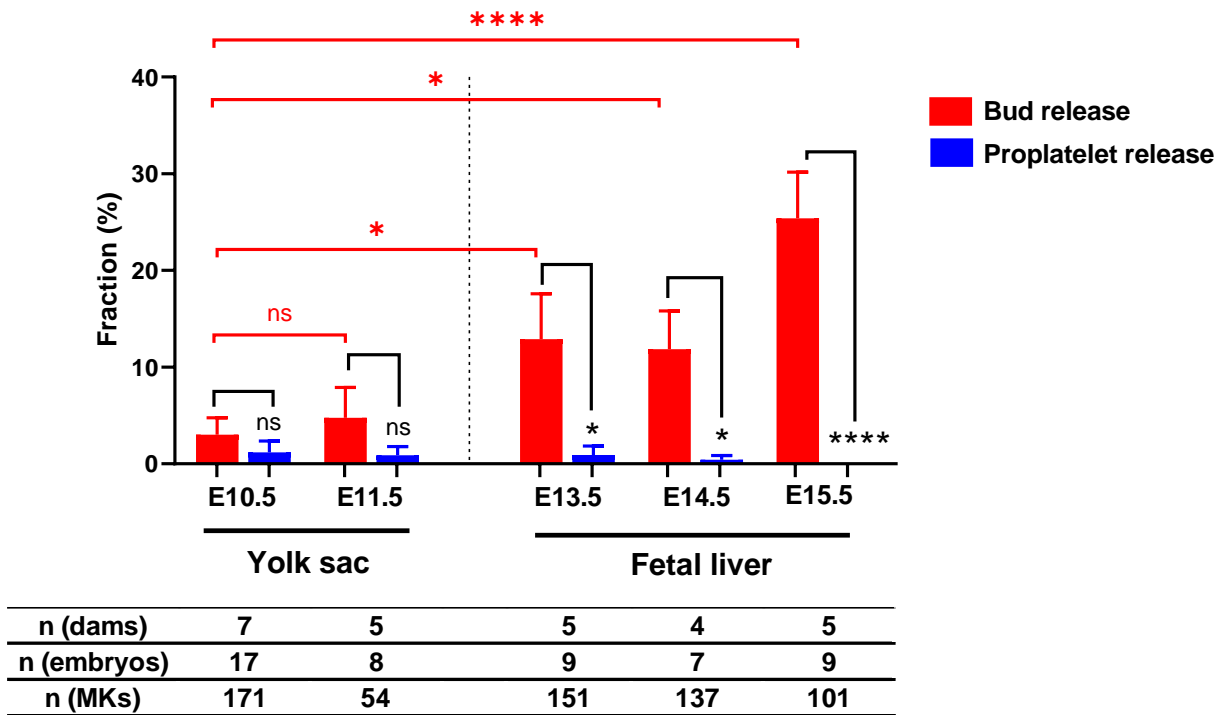
**Figure 3.40    Prevalence of membrane bud and proplatelet release from fetal liver and yolk sac megakaryocytes**

We analysed MP-IVM datasets from both YS and FL. We observed frequently definitive membrane bud release events into the circulation. At the same time, we also observed release events of large proplatelets into vasculature. The latter has been observed and thus proposed as the major form of platelet generation in adult bone marrow [18].

Here, we showed the fraction of megakaryocytes with a membrane bud and proplatelet release event from all present megakaryocytes within the MP-IVM dataset. Release events were counted if the particle was visibly disconnected with increasing distance from the MK cell body.

In YS, the fraction of MKs with membrane bud release (3.0 ± 1.7 %) was similar to

proplatelet release (1.2 ± 1.2 %) at E10.5. At E11.5, there was a numerical increase in membrane bud release (4.7 ± 3.2 %) compared to E10.5, which did not reach statistical significance. The difference of membrane bud release to proplatelet release grew at E11.5, but did not reach statistical significance. Proplatelet release frequency (0.9 ± 0.9 %) at E11.5 was similar to E10.5.

In FL at E13.5, the fraction of MKs with membrane bud release (12.9 ± 4.7 %) was 10-fold higher than proplatelets release (0.9 ± 0.9 %, p= 0.03). This difference was also present at E14.5 (11.9 ± 3.9 % vs. 0.4 ± 0.4 %, p =0.01). At E15.5, there were no proplatelets release events observed, compared to more than quarter of MKs with membrane buds release events (25.4 ± 4.9 %).

Overall, membrane bud release in FL was higher than that in YS. Over the observation period in YS, membrane bud release was similar between E10.5 and E11.5. In FL, membrane bud release was rising from E13.5 to E15.5, albeit without statistical significance. This could indicate a higher thrombopoietic activity of FL MKs at this developmental period, building up the platelet pool for the neonatal period.

Importantly, in both YS and FL, proplatelet release events were rare, indicating that this form of platelet generation is not as important in the embryonic setting.

The number of dams, embryos and observed MKs are noted below the graph.

### 3.4.7 Megakaryocyte position in embryonic vasculature of yolk sac and fetal liver

We further evaluated the spatial association of MKs with the vasculature within both hematopoietic compartments of YS and FL. This could provide information whether further differentiation of MKs over the embryonic development leads to more interactions with the vascular compartment.
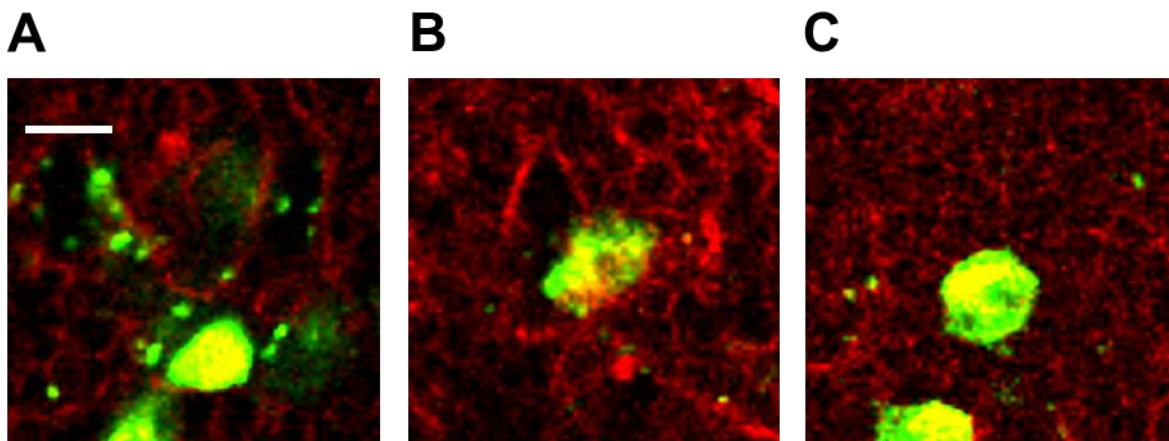


**Figure 3.41    Megakaryocyte position relative to the vasculature**

MP-IVM data showed found MK linage cells and platelets in green colour. Other cells and tissues were red. We can see very obvious lumen with platelets flowing inside. Besides, the lumens were usually showing clear border. This is how we define the vessels. We used our data to determine the position of MKs within the YS and FL in relation to the vasculature. MKs can be located intravascular (**A**, E15.5 FL), crossing the vessel wall (**B**, E14.5 FL), or extravascular **(C,** E13.5 FL**)**. Representative images. Bar, 20 µm

### 3.4.8 Quantification of megakaryocyte position in embryonic vasculature of yolk sac and fetal liver

**A**    **Yolk sac**



- intravascular MKs
- vessel wall-crossing MKs
- extravascular MKs

E10.5      E11.5

**Fetal liver**

E13.5      E14.5      E15.5

|            | E10.5 | E11.5 | E13.5 | E14.5 | E15.5 |
|------------|-------|-------|-------|-------|-------|
| n (dams)   | 8     | 7     | 4     | 6     | 4     |
| n (embryos)| 22    | 11    | 6     | 17    | 11    |
| n (MKs)    | 167   | 59    | 147   | 424   | 98    |

**B**

**Intravascular MK fraction**



|             |     |     |     |     |     |
|-------------|-----|-----|-----|-----|-----|
| n (dams)    | 8   | 7   | 4   | 6   | 4   |
| n (embryos) | 22  | 11  | 6   | 17  | 11  |
| n (MKs)     | 167 | 59  | 147 | 424 | 98  |

87
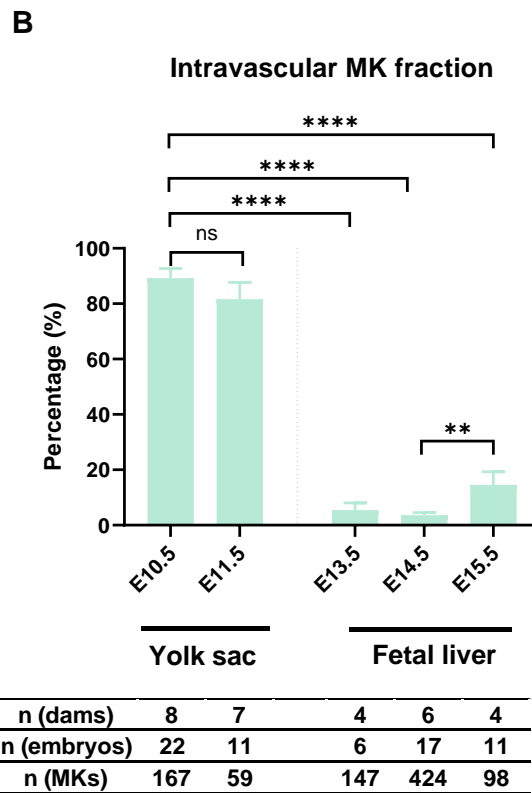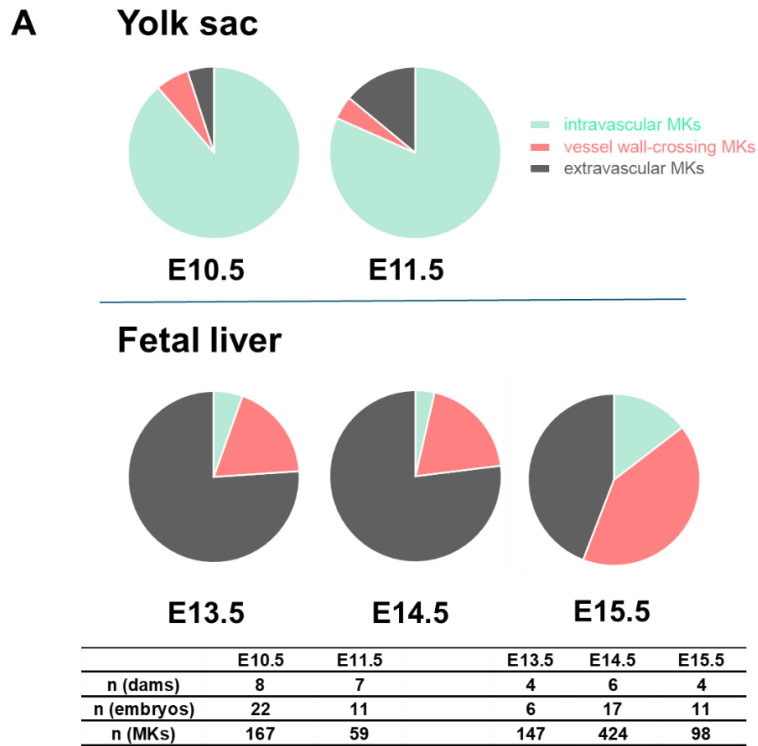
**C**

## Vessel wall-crossing MK fraction
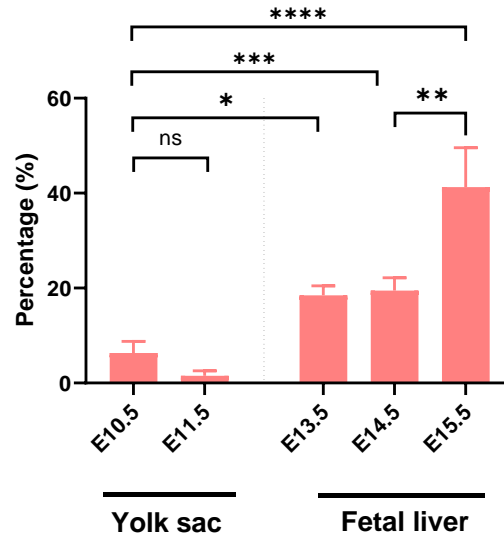


| n (dams) | 8 | 7 | | 4 | 6 | 4 |
|---|---|---|---|---|---|---|
| n (embryos) | 22 | 11 | | 6 | 17 | 11 |
| n (MKs) | 167 | 59 | | 147 | 424 | 98 |

**D**

## Extravascular MK fraction
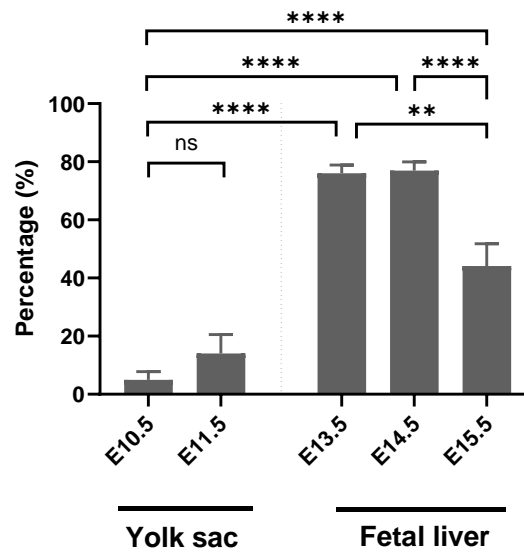


| n (dams) | 8 | 7 | | 4 | 6 | 4 |
|---|---|---|---|---|---|---|
| n (embryos) | 22 | 11 | | 6 | 17 | 11 |
| n (MKs) | 167 | 59 | | 147 | 424 | 98 |

**Figure 3.42   Quantification of megakaryocyte position in yolk sac and fetal liver**

From MP-IVM 3D datasets, we quantified the MK positions in the vasculature of YS and FL. The number of dams, embyros and observed MKs are noted below the graph.

In YS, the majority MKs (>80%) are intravascular (**A**, upper row of pie charts). In contrast, intravascular position of MKs was seldom in FL, with extravascular MKs being the majority (**A**, lower row of pie charts).

In YS, the fraction of intravascular MKs at E10.5 and E11.5 were similar (89.2 ± 3.5% vs. 81.6 ± 6.1%, p=ns). In FL, fraction of intravascular MKs was increasing from E14.5 to E15.5 (3.6 ± 1.0% vs. 14.6 ± 4.7%, p=0.007) **(B).**

As for vessel wall-crossing MKs, their fraction was low in YS at E10.5 (6.3 ± 2.4%) and at E11.5 (1.5 ± 1.0%) **(C)**. This fraction was significantly higher in FL at all observed days, with a strong increase from E14.5 to E15.5 (19.5 ± 2.7% vs. 41.3 ± 8.3%, p=0.005)**.**

Similar to vessel wall-crossing MKs, extravascular MKs were a minority in YS at E10.5 (5.0 ± 2.8%) and at E11.5 (14.0 ± 6.5%). As such, the fraction of extravascular MKs in YS was lower than in fetal liver. In FL, extravascular MKs were the majority, but with declining fractions from E14.5 to E15.5 (76.1 ± 2.8% vs. 44.1 ± 7.7%, p=0.008) **(D)**.

In FL with further development (i.e., at E15.5), more MKs were crossing vessel wall and locating intravascular compared with the situation at E13.5 and E14.5. This could suggest that more MKs and/or their progenitors are transmigrating from the extravascular niche into the vasculature with potential relocation to other organs.

### 3.4.9 Assessment of vessel contact of extravascular megakaryocytes
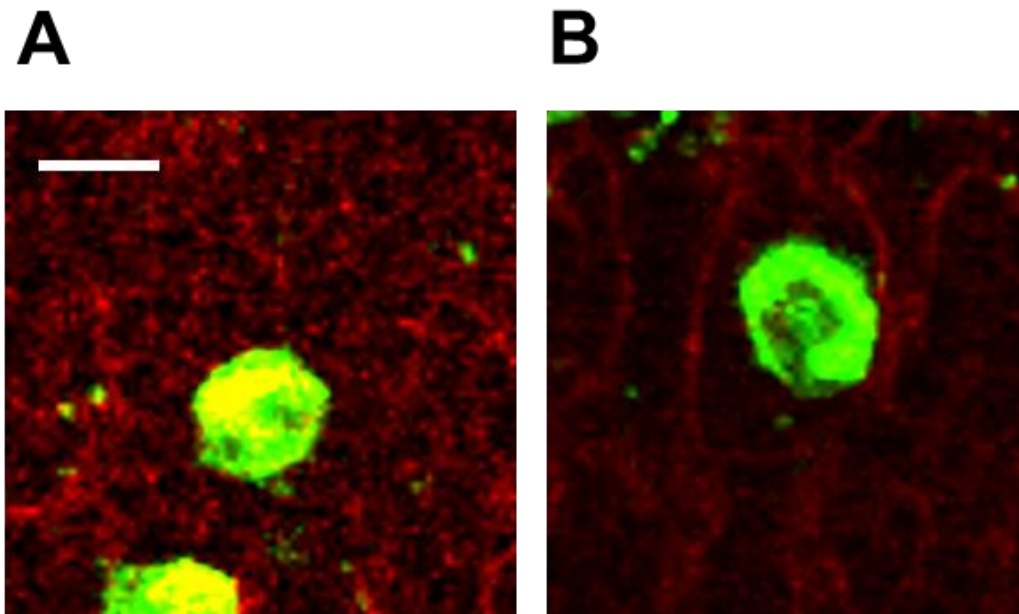


**Figure 3.43    Extravascular megakaryocyte positions with and without direct vessel wall contact**

Here, we show representative images of extravascular MKs in vessel sinusoids (**A**, E13.5 FL). Several MKs contacting the vessel wall were found (**B**, E15.5 FL). Additionally, we performed further analysis to subdivide extravascular MKs into fractions with and without contact with the vessel wall as embryo development.

Bar, 20 µm

### 3.4.10 Quantification of vessel contact of extravascular megakaryocytes



| | E13.5 | E14.5 | E15.5 |
|---|---|---|---|
| n (dams) | 4 | 6 | 4 |
| n (embryos) | 6 | 17 | 11 |
| n (MKs) | 112 | 326 | 43 |
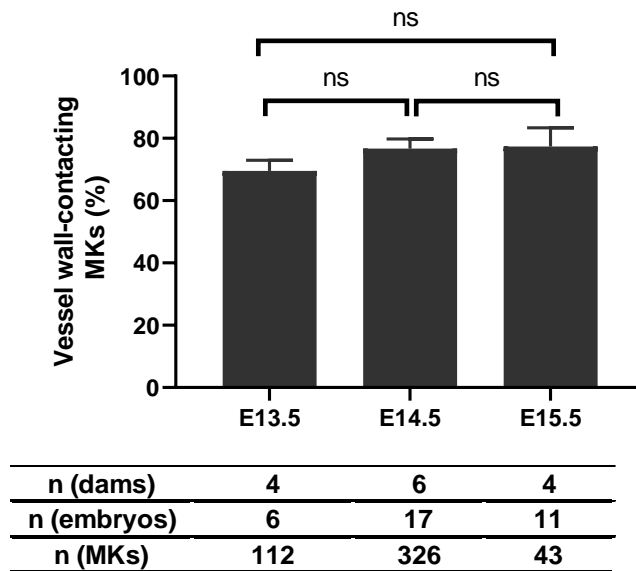
**Figure 3.44   Fraction of megakaryocyte with and without direct vessel wall contact among extravascular MKs in fetal liver**

We quantified the fraction of vessel wall-contacting MKs among extravascular MKs from MP-IVM 3D datasets of the FL. We found that the majority of extravascular MKs had in fact vessel contact, ranging from 69.5 ± 3.5 % at E13.5 to 77.4 ± 6.0 % at E15.5. There were no significant differences between the different embryo ages.

The number of dams, embryos and observed MKs are noted below the graph.

This shows the strong association of FL MKs with the dense vasculature, as the majority of MKs are either positioned within, crossing, or in contact with vessels.

## 3.5 Intramaternal and intraperitoneal injection of thrombopoietin and its effect on thrombopoiesis in dams and embryos

Thrombopoietin (TPO) is the most important factor to stimulate megakaryopoiesis and platelet biogenesis. Here, we did intraperitoneal injection (IP injection) to mother mice to test whether this can manipulate platelet level in embryos.

### 3.5.1 Serum thrombopoietin levels in dams and embryos with and without intraperitoneal thrombopoietin injection into dams
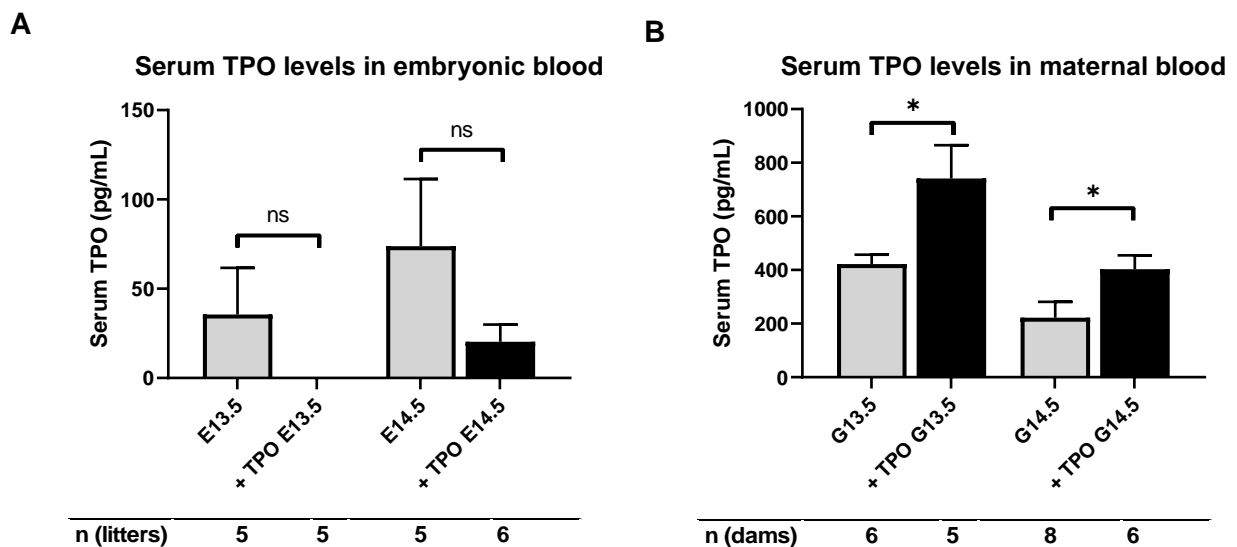


**Figure 3.45   Thrombopoietin level in maternal and embryonic serum after intramaternal intraperitoneal recombinant thrombopoietin injection**

We performed once daily intraperitoneal injections of recombinant murine thrombopoietin (rmTPO) into dams with a dose of 8ng/g/day over three consecutive days.

In E13.5 embryos from the injected dams **(A)**, the overall TPO level in embryonic blood did not show difference between the rmTPO-injected group (0 ± 0 pg/mL) and non-injected group (35.59 ± 26.06 pg/mL). Likewise, at E14.5, the rmTPO-injected group (20.37 ± 9.55 pg/mL) was similar with non-injected group (73.85 ± 37.58 pg/mL).

In dams **(B)**, at gestational age G13.5, the rmTPO-injected group showed an increased overall serum TPO level (741.4 ± 277.7 pg/mL) compared the non-injected group (421.8 ± 87.10 pg/mL). At G14.5, the overall serum TPO levels of the rmTPO-injected group (402.6 ± 126.3 pg/mL) were higher than non-injected group (221.8 ± 168.8 pg/mL).

The number of dams and litters are noted below the graph.

+ TPO: intraperitoneal intramaternal rmTPO injection.

### 3.5.2 Comparison of platelet count in dams and embryos after intraperitoneal thrombopoietin injection into dams

**A**

**Platelet count in embryonic blood**



| n (litters) | 4 | 3 | 4 | 4 |

**B**

**Platelet count in maternal blood**



| n (dams) | 4 | 3 | 4 | 4 |
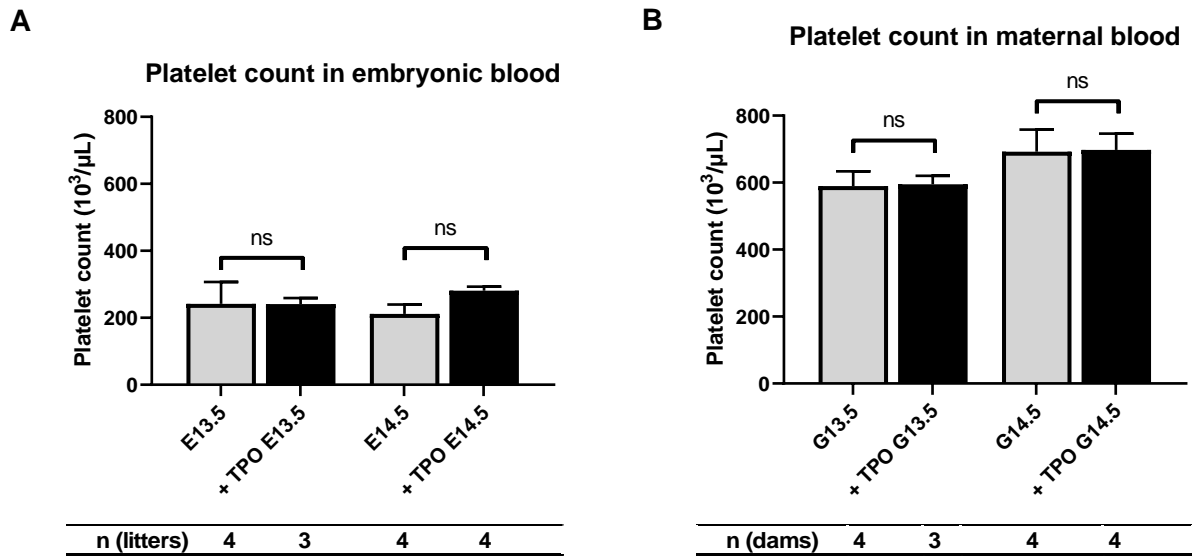
**Figure 3.46    Platelet counts in maternal and embryonic blood after intramaternal intraperitoneal recombinant thrombopoietin injection**

In embryonic blood at E13.5 **(A)**, the platelet count was similar between the rmTPO-injected group (241.0 ± 31.21 x $10^3$/µL) and non-injected group (241.6 ± 130.8 x $10^3$/µL). As such, platelet counts were similar between the rmTPO-injected group (280.9 ± 24.62 x $10^3$/µL) and non-injected group (211.8 ± 55.88 x $10^3$/µL) at E14.5,

In maternal blood at gestational age G13.5 **(B)**, the mTPO-injected group (595.0 ± 44.33 x $10^3$/µL) showed similar platelet counts with the non-injected group (589.8 ± 87.86 x $10^3$/µL). Also, at G14.5, the mTPO-injected group (697.8 ± 96.84 x $10^3$/µL) platelet count was comparable with non-injected group (692.3 ± 132.1 x $10^3$/µL).

The number of dams and litters are noted below the graph.

+ TPO: intraperitoneal intramaternal rmTPO injection.

## 3.5.3 Comparison of mean platelet volume in dams and embryos after intraperitoneal thrombopoietin injection into dams
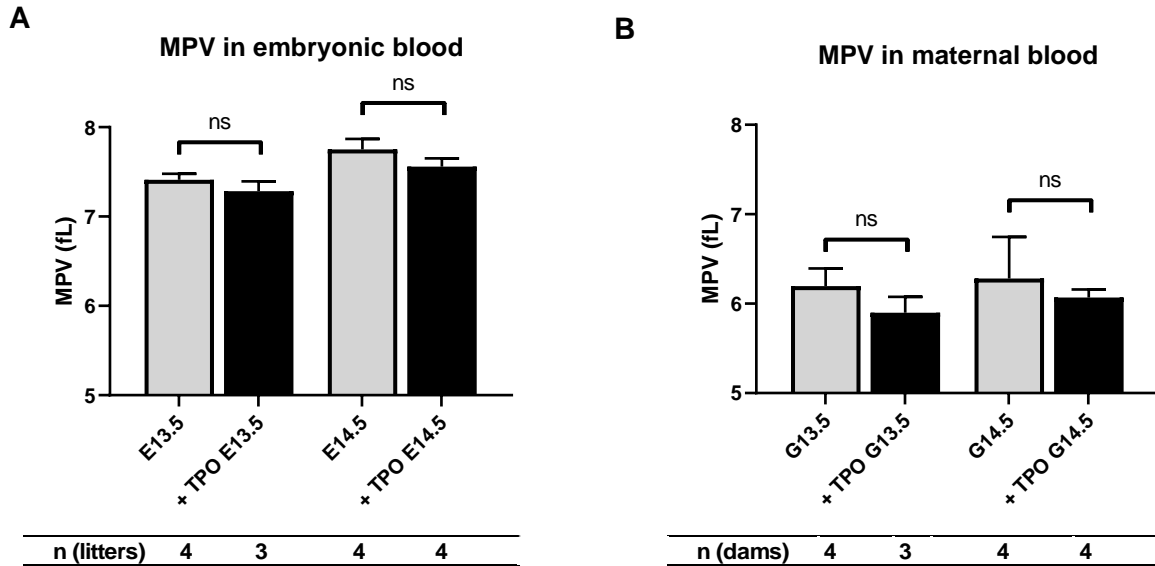


**Figure 3.47 Mean platelet volume after intramaternal intraperitoneal recombinant thrombopoietin injection**

The mean embryonic platelet volume (MPV) was similar between the rmTPO-injected group and non-injected group at E13.5 (7.28 ± 0.19 fL vs. (7.41 ± 0.13 fL) and at E14.5 (7.56 ± 0.18 fL vs. 7.75 ± 0.24 fL) **(A)**.

The maternal MPV was similar between the rmTPO-injected group and non-injected group at G13.5 (5.90 ± 0.31 fL vs. 6.20 ± 0.40 fL) and at G14.5 (6.07 ± 0.18 fL vs. 6.07 ± 0.18 fL) **(B)**.

The number of dams and litters are noted below the graph.

+ TPO: intraperitoneal intramaternal rmTPO injection.

In summarys, intraperitoneal intramaternal injection of rmTPO increase overall TPO level in maternal serum, but not embryonic serum. This may indicate that rmTPO might not cross the mouse placenta, despite its small size which would theoretically enable placenta crossing. However, the rmTPO injection did not influence the platelet count and MPV neither in maternal blood nor embryonic blood. Potts et al.

researched the function of TPO receptor (MPL) in embryonic thrombopoiesis. They found platelet-forming lineage production was not rely on MPL at early stage, but MPL was required in the late fetus for efficient thrombopoiesis [32]. We cannot rule out that rmTPO could have an influence on embryonic thrombopoiesis, but our results are in line with other findings that show that *in vivo* embryonic thrombopoiesis is less TPO dependent than adult thrombopoiesis.

# 4. Discussion and conclusion

## 4.1 Discussion of methodology

### 4.1.1 Methodology of platelet quantification

With flow cytometry techniques, we acquired patterns of platelets and MKs in BL6, c-Myb and NFE2 embryos. Flow cytometry is a standard method used for platelet research [90, 91]. It has many benefits, such as measuring specific surface markers on each platelet on a single event level[92], so it is able to examine platelets even in conditions of thrombocytosis or thrombocytopenia [93, 94]. Furthermore, there is no requirement for excessive blood volumes to gain data [95]. There are naturally limitations to this technique as only certain reagents and antibodies could be used and the probes have to processed with constant care under standardized protocols [83].

Flow cytometry was used to assess reticulated platelets, which are believed to be immature platelets. They are released by megakaryocytic fragmentation into the circulation if there is an increased demand for platelets, e.g. due to bleeding, thrombocytopenia and infection [96]. Thus, they can serve as an indicator for the activity of thrombopoiesis [97]. Reticulated platelets, although anucleated, contain some rough endoplasmic reticulum and messenger RNA and are also able to synthesize small amounts of protein [85, 98].  Thiazole orange (TO) has been established by Kienast et al [99] as a fluorescent nucleic acid dye [85] binding to RNA, and is therefore suitable for quantifying reticulated platelets by flow cytometry. For platelet and MK size estimation, we chose the forward scatter parameter, which has been shown to correlate with particle size [83, 89]. Flow cytometry was evidently useful to handle the small amounts of blood drawn from embryos, still providing the necessary flow cytometry event numbers needed for a reasonable analysis of platelet and MK numbers.

### 4.1.2 Methodology of multiphoton intravital microscopy

Advanced MP-IVM combined with transgenic mice expressing specific fluorescent labeling is a powerful tool to directly visualize organ development, cell movement and

interaction *in vivo* and in real-time*,* enabling a deeper understanding of embryonic physiology and pathological processes [100]. Previous studies have shown that MP-IVM can provide novel insights of adult thrombopoiesis [101]. It has been shown that in adult mice, MKs generate platelets by forming large intravascular extensions in the BM. MKs in BM migrate slowly and thrombopoiesis is spatially regulated by the BM vasculature [17]. Besides, the lung can be also an important organ for platelet generation in adult mice [9]. All these findings rely on well-developed MP-IVM technology.

Since the dynamic cellular interactions during fetal development are less understood, particularly the thrombopoietic system, MP-IVM could provide valuable data on these dynamic changes. Conventional imaging methods were of limited use for our aims, due to fragility of the embryo, difficulty to maintain circulation, and quick changes in cellular dynamics and interactions. To overcome these limitations, we established an embryonic tissue model combined with MP-IVM for studying murine embryonic thrombopoiesis in 3D, over time, and *in vivo.* As previously shown, MP-IVM has the advantage of increased sensitivity and imaging depth and reduced tissue damage [75]. Although the preparation of the embryo required anesthesia and surgical exposure of the YS and FL with potential deterioration of tissue integrity, our observations revealed that fetal circulation and organ functions are intact. Most importantly, thrombopoiesis was active in both YS and FL. We were able to improve our experimental setup to prolong continuous *in vivo* observation lengths up to 83 min for FL and 25 min for YS, notably with intact maternal-fetal circulation. To overcome difficulties of keeping a stable image acquisition due to fetal/maternal heart beat and maternal respiratory motions, we strengthened the fixation of our tissue holders and applied a real-time drift correction software. Optional post-acquisition image processing enabled further stabilization of tissue motion by additional drift correction. The sum of these protocol improvements in addition to the advanced image analysis software, enabled us to perform the first in-depth analysis and quantification of the dynamic process of embryonic thrombopoiesis *in vivo.* The generalizability of our imaging method could enable widespread use and rapid adoption in murine embryo research.

## 4.2 Discussion of results

### 4.2.1 Embryonic platelet dynamics

Platelet has been well studied in adult mammals, they are function not only in hemostasis, but also in infections and cancer [102]. In embryos, the platelet showed a very different functional pattern. Platelets are less active when stimulated with physiological agonists in human newborns [103, 104]. Interestingly, platelet activity and platelet counts were found to correlate with gestational age. The platelet in early stage is less active [105, 106]. These are due to different characters of platelet in embryos.

Using flow cytometry, we were able to monitor overall platelet and reticulated platelet numbers over different developmental ages. We found that the overall platelet count is lower than in adult mice, yet the fraction of reticulated platelet was particularly high in the embryo. Platelet counts were particularly low at E11.5, but expanded massively until E15.5. Embryonic platelet seemed to be larger than maternal peripheral blood platelets by FSC parameter. This finding is consistent with other reports showing lower fetal platelet numbers, but increased size [6]. We assume that embryonic platelets are larger because of the higher fraction of reticulated platelets, since the latter are also larger in the adult organism [107]. As megakaryocyte and platelet are probably more mature towards later developmental ages, we found also a decrease in platelet size over time. In a fetal thrombosis model under intravital microscopy, platelets presented hyporeactivity during early fetal development. They showed less adhesion and spreading capacity compared with adults [6].

### 4.2.2 Fetal liver development and megakaryopoiesis

The FL has a complex developmental process, originating from the ventral foregut endoderm [108] and differentiating into liver and biliary cells, fibroblasts and stellate cells, with phases of accelerated growth as it is vascularized and colonized by hematopoietic cells to become the major fetal hematopoietic organ [36]. Since the FL has such a prominent role for embryonic hematopoiesis, we assessed also its role for thrombopoiesis. Among others, MK numbers and overall FL cell numbers were quantified. Total FL cell numbers increased dramatically between E11.5 and E16.5,

representing the expanse of the hematopoietic system. According to previous reports, immature or pre-HSCs from the YS colonize the FL where the definitive hematopoiesis is achieved through HSC expansion (up to 40-fold [26]) and subsequent lineage commitment [28]. Beyond the FL, also the spleen is a site of hematopoiesis colonized by HSCs [38, 109]. Among the earliest lineage commitments in the YS and FL are macrophages and MK progenitors [110, 111]. These MK progenitors can apparently give rise to MKs *in vitro*, with a greater magnitude of *in vitro* expansion of FL progenitors than from adult marrow progenitors [112]. These MK progenitors then give rise to MKs. Although MKs were only a small fraction of total FL cells, their numbers increased substantially over time and gained in ploidy, which could represent the necessary MK maturation to achieve the aforementioned platelet expansion.

### 4.2.3  c-Myb is dispensable for early embryonic thrombopoiesis

The transcription factor c-Myb is essential for the development of definitive hematopoiesis which will sustain into the adult organism. Therefore, c-Myb deficient embryos have a deleterious phenotype due to lack of erythrocytes. Experiments with this model showed that other hematopoietic cells from more primitive sources exist throughout the embryo and survive into adulthood, namely YS macrophages. Our experiments with transgenic c-Myb knockout embryos showed that MKs are very well present in the FL until demise of the embryo. Therefore, total megakaryopoiesis and thrombopoiesis do not seem to be altered quantitively by this important transcription factor, as platelet and MK numbers were comparable to heterozygous embryos. Conversely, platelet (larger) and MK (smaller) size as well as MK ploidy (lower) showed a less mature phenotype. This could also be due to a compensatory mechanism that potentially upregulates primitive megakaryopoiesis and thrombopoiesis in the absence of definitive hematopoiesis. Similar reports showed that c-Myb deficient embryos had normal platelet numbers at E12.5 but became thrombocytopenic by E15.5, suggesting that c-myb is required for sustained definitive thrombopoiesis in the third semester and beyond [113]. As we have outlined, it is hypothesized that MKs can be generated from both primitive or definitive hematopoiesis and be present at the same time in the embryo [25]. YS-derived MKs

or their progenitors could migrate to and colonize the FL, apparently c-Myb independent. However, MKs generated during primitive hematopoiesis are not well distinguishable from their definitive counterparts [111].

### 4.2.4 NFE2 is involved in embryonic thrombopoiesis

One of the master regulators of thrombopoiesis is the transcription factor NFE2, which is responsible for differentiation of MKs to become highly effective in platelet generation. In case of NFE2 depletion, severe thrombocytopenia is observed in adult mice. NFE2 is dispensable for erythroid cell development, and organ development [114], but only the minority of NFE2 deficient embryos survive into adulthood. However, it is obligatory for megakaryocyte maturation and thrombopoiesis [58]. Moreover, absolute thrombocytopenia in NFE2 -/- mice does not result from absence of thrombopoietin or from failed respond to thrombopoietin [58]. Those mice were also shown to lack production of proplatelets, identifying the pathology of platelet release [59]. In our results, we saw indeed a role of NFE2 for embryonic thrombopoiesis from FL MKs. NFE2 deficient embryos had also thrombocytopenia, but platelets were still present in contrast to absolute thrombocytopenia in adults. Conversely, FL MK numbers were elevated. Furthermore, FL MK size as well as MK ploidy showed a less mature phenotype. This could explain, why we still found embryonic platelets which were larger than their wild type embryonic counterparts and could represent immature forms generated from immature MKs. Interestingly, surviving NFE2 deficient adults do not die of hemorrhage or display signs of bleeding despite absolute thrombocytopenia, indicating that other elements of the coagulation system play crucial roles. Potentially, an immature embryonic coagulation system cannot fully compensate the thrombocytopenia of NFE2 deficient embryos, which therefore die of hemorrhage intrauterine or peripartum.

### 4.2.5 Patterns of thrombopoiesis in yolk sac and fetal liver revealed by multiphoton intravital microscopy

First, MP-IVM unveiled the presence of active thrombopoiesis in both YS and FL. In general, we found higher concentration of MKs in FL than in YS. The FL MKs were larger than YS MKs. This could indicate higher activity of thrombopoiesis in FL. In FL, a large fraction of MKs was extravascular, although the majority had vessel wall

contact. The role of these extravascular MKs is unknown, both in adults and embryos. One possibility is that these MKs modulate the resident hematopoietic niche. Previous studies showed that MKs can be passive obstacles for HSCs in the BM[115]. Depletion of MKs activates quiescent HSC, expands the HSC pool, and increase HSC proliferation[116, 117]. Therefore, MKs have a prominent role in niche homeostasis.

Second, diverse MK and proplatelet/platelet forms were observed in the embryo. We identified different types of proplatelets *in vivo,* ranging substantially in length from 5 µm to 200 µm. Our imaging protocol enabled us to identify distinct modes of embryonic platelet generation. Compared with the classic proplatelet formation and shedding pattern in adult bone marrow and lung [9, 18], we found small cytoplasmatic extensions we termed buds. The latter were released and directly shed into circulation from FL and YS MKs and represented the majority of release events. It is noteworthy that *in vitro*, the vast majority of MKs do not form buds, but long proplatelets. The discrepancy of these *in vitro* and *in vivo* results has been shown by others recently [118]. Furthermore, if canonical proplatelet protrusions were observed, there were shorter than their adult counterparts [101]. Importantly, also in adults there seem to be different modes of platelet generation Brown et al. found that most megakaryocytes enter the sinusoidal space as large protrusions rather than extruding fine proplatelet extensions [119].

The potential mechanisms of budding vs. proplatelet shedding are still not clear. Surely, the cytoskeleton and membrane re-organization will play an important role. regulators of this process are proteins of the Rho family (eg, RhoA, Rac1), which are also required for many cellular functions beyond cell mobility and cytokinesis [120]. These proteins, e.g., RhoA and Rock, play an important role in the MK endomitotic process [121, 122]. Rock inhibitor treatments in mature MKs also lead to the downregulation of MYC, NFE2, MAFG and MAFK transcript levels, suggesting that lowering the levels of these transcription factors is a prerequisite to drive the late stages of megakaryocyte maturation [123]. These transcription factors could be less important in the embryonic setting, therefore biasing platelet generation towards bud formation. Because NFE2−/− mice can form, release, and fragment proplatelets *in*

*vivo,* are not able to form and release membrane buds [118]. This suggest NFE2 could be critical for embryonic membrane budding alone.

### 4.2.6 Limitations of methods

Choosing the right transgenic mouse models is essential for adequate experimental setup and interpretation of results. This is evidently true for research of embryonic development. It is very difficult to perform conditional gene knockouts by e.g. application of chemical compounds in embryos due to the placenta barrier. Surprisingly, there is a sparsity of data regarding the capability of chemical compounds or small molecules to cross this barrier. In our project, we also injected diphtheria toxin to PF4 Cre ✕ Rosa26-iDTR pregnant mice and did not observe any Cre mediated recombination with subsequent depletion of the thrombopoietic lineage. Therefore, we chose the c-Myb and NFE2 transgenic mice to perform constitutional knockouts of these transcriptional factors with major impact on definitive hematopoiesis and thrombopoiesis.

Although MP-IVM has certain advantages, it also has disadvantages such as a lower spatial resolution compared to confocal microscopy. This is due to the principle that the longer the wavelength of the excitation light, the lower is the spatial resolution. Two-photon excitation requires the usage of excitation that is twice that of the one-photon wavelength, leading to approximately half the resolution. Therefore, we cannot exclude that certain biologic processes are not detected by MP-IVM.

The Rosa 26 mTmG x Pf4 Cre mouse model has been widely used to study the MK/platelet lineage. However, Pf4 could have a broader expression beyond MKs under certain circumstances. The Pf4 Cre transgene is also believed to be expressed in a variety of leukocyte populations [124] as well as a subset of epithelial cells from distal colon [125]. In embryonic intravital imaging, it could therefore be difficult to distinguish MK, MK progenitors or monocytes progenitors only based on Pf4 expression. Nonetheless, several groups have used this model for deciphering thrombopoiesis [9], as additional parameters such as size and shedding activity were used to identify MKs.

## 4.3 Summary

Platelet generation and function in embryos is not fully understood. This is partly due to the challenges in handling embryonic structures for experimental setups and limitations of conventional imaging methods which do not allow for direct and real-time visualization of MKs and platelets *in vivo*. As such, dynamic development of MKs and their mode of embryonic platelet production has not been studied in detail.

To gain further insights into embryonic thrombopoiesis, we first performed global quantitative assessments of MKs and platelets. Platelet count, reticulated platelet count and MK numbers were quantified using flow cytometry and specific stainings. Our results show that platelet count starts low but expand dramatically with further development. Moreover, a higher fraction of reticulated platelets is present in the embryo than adults. Both observations could be related to a strong increase of fetal liver MK numbers and their ploidy reflecting maturation. Experiments with transgenic c-Myb knockout embryos with a known deficiency of definitive hematopoiesis showed that megakaryopoiesis and thrombopoiesis do not seem to be influenced by this important transcription factor quantitatively, as platelet and MK numbers were comparable to heterozygous embryos. Conversely, platelet and MK size as well as MK ploidy showed a less mature phenotype. Furthermore, the major canonical transcription factor responsible for MK maturation in adults, NFE2, did also affect embryonic platelet number with severe thrombocytopenia in NFE2 knockout embryos. Again, fetal liver MK size as well as MK ploidy showed a less mature phenotype, with higher numbers of these more immature MKs. Our results suggest that potentially two waves of embryonic megakaryopoiesis could occur with different regulators of platelet production, where the early wave is less affected by c-Myb and NFE2.

In a second step, we aimed at developing a new protocol for intravital, real-time three-dimensional imaging to visualize embryonic thrombopoiesis in hematopoietic organs (yolk sac, fetal liver) across different stages of embryonic development. We applied multiphoton microscopy to enable the imaging of different forms of platelet generation from yolk sac and fetal liver MKs using the Rosa 26 mTmG x Pf4 Cre mouse model. At least two patterns of platelet shedding from MKs exist, either by conventional proplatelet release or by a novel process we termed membrane budding. The latter

seems to be the predominant form. We observed also that fetal liver MKs presented higher thrombopoietic activity than yolk sac MKs. Accordingly, and in line with our results from flow cytometry, fetal liver MKs seemed to be larger and more mature. Our imaging method revealed that fetal liver MKs were positioned mainly extravascular, whereas yolk sac MKs were found primarily intravascular.

Both our flow cytometry protocols and our novel three-dimensional intravital imaging protocol can be applied for further studies of thrombopoiesis and for other dynamic developmental processes and embryonic disease modeling. Understanding the mechanism by which platelets are generated at the embryonic stage could be critical to develop novel therapeutic strategies for congenital defects of hematopoiesis and thrombopoiesis such as neonatal thrombocytopenia.

# References

1.      Thon JN, Dykstra BJ, Beaulieu LM: **Platelet bioreactor: accelerated evolution of design and manufacture**. *Platelets* 2017, **28**(5):472-477.

2.      van der Meijden PEJ, Heemskerk JWM: **Platelet biology and functions: new concepts and clinical perspectives**. *Nat Rev Cardiol* 2019, **16**(3):166-179.

3.      Nurden AT: **The biology of the platelet with special reference to inflammation, wound healing and immunity**. *Front Biosci (Landmark Ed)* 2018, **23**:726-751.

4.      Haemmerle M, Stone RL, Menter DG, Afshar-Kharghan V, Sood AK: **The Platelet Lifeline to Cancer: Challenges and Opportunities**. *Cancer Cell* 2018, **33**(6):965-983.

5.      Engelmann B, Massberg S: **Thrombosis as an intravascular effector of innate immunity**. *Nat Rev Immunol* 2013, **13**(1):34-45.

6.      Margraf A, Nussbaum C, Rohwedder I, Klapproth S, Kurz ARM, Florian A, Wiebking V, Pircher J, Pruenster M, Immler R *et al*: **Maturation of Platelet Function During Murine Fetal Development In Vivo**. *Arterioscler Thromb Vasc Biol* 2017, **37**(6):1076-1086.

7.      Yang Y, Oliver G: **Development of the mammalian lymphatic vasculature**. *J Clin Invest* 2014, **124**(3):888-897.

8.      Echtler K, Stark K, Lorenz M, Kerstan S, Walch A, Jennen L, Rudelius M, Seidl S, Kremmer E, Emambokus NR *et al*: **Platelets contribute to postnatal occlusion of the ductus arteriosus**. *Nat Med* 2010, **16**(1):75-82.

9.      Lefrancais E, Ortiz-Munoz G, Caudrillier A, Mallavia B, Liu F, Sayah DM, Thornton EE, Headley MB, David T, Coughlin SR *et al*: **The lung is a site of platelet biogenesis and a reservoir for haematopoietic progenitors**. *Nature* 2017, **544**(7648):105-109.

10.     Noetzli LJ, French SL, Machlus KR: **New Insights Into the Differentiation of Megakaryocytes From Hematopoietic Progenitors**. *Arteriosclerosis, Thrombosis, and Vascular Biology* 2019, **39**(7):1288-1300.

11.     Akashi K, Traver D, Miyamoto T, Weissman IL: **A clonogenic common myeloid progenitor that gives rise to all myeloid lineages**. *Nature* 2000, **404**(6774):193-197.

12.     Debili N, Coulombel L, Croisille L, Katz A, Guichard J, Breton-Gorius J, Vainchenker W: **Characterization of a bipotent erythro-megakaryocytic progenitor in human bone marrow**. *Blood* 1996, **88**(4):1284-1296.

13.     Woolthuis CM, Park CY: **Hematopoietic stem/progenitor cell commitment to the megakaryocyte lineage**. *Blood* 2016, **127**(10):1242-1248.

14.     Pronk CJ, Rossi DJ, Mansson R, Attema JL, Norddahl GL, Chan CK, Sigvardsson M, Weissman IL, Bryder D: **Elucidation of the phenotypic, functional, and molecular topography of a myeloerythroid progenitor cell hierarchy**. *Cell Stem Cell* 2007, **1**(4):428-442.

15.     Mazzi S, Lordier L, Debili N, Raslova H, Vainchenker W: **Megakaryocyte and polyploidization**. *Exp Hematol* 2018, **57**:1-13.

16.     Machlus KR, Italiano JE, Jr.: **The incredible journey: From megakaryocyte development to platelet formation**. *J Cell Biol* 2013, **201**(6):785-796.

17.     Stegner D, vanEeuwijk JMM, Angay O, Gorelashvili MG, Semeniak D, Pinnecker J, Schmithausen P, Meyer I, Friedrich M, Dutting S *et al*: **Thrombopoiesis is spatially regulated by the bone marrow vasculature**. *Nat Commun* 2017, **8**(1):127.

18. Zhang L, Orban M, Lorenz M, Barocke V, Braun D, Urtz N, Schulz C, von Bruhl ML, Tirniceriu A, Gaertner F *et al*: **A novel role of sphingosine 1-phosphate receptor S1pr1 in mouse thrombopoiesis**. *J Exp Med* 2012, **209**(12):2165-2181.

19. Italiano JE, Jr., Patel-Hett S, Hartwig JH: **Mechanics of proplatelet elaboration**. *J Thromb Haemost* 2007, **5 Suppl 1**:18-23.

20. Nishimura S, Nagasaki M, Kunishima S, Sawaguchi A, Sakata A, Sakaguchi H, Ohmori T, Manabe I, Italiano JE, Jr., Ryu T *et al*: **IL-1alpha induces thrombopoiesis through megakaryocyte rupture in response to acute platelet needs**. *J Cell Biol* 2015, **209**(3):453-466.

21. Medvinsky A, Rybtsov S, Taoudi S: **Embryonic origin of the adult hematopoietic system: advances and questions**. *Development* 2011, **138**(6):1017-1031.

22. de Bruijn MF, Speck NA, Peeters MC, Dzierzak E: **Definitive hematopoietic stem cells first develop within the major arterial regions of the mouse embryo**. *EMBO J* 2000, **19**(11):2465-2474.

23. Gekas C, Dieterlen-Lièvre F, Orkin SH, Mikkola HKA: **The placenta is a niche for hematopoietic stem cells**. *Dev Cell* 2005, **8**(3):365-375.

24. Ottersbach K, Dzierzak E: **The murine placenta contains hematopoietic stem cells within the vascular labyrinth region**. *Dev Cell* 2005, **8**(3):377-387.

25. Lacaud G, Kouskoff V: **Hemangioblast, hemogenic endothelium, and primitive versus definitive hematopoiesis**. *Exp Hematol* 2017, **49**:19-24.

26. Golub R, Cumano A: **Embryonic hematopoiesis**. *Blood Cells Mol Dis* 2013, **51**(4):226-231.

27. Palis J: **Hematopoietic stem cell-independent hematopoiesis: emergence of erythroid, megakaryocyte, and myeloid potential in the mammalian embryo**. *FEBS Lett* 2016, **590**(22):3965-3974.

28. Samokhvalov IM, Samokhvalova NI, Nishikawa S: **Cell tracing shows the contribution of the yolk sac to adult haematopoiesis**. *Nature* 2007, **446**(7139):1056-1061.

29. Yu H, Bauer B, Lipke G, Phillips R, Van Zant G: **Apoptosis and hematopoiesis in murine fetal liver**. *Blood* 1993, **81**(2):373-384.

30. Hadland B, Yoshimoto M: **Many layers of embryonic hematopoiesis: new insights into B-cell ontogeny and the origin of hematopoietic stem cells**. *Exp Hematol* 2018, **60**:1-9.

31. Mukai HY, Motohashi H, Ohneda O, Suzuki N, Nagano M, Yamamoto M: **Transgene insertion in proximity to the c-myb gene disrupts erythroid-megakaryocytic lineage bifurcation**. *Mol Cell Biol* 2006, **26**(21):7953-7965.

32. Potts KS, Sargeant TJ, Dawson CA, Josefsson EC, Hilton DJ, Alexander WS, Taoudi S: **Mouse prenatal platelet-forming lineages share a core transcriptional program but divergent dependence on MPL**. *Blood* 2015, **126**(6):807-816.

33. Potts KS, Sargeant TJ, Markham JF, Shi W, Biben C, Josefsson EC, Whitehead LW, Rogers KL, Liakhovitskaia A, Smyth GK *et al*: **A lineage of diploid platelet-forming cells precedes polyploid megakaryocyte formation in the mouse embryo**. *Blood* 2014, **124**(17):2725-2729.

34. Porcelijn L, Van den Akker ESA, Oepkes D: **Fetal thrombocytopenia**. *Seminars in Fetal and Neonatal Medicine* 2008, **13**(4):223-230.

35. Hohlfeld P, Forestier F, Kaplan C, Tissot JD, Daffos F: **Fetal thrombocytopenia: a retrospective survey of 5,194 fetal blood samplings**. *Blood* 1994, **84**(6):1851-1856.

36. Zorn AM: **Liver development**. In: *StemBook*. edn. Cambridge (MA); 2008.

37. Schmelzer E, Wauthier E, Reid LM: **The phenotypes of pluripotent human hepatic progenitors**. *Stem Cells* 2006, **24**(8):1852-1858.

38. Christensen JL, Wright DE, Wagers AJ, Weissman IL: **Circulation and chemotaxis of fetal hematopoietic stem cells**. *PLoS Biol* 2004, **2**(3):E75.

39. Zanjani ED, Ascensao JL, Tavassoli M: **Liver-derived fetal hematopoietic stem cells selectively and preferentially home to the fetal bone marrow**. *Blood* 1993, **81**(2):399-404.

40. Wolff L: **Myb-induced transformation**. *Crit Rev Oncog* 1996, **7**(3-4):245-260.

41. Greig KT, Carotta S, Nutt SL: **Critical roles for c-Myb in hematopoietic progenitor cells**. *Semin Immunol* 2008, **20**(4):247-256.

42. Oh IH, Reddy EP: **The myb gene family in cell growth, differentiation and apoptosis**. *Oncogene* 1999, **18**(19):3017-3033.

43. Mucenski ML, McLain K, Kier AB, Swerdlow SH, Schreiner CM, Miller TA, Pietryga DW, Scott WJ, Jr., Potter SS: **A functional c-myb gene is required for normal murine fetal hepatic hematopoiesis**. *Cell* 1991, **65**(4):677-689.

44. Yanagisawa H, Nagasawa T, Kuramochi S, Abe T, Ikawa Y, Todokoro K: **Constitutive expression of exogenous c-myb gene causes maturation block in monocyte-macrophage differentiation**. *Biochim Biophys Acta* 1991, **1088**(3):380-384.

45. Sandberg ML, Sutton SE, Pletcher MT, Wiltshire T, Tarantino LM, Hogenesch JB, Cooke MP: **c-Myb and p300 regulate hematopoietic stem cell proliferation and differentiation**. *Dev Cell* 2005, **8**(2):153-166.

46. Metcalf D, Carpinelli MR, Hyland C, Mifsud S, Dirago L, Nicola NA, Hilton DJ, Alexander WS: **Anomalous megakaryocytopoiesis in mice with mutations in the c-Myb gene**. *Blood* 2005, **105**(9):3480-3487.

47. Carpinelli MR, Hilton DJ, Metcalf D, Antonchuk JL, Hyland CD, Mifsud SL, Di Rago L, Hilton AA, Willson TA, Roberts AW *et al*: **Suppressor screen in Mpl-/- mice: c-Myb mutation causes supraphysiological production of platelets in the absence of thrombopoietin signaling**. *Proc Natl Acad Sci U S A* 2004, **101**(17):6553-6558.

48. Emambokus N, Vegiopoulos A, Harman B, Jenkinson E, Anderson G, Frampton J: **Progression through key stages of haemopoiesis is dependent on distinct threshold levels of c-Myb**. *EMBO J* 2003, **22**(17):4478-4488.

49. Gasiorek JJ, Blank V: **Regulation and function of the NFE2 transcription factor in hematopoietic and non-hematopoietic cells**. *Cell Mol Life Sci* 2015, **72**(12):2323-2335.

50. Andrews NC, Kotkow KJ, Ney PA, Erdjument-Bromage H, Tempst P, Orkin SH: **The ubiquitous subunit of erythroid transcription factor NF-E2 is a small basic-leucine zipper protein related to the v-maf oncogene**. *Proc Natl Acad Sci U S A* 1993, **90**(24):11488-11492.

51. Andrews NC, Erdjument-Bromage H, Davidson MB, Tempst P, Orkin SH: **Erythroid transcription factor NF-E2 is a haematopoietic-specific basic-leucine zipper protein**. *Nature* 1993, **362**(6422):722-728.

52. Ney PA, Andrews NC, Jane SM, Safer B, Purucker ME, Weremowicz S, Morton CC, Goff SC, Orkin SH, Nienhuis AW: **Purification of the human NF-E2 complex: cDNA cloning**

of the hematopoietic cell-specific subunit and evidence for an associated partner. *Mol Cell Biol* 1993, **13**(9):5604-5612.

53. Romeo PH, Prandini MH, Joulin V, Mignotte V, Prenant M, Vainchenker W, Marguerie G, Uzan G: **Megakaryocytic and erythrocytic lineages share specific transcription factors**. *Nature* 1990, **344**(6265):447-449.

54. Deveaux S, Cohen-Kaminsky S, Shivdasani RA, Andrews NC, Filipe A, Kuzniak I, Orkin SH, Romeo PH, Mignotte V: **p45 NF-E2 regulates expression of thromboxane synthase in megakaryocytes**. *EMBO J* 1997, **16**(18):5654-5661.

55. Glembotsky AC, Bluteau D, Espasandin YR, Goette NP, Marta RF, Marin Oyarzun CP, Korin L, Lev PR, Laguens RP, Molinas FC *et al*: **Mechanisms underlying platelet function defect in a pedigree with familial platelet disorder with a predisposition to acute myelogenous leukemia: potential role for candidate RUNX1 targets**. *J Thromb Haemost* 2014, **12**(5):761-772.

56. Motohashi H, Kimura M, Fujita R, Inoue A, Pan X, Takayama M, Katsuoka F, Aburatani H, Bresnick EH, Yamamoto M: **NF-E2 domination over Nrf2 promotes ROS accumulation and megakaryocytic maturation**. *Blood* 2010, **115**(3):677-686.

57. Chen S, Su Y, Wang J: **ROS-mediated platelet generation: a microenvironment-dependent manner for megakaryocyte proliferation, differentiation, and maturation**. *Cell Death Dis* 2013, **4**:e722.

58. Shivdasani RA, Rosenblatt MF, Zucker-Franklin D, Jackson CW, Hunt P, Saris CJ, Orkin SH: **Transcription factor NF-E2 is required for platelet formation independent of the actions of thrombopoietin/MGDF in megakaryocyte development**. *Cell* 1995, **81**(5):695-704.

59. Lecine P, Villeval JL, Vyas P, Swencki B, Xu Y, Shivdasani RA: **Mice lacking transcription factor NF-E2 provide in vivo validation of the proplatelet model of thrombocytopoiesis and show a platelet production defect that is intrinsic to megakaryocytes**. *Blood* 1998, **92**(5):1608-1616.

60. Kelemen E, Cserhati I, Tanos B: **Demonstration and some properties of human thrombopoietin in thrombocythaemic sera**. *Acta Haematol* 1958, **20**(6):350-355.

61. Bartley TD, Bogenberger J, Hunt P, Li YS, Lu HS, Martin F, Chang MS, Samal B, Nichol JL, Swift S *et al*: **Identification and cloning of a megakaryocyte growth and development factor that is a ligand for the cytokine receptor Mpl**. *Cell* 1994, **77**(7):1117-1124.

62. Lok S, Kaushansky K, Holly RD, Kuijper JL, Lofton-Day CE, Oort PJ, Grant FJ, Heipel MD, Burkhead SK, Kramer JM *et al*: **Cloning and expression of murine thrombopoietin cDNA and stimulation of platelet production in vivo**. *Nature* 1994, **369**(6481):565-568.

63. de Sauvage FJ, Hass PE, Spencer SD, Malloy BE, Gurney AL, Spencer SA, Darbonne WC, Henzel WJ, Wong SC, Kuang WJ *et al*: **Stimulation of megakaryocytopoiesis and thrombopoiesis by the c-Mpl ligand**. *Nature* 1994, **369**(6481):533-538.

64. Folman CC, de Jong SM, de Haas M, von dem Borne AE: **Analysis of the kinetics of TPO uptake during platelet transfusion**. *Transfusion* 2001, **41**(4):517-521.

65. de Graaf CA, Metcalf D: **Thrombopoietin and hematopoietic stem cells**. *Cell Cycle* 2011, **10**(10):1582-1589.

66. Geddis AE, Linden HM, Kaushansky K: **Thrombopoietin: a pan-hematopoietic cytokine**. *Cytokine Growth Factor Rev* 2002, **13**(1):61-73.

67. Wolber EM, Jelkmann W: **Interleukin-6 increases thrombopoietin production in human hepatoma cells HepG2 and Hep3B**. *J Interferon Cytokine Res* 2000, **20**(5):499-506.

68. Zucker-Franklin D, Kaushansky K: **Effect of thrombopoietin on the development of megakaryocytes and platelets: an ultrastructural analysis**. *Blood* 1996, **88**(5):1632-1638.

69. Takayama N, Eto K: **Pluripotent stem cells reveal the developmental biology of human megakaryocytes and provide a source of platelets for clinical application**. *Cell Mol Life Sci* 2012, **69**(20):3419-3428.

70. Cho J, Kim H, Song J, Cheong JW, Shin JW, Yang WI, Kim HO: **Platelet storage induces accelerated desialylation of platelets and increases hepatic thrombopoietin production**. *J Transl Med* 2018, **16**(1):199.

71. Hitchcock IS, Kaushansky K: **Thrombopoietin from beginning to end**. *Br J Haematol* 2014, **165**(2):259-268.

72. Vadhan-Raj S, Murray LJ, Bueso-Ramos C, Patel S, Reddy SP, Hoots WK, Johnston T, Papadopolous NE, Hittelman WN, Johnston DA *et al*: **Stimulation of megakaryocyte and platelet production by a single dose of recombinant human thrombopoietin in patients with cancer**. *Ann Intern Med* 1997, **126**(9):673-681.

73. Denk W, Strickler JH, Webb WW: **Two-photon laser scanning fluorescence microscopy**. *Science* 1990, **248**(4951):73-76.

74. Zheng Y, Chen J, Shi X, Zhu X, Wang J, Huang L, Si K, Sheppard CJR, Gong W: **Two-photon focal modulation microscopy for high-resolution imaging in deep tissue**. *J Biophotonics* 2019, **12**(1):e201800247.

75. Ishikawa-Ankerhold HC, Ankerhold R, Drummen GP: **Advanced fluorescence microscopy techniques--FRAP, FLIP, FLAP, FRET and FLIM**. *Molecules* 2012, **17**(4):4047-4132.

76. Helmchen F, Denk W: **Deep tissue two-photon microscopy**. *Nat Methods* 2005, **2**(12):932-940.

77. Weigert R, Porat-Shliom N, Amornphimoltham P: **Imaging cell biology in live animals: ready for prime time**. *J Cell Biol* 2013, **201**(7):969-979.

78. Tiedt R, Schomber T, Hao-Shen H, Skoda RC: **Pf4-Cre transgenic mice allow the generation of lineage-restricted gene knockouts for studying megakaryocyte and platelet function in vivo**. *Blood* 2007, **109**(4):1503-1506.

79. Muzumdar MD, Tasic B, Miyamichi K, Li L, Luo L: **A global double-fluorescent Cre reporter mouse**. *Genesis* 2007, **45**(9):593-605.

80. Proulx C, Boyer L, Hurnanen DR, Lemieux R: **Preferential ex vivo expansion of megakaryocytes from human cord blood CD34+-enriched cells in the presence of thrombopoietin and limiting amounts of stem cell factor and Flt-3 ligand**. *J Hematother Stem Cell Res* 2003, **12**(2):179-188.

81. Hartley PS, Sheward J, Scholefield E, French K, Horn JM, Holmes MC, Harmar AJ: **Timed feeding of mice modulates light-entrained circadian rhythms of reticulated platelet abundance and plasma thrombopoietin and affects gene expression in megakaryocytes**. *Br J Haematol* 2009, **146**(2):185-192.

82. Stremmel C, Schuchert R, Wagner F, Thaler R, Weinberger T, Pick R, Mass E, Ishikawa-Ankerhold HC, Margraf A, Hutter S *et al*: **Yolk sac macrophage progenitors traffic to the embryo during defined stages of development**. *Nat Commun* 2018, **9**(1):75.

83. Cossarizza A, Chang HD, Radbruch A, Acs A, Adam D, Adam-Klages S, Agace WW, Aghaeepour N, Akdis M, Allez M *et al*: **Guidelines for the use of flow cytometry and cell sorting in immunological studies (second edition)**. *Eur J Immunol* 2019, **49**(10):1457-1973.

84. Ault KA: **Flow cytometric measurement of platelet function and reticulated platelets**. *Ann N Y Acad Sci* 1993, **677**:293-308.

85. Robinson MS, Mackie IJ, Khair K, Liesner R, Goodall AH, Savidge GF, Machin SJ, Harrison P: **Flow cytometric analysis of reticulated platelets: evidence for a large proportion of non-specific labelling of dense granules by fluorescent dyes**. *Br J Haematol* 1998, **100**(2):351-357.

86. Debili N, Louache F, Vainchenker W: **Isolation and culture of megakaryocyte precursors**. *Methods Mol Biol* 2004, **272**:293-308.

87. Brown AS, Hong Y, de Belder A, Beacon H, Beeso J, Sherwood R, Edmonds M, Martin JF, Erusalimsky JD: **Megakaryocyte ploidy and platelet changes in human diabetes and atherosclerosis**. *Arterioscler Thromb Vasc Biol* 1997, **17**(4):802-807.

88. Shivdasani RA: **The role of transcription factor NF-E2 in megakaryocyte maturation and platelet production**. *Stem Cells* 1996, **14 Suppl 1**:112-115.

89. Tzur A, Moore JK, Jorgensen P, Shapiro HM, Kirschner MW: **Optimizing optical flow cytometry for cell volume-based sorting and analysis**. *PLoS One* 2011, **6**(1):e16053.

90. Pedersen OH, Nissen PH, Hvas AM: **Platelet function investigation by flow cytometry: Sample volume, needle size, and reference intervals**. *Platelets* 2018, **29**(2):199-202.

91. Aurbach K, Spindler M, Haining EJ, Bender M, Pleines I: **Blood collection, platelet isolation and measurement of platelet count and size in mice-a practical guide**. *Platelets* 2019, **30**(6):698-707.

92. Ramstrom S, Sodergren AL, Tynngard N, Lindahl TL: **Platelet Function Determined by Flow Cytometry: New Perspectives?** *Semin Thromb Hemost* 2016, **42**(3):268-281.

93. Michelson AD: **Evaluation of platelet function by flow cytometry**. *Pathophysiol Haemost Thromb* 2006, **35**(1-2):67-82.

94. Vinholt PJ, Frederiksen H, Hvas AM, Sprogoe U, Nielsen C: **Measurement of platelet aggregation, independently of patient platelet count: a flow-cytometric approach**. *J Thromb Haemost* 2017, **15**(6):1191-1202.

95. Grove EL, Hvas AM, Johnsen HL, Hedegaard SS, Pedersen SB, Mortensen J, Kristensen SD: **A comparison of platelet function tests and thromboxane metabolites to evaluate aspirin response in healthy individuals and patients with coronary artery disease**. *Thromb Haemost* 2010, **103**(6):1245-1253.

96. Buttarello M, Mezzapelle G, Freguglia F, Plebani M: **Reticulated platelets and immature platelet fraction: Clinical applications and method limitations**. *Int J Lab Hematol* 2020, **42**(4):363-370.

97. Meintker L, Krause SW: **Reticulated platelets – clinical application and future perspectives**. *Journal of Laboratory Medicine* 2020, **0**(0).

98. Kieffer N, Guichard J, Farcet JP, Vainchenker W, Breton-Gorius J: **Biosynthesis of major platelet proteins in human blood platelets**. *Eur J Biochem* 1987, **164**(1):189-195.

99.    Kienast J, Schmitz G: **Flow cytometric analysis of thiazole orange uptake by platelets: a diagnostic aid in the evaluation of thrombocytopenic disorders**. *Blood* 1990, **75**(1):116-121.

100.   Levario TJ, Zhao C, Rouse T, Shvartsman SY, Lu H: **An integrated platform for large-scale data collection and precise perturbation of live Drosophila embryos**. *Sci Rep* 2016, **6**:21366.

101.   Junt T, Schulze H, Chen Z, Massberg S, Goerge T, Krueger A, Wagner DD, Graf T, Italiano JE, Jr., Shivdasani RA *et al*: **Dynamic visualization of thrombopoiesis within bone marrow**. *Science* 2007, **317**(5845):1767-1770.

102.   Gaertner F, Massberg S: **Patrolling the vascular borders: platelets in immunity to infection and cancer**. *Nat Rev Immunol* 2019, **19**(12):747-760.

103.   Sola-Visner M: **Platelets in the neonatal period: developmental differences in platelet production, function, and hemostasis and the potential impact of therapies**. *Hematology Am Soc Hematol Educ Program* 2012, **2012**:506-511.

104.   Israels SJ, Cheang T, Roberston C, McMillan-Ward EM, McNicol A: **Impaired signal transduction in neonatal platelets**. *Pediatr Res* 1999, **45**(5 Pt 1):687-691.

105.   Sitaru AG, Holzhauer S, Speer CP, Singer D, Obergfell A, Walter U, Grossmann R: **Neonatal platelets from cord blood and peripheral blood**. *Platelets* 2005, **16**(3-4):203-210.

106.   Patrick CH, Lazarchick J, Stubbs T, Pittard WB: **Mean platelet volume and platelet distribution width in the neonate**. *Am J Pediatr Hematol Oncol* 1987, **9**(2):130-132.

107.   Harrison P, Robinson MS, Mackie IJ, Machin SJ: **Reticulated platelets**. *Platelets* 1997, **8**(6):379-383.

108.   Tremblay KD, Zaret KS: **Distinct populations of endoderm cells converge to generate the embryonic liver bud and ventral foregut tissues**. *Dev Biol* 2005, **280**(1):87-99.

109.   Wolber FM, Leonard E, Michael S, Orschell-Traycoff CM, Yoder MC, Srour EF: **Roles of spleen and liver in development of the murine hematopoietic system**. *Exp Hematol* 2002, **30**(9):1010-1019.

110.   Palis J, Robertson S, Kennedy M, Wall C, Keller G: **Development of erythroid and myeloid progenitors in the yolk sac and embryo proper of the mouse**. *Development* 1999, **126**(22):5073-5084.

111.   Tober J, Koniski A, McGrath KE, Vemishetti R, Emerson R, de Mesy-Bentley KK, Waugh R, Palis J: **The megakaryocyte lineage originates from hemangioblast precursors and is an integral component both of primitive and of definitive hematopoiesis**. *Blood* 2007, **109**(4):1433-1441.

112.   Italiano JE, Jr., Lecine P, Shivdasani RA, Hartwig JH: **Blood platelets are assembled principally at the ends of proplatelet processes produced by differentiated megakaryocytes**. *J Cell Biol* 1999, **147**(6):1299-1312.

113.   Tober J, McGrath KE, Palis J: **Primitive erythropoiesis and megakaryopoiesis in the yolk sac are independent of c-myb**. *Blood* 2008, **111**(5):2636-2639.

114.   Chan K, Lu R, Chang JC, Kan YW: **NRF2, a member of the NFE2 family of transcription factors, is not essential for murine erythropoiesis, growth, and development**. *Proc Natl Acad Sci U S A* 1996, **93**(24):13943-13948.

115.    Gorelashvili MG, Angay O, Hemmen K, Klaus V, Stegner D, Heinze KG: **Megakaryocyte volume modulates bone marrow niche properties and cell migration dynamics**. *Haematologica* 2020, **105**(4):895-904.

116.    Bruns I, Lucas D, Pinho S, Ahmed J, Lambert MP, Kunisaki Y, Scheiermann C, Schiff L, Poncz M, Bergman A *et al*: **Megakaryocytes regulate hematopoietic stem cell quiescence through CXCL4 secretion**. *Nat Med* 2014, **20**(11):1315-1320.

117.    Nakamura-Ishizu A, Takubo K, Fujioka M, Suda T: **Megakaryocytes are essential for HSC quiescence through the production of thrombopoietin**. *Biochem Biophys Res Commun* 2014, **454**(2):353-357.

118.    Potts KS, Farley A, Dawson CA, Rimes J, Biben C, de Graaf C, Potts MA, Stonehouse OJ, Carmagnac A, Gangatirkar P *et al*: **Membrane budding is a major mechanism of in vivo platelet biogenesis**. *J Exp Med* 2020, **217**(9).

119.    Brown E, Carlin LM, Nerlov C, Lo Celso C, Poole AW: **Multiple membrane extrusion sites drive megakaryocyte migration into bone marrow blood vessels**. *Life Sci Alliance* 2018, **1**(2).

120.    Jaffe AB, Hall A: **Rho GTPases: biochemistry and biology**. *Annu Rev Cell Dev Biol* 2005, **21**:247-269.

121.    Lordier L, Jalil A, Aurade F, Larbret F, Larghero J, Debili N, Vainchenker W, Chang Y: **Megakaryocyte endomitosis is a failure of late cytokinesis related to defects in the contractile ring and Rho/Rock signaling**. *Blood* 2008, **112**(8):3164-3174.

122.    Hickson GR, Echard A, O'Farrell PH: **Rho-kinase controls cell shape changes during cytokinesis**. *Curr Biol* 2006, **16**(4):359-370.

123.    Avanzi MP, Goldberg F, Davila J, Langhi D, Chiattone C, Mitchell WB: **Rho kinase inhibition drives megakaryocyte polyploidization and proplatelet formation through MYC and NFE2 downregulation**. *Br J Haematol* 2014, **164**(6):867-876.

124.    Nagy Z, Vogtle T, Geer MJ, Mori J, Heising S, Di Nunzio G, Gareus R, Tarakhovsky A, Weiss A, Neel BG *et al*: **The Gp1ba-Cre transgenic mouse: a new model to delineate platelet and leukocyte functions**. *Blood* 2019, **133**(4):331-343.

125.    Pertuy F, Aguilar A, Strassel C, Eckly A, Freund JN, Duluc I, Gachet C, Lanza F, Leon C: **Broader expression of the mouse platelet factor 4-cre transgene beyond the megakaryocyte lineage**. *J Thromb Haemost* 2015, **13**(1):115-125.

# Acknowledgement

I want to thank Prof. Dr. med Steffen Massberg for the opportunity to study and work on this project in his laboratory. I would also like to thank Mathias Orban for supervising and helping in research as well as in life. With his support, I quickly adapted to studying and living in Germany.

Furthermore, I would like to thank the members of my thesis advisory committee, Prof. Dr. Markus Sperandio and Prof. Dr. Christian Schulz, for their constructive advices on my PhD project. I would further like to thank the members of our lab for the great work atmosphere, in particular Hellen for helping me with multiphoton microscopy techniques, Michael, and Susanne for their continuous advice on animal experiments. Thanks to Sara who patiently check the writing and spells of the thesis.

I want to thank the IRTG914 for giving me the opportunity to participate in this structured PhD program. They provided interesting lectures, helpful seminars about soft skills and organized great retreats. I benefited a lot from this program. I learned not only lab skills but also communication skills. I would like to thank Dr. Verena Kochan for coordinating the program. She always treated me with patient and helpful advice, giving me much support.

I would also like to thank my family. My parents and sisters gave me tremendous support and trust. They were always the best listener and provided me the best self-confidence. My little nephew was always delivering joy to us. I am also grateful to had my excellent friends (Yao Ye, Lin Peng and Xiaolan) accompanying with me during my hard time and exploring different things together out of the lab. Thanks to my boyfriend Wei Xue for his care and love.

# Affidavit

Liu, Huan
_____
Surname, first name


_____
Street


_____
Zip code, town, country


I hereby declare, that the submitted thesis entitled:

### Mechanisms of embryonic thrombopoiesis
…………………………………………………………………..

is my own work. I have only used the sources indicated and have not made unauthorised use of services of a third party. Where the work of others has been quoted or reproduced, the source is always given.
I further declare that the submitted thesis or parts thereof have not been presented as part of an examination degree to any other university.


Munich, 13.12.2021_____          __Huan Liu_____
place, date                                              Signature doctoral candidate

# Confirmation of congruency

| | | | |
|---|---|---|---|
| **LMU** LUDWIG-MAXIMILIANS-UNIVERSITÄT MÜNCHEN | Promotionsbüro Medizinische Fakultät | MMRS | |

**Confirmation of congruency between printed and electronic version of the doctoral thesis**

Liu, Huan
_____
Surname, first name


_____
Street


_____
Zip code, town, country


I hereby declare, that the submitted thesis entitled:

### Mechanisms of embryonic thrombopoiesis
………………………………………………………………….

is congruent with the printed version both in content and format.




Munich, 13.12.2021 _____          _Huan Liu_____
place, date                                                  Signature doctoral candidate